Bioactive Materials 43 (2025) 510–549

Contents lists available at ScienceDirect

Bioactive Materials

journal homepage: www.keaipublishing.com/en/journals/bioactive-materials

Review article

Biomimetic multizonal scaffolds for the reconstruction of zonal articular cartilage in chondral and osteochondral defects

Xiaoqi Lin [a], Ye Zhang [b], Jiarong Li [a], Brian G. Oliver [b,c], Bin Wang [d], Haiyan Li [e], Ken-Tye Yong [f], Jiao Jiao Li [a,c,*]

[a] School of Biomedical Engineering, Faculty of Engineering and IT, University of Technology Sydney, NSW, 2007, Australia
[b] School of Life Sciences, Faculty of Science, University of Technology Sydney, NSW, 2007, Australia
[c] Woolcock Institute of Medical Research, Macquarie University, Macquarie Park, NSW, 2113, Australia
[d] Department of Orthopaedic Surgery, The First Affiliated Hospital, Zhejiang University School of Medicine, Hangzhou, 310006, China
[e] Chemical and Environmental Engineering Department, School of Engineering, STEM College, RMIT University, Melbourne, VIC, 3000, Australia
[f] School of Biomedical Engineering, Faculty of Engineering, The University of Sydney, Sydney, NSW, 2006, Australia

ARTICLE INFO

Keywords:
Cartilage tissue engineering
Zonal cartilage
Osteochondral scaffolds
Multizonal scaffolds
Biomimetic scaffolds

ABSTRACT

Chondral and osteochondral injuries are frequently encountered in clinical practice. However, articular cartilage has limited self-healing capacity due to its sophisticated zonal structure and avascular nature, introducing significant challenges to the restoration of chondral and osteochondral tissues after injury. Improperly repaired articular cartilage can lead to irreversible joint damage and increase the risk of osteoarthritis progression. Cartilage tissue engineering using stratified scaffolds with multizonal design to match the zonal structure of articular cartilage may help to meet the complex regeneration requirements of chondral and osteochondral tissues, and address the drawbacks experienced with single-phase scaffolds. Navigating the heterogeneity in matrix organisation and cellular composition across cartilage zones is a central consideration in multizonal scaffold design. With emphasis on recent advances in scaffold design and fabrication strategies, this review captures emerging approaches on biomimetic multizonal scaffolds for the reconstruction of zonal articular cartilage, including strategies on replicating native tissue structure through variations in fibre orientation, porous structure, and cell types. Exciting progress in this dynamic field has highlighted the tremendous potential of multizonal scaffolding strategies for regenerative medicine in the recreation of functional tissues.

1. Introduction

Chondral and osteochondral injuries frequently lead to osteochondral defects (OCDs) within the joint tissue, typically originating in the articular cartilage and may extend into the underlying subchondral bone. OCDs predominantly occur in the knee and ankle joints, but are also observed in other anatomical sites such as the hands and spine [1]. Symptomatic cases often present with severe pain, swelling, and impaired mobility, significantly impacting patients' quality of life. Possible aetiology of OCDs includes genetics, overeating, sedentary lifestyle, microtrauma, post-traumatic arthritis, acute and repetitive sports injuries, ligament instability, meniscus tears, and chronic stress caused by limb axis malalignment. Studies have shown a higher incidence of knee OCDs among athletes compared to the general population, with more than half of asymptomatic athletes showing full-thickness defects [2]. Meanwhile, osteochondritis dissecans is more prevalent in individuals aged 10 to 20, with higher occurrence in males [3]. Anatomically, within a joint, the bone surface is covered with a thin layer of articular (hyaline) cartilage, which serves as lubrication during movement and supports the distribution of loading forces to the subchondral bone [4]. Due to the inherent characteristics of the joint microenvironment, characterised by limited blood supply and availability of stem/progenitor cells, mature chondrocytes exhibit low metabolic activity and restricted ability to proliferate and migrate [5]. After cartilage injury and even with reconstructive surgery, critical-sized chondral or osteochondral defects have poor capacity for long-term repair. This diminished self-repair capacity leaves OCDs vulnerable to weight bearing, leading to altered force distribution within the joint that

Peer review under responsibility of KeAi Communications Co., Ltd.
* Corresponding author. School of Biomedical Engineering, Faculty of Engineering and IT, University of Technology Sydney, NSW, 2007, Australia.
E-mail address: jiaojiao.li@uts.edu.au (J.J. Li).

https://doi.org/10.1016/j.bioactmat.2024.10.001
Received 30 May 2024; Received in revised form 2 September 2024; Accepted 1 October 2024
Available online 11 October 2024

can accelerate the deterioration of tissues surrounding the defect, potentially culminating in the onset of joint pathology [6]. The combination of tissue damage and biomechanical instability often results in irreversible tissue degeneration and the progression of osteoarthritis (OA) [7]. Without curative treatment, OA causes severe chronic pain and disability due to structural joint damage characterised by articular cartilage thinning and degeneration, joint space narrowing, osteophyte formation, and subchondral bone remodelling, eventually necessitating total joint replacement although this surgery is associated with many complications [8].

Cartilage lesion grade is critical in determining the appropriate treatment and pain management plan. According to the International Cartilage Repair Society Classification (ICRSC), cartilage defects are classified into four grades based on severity. ICRS Grades 1–3 are known as 'chondral tissue defect' [9–11]. In Grade 3, the lesion extends to more than 50 % of the cartilage thickness, but it does not reach the subchondral bone. OCDs belong to the most severe form of defect identified as Grade 4, characterised by the complete loss of articular and calcified cartilage accompanied by extension of the defect down to the subchondral bone [12]. In this review, both the Grade 3 full-thickness cartilage defects and the Grade 4 osteochondral defects are considered, which are classified as 'Severely Abnormal' requiring full-layer reconstruction to relieve pain and prevent secondary arthritis [13].

Current clinical methods of chondral and osteochondral repair present numerous drawbacks, often resulting in limited applicability or suboptimal long-term outcomes, necessitating the development of emerging tissue engineering strategies based on multiphasic scaffolds to improve repair outcomes [14,15]. Advances in biomaterials and fabrication technologies have propelled the development of implantable biomimetic scaffold constructs, offering promising avenues for improving clinical outcomes in osteochondral repair [6]. However, the intricate hierarchical structure of osteochondral tissue, incorporating stratified layers with variations in cell type and morphology, matrix composition and arrangement, and biomechanical properties pose significant challenges to regeneration using scaffold-based approaches [16]. Key hurdles include the creation of bioactive scaffolds capable of accurately mimicking the natural structure and functionality of different osteochondral tissue regions, particularly the zonal architecture of articular cartilage.

The development of biomimetic scaffolds utilising novel combinations and designs of biomaterials has emerged as a promising approach for the treatment of osteochondral injuries [17–19]. Biomimetic scaffolding strategies aim to restore joint anatomy and function by mimicking the natural composition and structure of osteochondral tissue, thereby preventing further joint degeneration or the development of OA. A number of recent studies have highlighted the advantages of regenerating full-thickness cartilage or osteochondral defects using multizonal scaffolds in animal models. By providing a more biomimetic structure with zonal variations in scaffold properties that better matched native tissues, multizonal scaffolds tested in rabbit osteochondral defects were found to achieve improved defect filling and integration with host tissues [20], more faithful reconstruction of hyaline-like cartilage with zone-specific variations in cells and ECM [21], and simultaneous regeneration of cartilage and subchondral bone accompanied by a more wear-resistant articulating surface [22], compared to single-layer scaffolds without a multizonal design. Biomimetic multizonal scaffolds, particularly those that specifically replicate the zonal variations seen in native articular cartilage, are an emerging direction for the effective treatment of chondral and osteochondral injuries.

Although other reviews have captured biomimetic scaffolding strategies for the repair of osteochondral tissues, such as multiphasic and gradient scaffolds [14–16,23], they focused on studies that attempted to replicate the whole osteochondral unit. Despite heterogeneous naming conventions including 'multiphasic', 'multilayered', 'multizonal', and 'gradient', these reviews tended to focus on scaffolds that treated the articular cartilage as a bulk tissue rather than differentiating among the superficial, middle, and deep cartilage zones. The zonal architecture of articular cartilage introduces significant vertical heterogeneity in biophysical, biochemical, and cellular properties along the cartilage compartment of osteochondral tissue, which is a critical consideration for successful osteochondral reconstruction. In light of this, our review will provide a comprehensive evaluation of the current studies on constructing biomimetic chondral and osteochondral scaffolds, which specifically focused on faithfully replicating the zonal structure of articular cartilage. Our definition of 'multizonal' scaffolds in the rest of this review refers to scaffolds that attempted to mimic zonal cartilage architecture by incorporating different scaffold regions to match the superficial, middle, and deep cartilage zones. Diverging from the prevalent use of homogeneous hydrogels in existing research on cartilage tissue engineering, our review captures the latest research on a diverse range of scaffolding approaches to recreate the hierarchical structure of zonal articular cartilage.

This review will first briefly introduce the zonal organisation of articular cartilage and conventional treatment approaches, followed by an examination of biomimetic approaches for designing chondral and osteochondral scaffolds. It will then delve into the current scaffolding strategies that have specifically tried to recreate the zonal structure of articular cartilage, focusing on multizonal cartilage scaffolds incorporating design features such as fibre orientation, gradient composition and porous architecture, and the possible inclusion of cells and growth factors. This comprehensive review provides fresh insights into designing biomimetic zonal scaffolds for cartilage tissue engineering, and how these can be optimised to address a critical need in the realm of osteochondral tissue repair.

2. Characteristics of articular cartilage and current treatment approaches

2.1. Zonal articular cartilage and regional osteochondral hierarchy

Osteochondral tissue consists of articular cartilage ('chondral region') and underlying subchondral bone ('osseous region') [24]. As illustrated in Fig. 1A, native osteochondral tissue can be divided into three distinct but integrated layers: articular cartilage, calcified cartilage (interface or transition region between cartilage and bone), and subchondral bone (mainly trabecular bone) [25]. Within the chondral region, articular cartilage exhibits a transitional composition characterised by superficial, middle, and deep zones. Osteochondral tissue in different zones and regions exhibits different cellular and matrix compositions as well as unique structural and mechanical characteristics.

Articular cartilage, covering articular joint surfaces and comprising hyaline cartilage tissue, exhibits elastic properties and remarkable resistance to compression. Its smooth surface provides optimal lubrication, making it a crucial covering for the epiphyseal surface of joints that plays a vital role in supporting and cushioning the human body during movement. The thickness of articular cartilage varies depending on its location within the joint and the age of the individual. On average, it has a pore size of 6 nm, with normal thickness ranging 2.41 ± 0.53 mm [25]. Structurally, articular cartilage is a horizontally stratified tissue characterised by heterogeneity and anisotropy. This multilayered composition consists of superficial, middle, and deep zones, distinguished by variations in glycosaminoglycan (GAG) and collagen content and differences in collagen fibril orientation and cell density [26], as depicted in Fig. 1B. The superficial zone comprises 10–20 % of the total thickness, with densely packed, thin, aligned collagen fibres parallel to the cartilage surface. This zone has the lowest GAG concentration and highest permeability, with chondrocytes that are flat and tightly packed. The middle zone represents 40–60 % of the thickness, characterised by thick collagen fibres, arcades linked by smaller diameter fibres, and a higher concentration of GAGs. Chondrocytes are rounded and randomly distributed in this zone. The deep zone, accounting for 30–40 % of

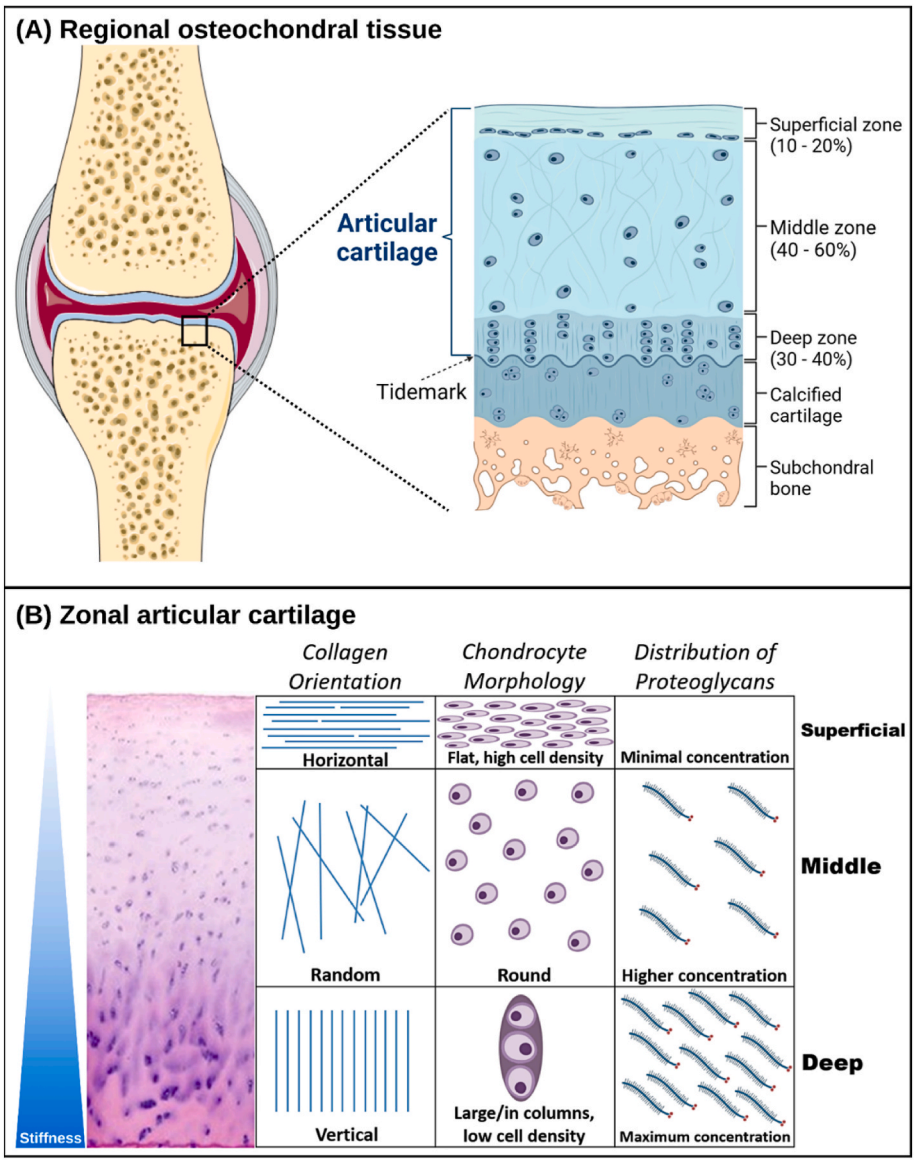

Fig. 1. Natural hierarchical structure of osteochondral tissue. **(A)** Organisation of osteochondral tissue regions. **(B)** Zonal structure of articular cartilage with variations in collagen fibril distribution, chondrocyte morphology, and mineral composition in the superficial, middle, and deep zones. Figure created using Microsoft PowerPoint.

cartilage thickness, features arranged collagen fibres and elongated chondrocytes perpendicular to the tidemark. It holds the highest GAG concentration but the lowest cell density, with low permeability and no fluid flow. The natural composition gradient, including collagen type and mineral content variations, imparts gradient biomechanical properties to the articular cartilage. Consequently, an increase in tissue depth from the superficial to deep layers is accompanied by a corresponding progressive increase in mechanical stiffness.

Between the hyaline articular cartilage and the subchondral bone, the calcified cartilage region is a transitional intermediate layer delimited by the upper tidemark and the lower cement line. Calcified cartilage contains dispersed, hypertrophic chondrocytes within lacunae in the calcified matrix, comprising collagen type I, sodium hyaluronate, and nanohydroxyapatite in varying proportions. Compared to adjacent regions, calcified cartilage exhibits transitional properties, with a lower content of collagen type II than articular cartilage and lower concentration of hydroxyapatite inorganic mineral than subchondral bone [27]. It hence endows osteochondral tissue with transitional mechanical properties characterised by a continuous increase in stiffness from top to bottom that minimises shear stress ('stiffness gradient'). In addition, calcified cartilage acts as a barrier that limits diffusion and inhibits vascular invasion from the subchondral bone, thereby helping to preserve the structure and function of articular cartilage, while also allowing the transport of small solutes from the subchondral circulation to nourish the deeper cartilage regions. Articular cartilage hence derives its nutrients from both the superficial synovial fluid and the underlying subchondral bone.

The subchondral bone is the region with the highest mechanical strength, allowing the joint to withstand stress and absorb shock, and facilitating nutrient delivery through its rich vascular network. Subchondral bone comprises a diverse array of cells, with osteocytes being the predominant type (constituting 90–95 %), and plays a pivotal role in regulating bone formation (by osteoblasts) and bone resorption (by osteoclasts) as well as maintaining bone homeostasis. Structurally, the subchondral bone is akin to cancellous or trabecular bone, characterised by a spongy architecture with interconnected large pores. Its porosity typically ranges from 75 to 90 %, with pore sizes varying between 50 and 300 μm [28].

2.2. Existing clinical treatments for cartilage restoration

Clinical treatments for full-thickness chondral and osteochondral defects are limited, generally involving microfracture drills and tissue transplantation using osteochondral autografts or allografts. However, these treatments are only applicable for small-to mid-sized lesions [29]. A critical-sized cartilage/osteochondral defect in humans is usually defined as $\geq$ 3.0 cm in diameter [30]. Clinical cases of osteochondral injuries vary widely in defect area, but have been estimated to have an average size of 4.1 cm^2 [25], and may exceed the repairable size range using tissue transplantation. Moreover, tissue grafts usually only help to relieve symptoms such as pain, but do not actually promote osteochondral tissue regeneration. The lack of long-term effectiveness of existing therapies, particularly for extensive osteochondral injuries, drives research towards exploring more innovative strategies. Unlike conventional treatments, scaffold-based cartilage tissue engineering can provide a temporary 3D structure to reconstitute the structure and function of the native cartilage extracellular matrix (ECM), substituting the anatomy, mechanical properties, and biochemical composition of the damaged tissue and creating an environment that is conducive to cellular repair processes.

2.2.1. Non-surgical strategies

Non-surgical strategies for cartilage and osteochondral repair include non-pharmacological management, pharmacological management, and orthobiologics. Non-pharmacological interventions often involve exercises, weight management, physical therapy, and resistance training [31,32]. Braces and other orthoses may be used to provide structural support, aiming to alleviate pain and enhance joint function [32]. However, these approaches are aimed at palliative care, where the patient has little or no prospect of a cure and only derives symptomatic relief.

Pharmacological management options may include oral supplements, steroid injections, injectable viscosupplements, and other drug therapies with the central aim of providing pain relief [32]. However, these have potential to induce severe side effects, including renal, cardiovascular, and gastrointestinal injuries [33], particularly in older patients who are often affected by multiple chronic conditions and polypharmacy becomes an issue. Oral supplements often comprise the commonly applied non-steroidal anti-inflammatory drugs (NSAIDs), which inhibit cyclo-oxygenase activity and stimulate anti-inflammatory, anti-depressant and analgesic effects [34]. However, in addition to the risk of causing acute kidney injury and stroke, the clinical efficacy of oral supplements such as NSAIDs has been variable, with mixed results reported in studies evaluating their effectiveness [35]. Steroid injections have been used in joint injuries to reduce pain and improve function due to their local anti-inflammatory effects. However, they typically provide short-term benefits and are best suited for acute pain onset in cartilage injuries or early OA [32]. Side effects are commonly experienced after injection such as injection site pain, elevated blood glucose, and skin atrophy [36]. Meanwhile, injectable viscosupplements such as high molecular weight hyaluronic acid (HA) base on the rationale that they may help to enhance joint lubrication by improving viscoelasticity, as well as provide anti-inflammatory effects [37]. However, they have shown variable therapeutic benefits and also do not prevent long-term progression of joint degeneration [38].

Orthobiologics treatment involves using biological substances, such as platelet-rich plasma (PRP) [39], stromal vascular fraction (SVF) [40], and stem cells [41] to promote osteochondral tissue repair after injury. PRP is derived from centrifuged autologous blood and contains a concentrated mixture of platelets, growth factors, and other bioactive molecules. It has been shown to inhibit catabolic cytokines such as IL-1β and TNF-α, which have integral roles in driving OA progression after joint injury, while promoting cellular secretion of anabolic factors such as fibroblast growth factor (FGF) and transforming growth factor-β (TGF-β) [42]. PRP injections have shown beneficial effects when used in conjunction with surgical approaches to manage knee and hip OA [43]. SVF is a concentrated mixture of heterogeneous cell populations, including adipose-derived stem cells (ADSCs), pre-adipocytes, endothelial progenitor cells, and various immune cells, along with platelets, growth factors, and ECM materials. Intra-articular injection of SVF has shown some beneficial effects as a treatment for knee OA [40]. Stem cells, particularly mesenchymal stem cells (MSCs), hold promise as a therapy for cartilage repair or OA, mainly due to their paracrine function or ability to exert anti-inflammatory and trophic effects on surrounding tissues [44]. For instance, autologous MSCs have been reported to induce functional improvement in knee OA patients over a 12-month period [45]. However, despite some promising results obtained with orthobiologics in the treatment of joint pathologies [46], the majority of studies have applied these to patients at an advanced stage of OA, and often reporting inconsistent long-term benefits [47,48]. Their therapeutic effects in clinical cases of chondral and osteochondral injuries are less well characterised, and possibly limited by the need for injections at high doses and/or frequency as well as injection-related side effects [49].

2.2.2. Surgical strategies

Surgical strategies for cartilage and osteochondral repair include microfracture, autologous chondrocyte implantation (ACI), and osteochondral grafts. Microfracture (bone marrow stimulation) creates micro-size or nano-size drills into the subchondral bone beneath the damaged cartilage. This induces rapid infiltration of stem cells from the bone marrow through microscopic injuries in the subchondral bone surface, and the subsequent formation of a fibrin clot. Being performed through arthroscopy, it has the advantages of being minimally invasive, resulting in shorter surgical time and reduced postoperative pain. However, microfracture stimulates unnatural cartilage healing through scarring, promoting the formation of fibrocartilage to fill the defect [50]. This repair tissue is substantially different from hyaline cartilage, being vulnerable to mechanical forces and is only helpful in the short-term for delaying cartilage degeneration, with degenerative changes typically expected beyond five years following microfracture surgery irrespective of the lesion size [51].

ACI involves treating cartilage injuries through transplantation of the patient's cultured chondrocytes into the damaged area, which may be aided by a biomaterial (matrix-induced ACI or MACI) [52]. ACI is capable of inducing hyaline-like cartilage formation that closely resembles the properties of native articular cartilage, hence providing better long-term outcomes compared to fibrocartilagous repair in microfracture [53]. However, although using cultured chondrocytes in ACI provides a personalised approach for repairing larger-sized defects, there are limitations associated with the surgical process and possible need for large amounts of chondrocytes [54]. For instance, the harvesting of healthy cartilage from a non-weight-bearing site in the patient and subsequent culturing of extracted chondrocytes inevitably prolong the treatment timeline, while the need to perform a complex surgery for implantation reduces the accessibility of this technique in some regions. Moreover, ACI is limited to the repair of cartilage damage, while a bone grafting procedure must also be performed for defects penetrating deeper than 6–8 mm into the subchondral bone [26]. For this reason, full-thickness osteochondral defects currently have limited and suboptimal surgical options for repair.

Osteochondral grafting can provide an option for restoring full-thickness osteochondral lesions. Conventional strategies are widely known as autograft and allograft cartilage implantation [55]. Autografting involves cartilage transplantation from another non-load-bearing joint in the same person, but is often limited by the amount of healthy cartilage available particularly in extensive injuries. Harvesting autologous tissue can also cause additional damage at the donor site. Allografting involves transplanting a cartilage tissue graft from another individual, often a deceased donor. However, this carries a risk of immune rejection and subsequent graft failure, as well as possible

tissue mismatch with the defect and lack of bioactivity in the transplanted graft.

Conventional treatment approaches for chondral and osteochondral injuries are largely ineffective at restoring original cartilage structure and properties to achieve adequate long-term repair and prevent further degenerative changes. Consequently, there is a pressing need for new therapeutic interventions that can effectively repair critical-sized cartilage defects. The design and application of biomimetic stratified scaffolds through tissue engineering approaches offer new hope for addressing current challenges.

3. Design considerations for biomimetic chondral and osteochondral scaffolds

Biomimetic chondral and osteochondral scaffolds are designed to closely mimic the spatial organisation, tissue composition, and functional properties of native tissues. Earlier approaches using homogeneous monolayer scaffolds were mostly shown to be suboptimal for regenerating zone-specific osteochondral tissues, as they were unable to satisfy variations in the conditions required for different types of tissue regeneration along the depth of the defect [14,15]. The design of a biomimetic, stratified zonal scaffold depends on several key factors (Fig. 2), including layered architecture, materials selection, corresponding fabrication methods, and optional incorporation of cells and growth factors [23]. The desired outcomes include a hierarchical structure and zonal properties within the regenerated cartilage region to match native tissue characteristics, which may include zone-specific variations in matrix composition, collagen fibre orientation, mechanical properties, cellular phenotypes, and bioactive growth factors. Fig. 3A illustrates a representative multizonal hydrogel model based on a 'full-thickness cartilage defect (grade 3)', replicating the zonal structure of the natural articular cartilage in the superficial, middle, and deep zones. Multizonal osteochondral scaffolds aim to restore the physical and biochemical properties of the stratified structure of articular cartilage zones, with additional considerations for calcified cartilage and subchondral bone to reconstruct the entire osteochondral unit, as depicted in Fig. 3B.

Current designs for chondral and osteochondral scaffolds still face some important challenges. Firstly, it is difficult to produce truly biomimetic scaffold designs that faithfully replicate the hierarchical structure and composition of zonal cartilage tissue and regional osteochondral tissue, particularly without involving complex fabrication processes that might pose hurdles in scale-up manufacturing. Secondly, there is a significant challenge in fabricating multiphasic scaffolds with integrated layers that respectively accommodate the regeneration requirements of superficial, middle, and deep zone cartilage as well as calcified cartilage and subchondral bone, while maintaining seamless integration between the different layers. Thirdly, chondral and osteochondral defects often occur at weight-bearing sites within the joint. However, much of the current biomimetic scaffold designs for treating these defects are created using hydrogels, which may not possess adequate mechanical properties for physiological load-bearing. These challenges form the basis of the design requirements for multizonal cartilage scaffolds discussed in detail later in this review, including biomimetic zone-specific architecture, seamless transition or integration between zones, and mechanical stability or biomimicry in mechanical properties. Current scaffold designs have attempted to meet these design needs through zone-specific modulation of fibre orientation, composition or pore structure, and cell types or growth factors.

3.1. Architecture comparison between multilayered and gradient scaffolds

Biomimetic multilayered scaffolds mimic natural osteochondral tissue structure and function, comprising both cartilage and subchondral

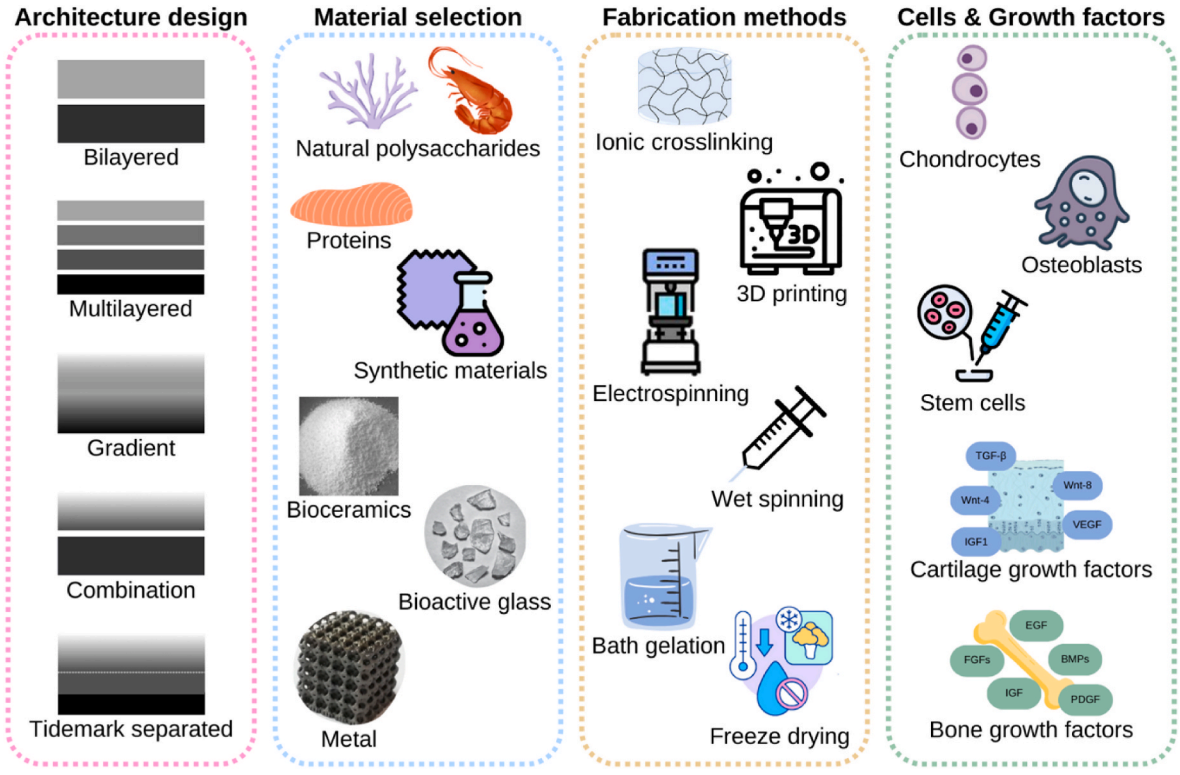

Fig. 2. Critical factors in the design of biomimetic zonal chondral/osteochondral scaffolds, such as architecture design and material selection, may define the success of reconstructing zonal properties and mechanical performance of native tissues. Fabrication methods need to be selected and adapted according to the materials used to increase the degree of control over structural and compositional parameters. Loading cells and/or growth factors is an additional strategy to promote chondrogenesis and osteogenesis in the corresponding regions by providing microenvironmental cues. Figure created using Microsoft PowerPoint.

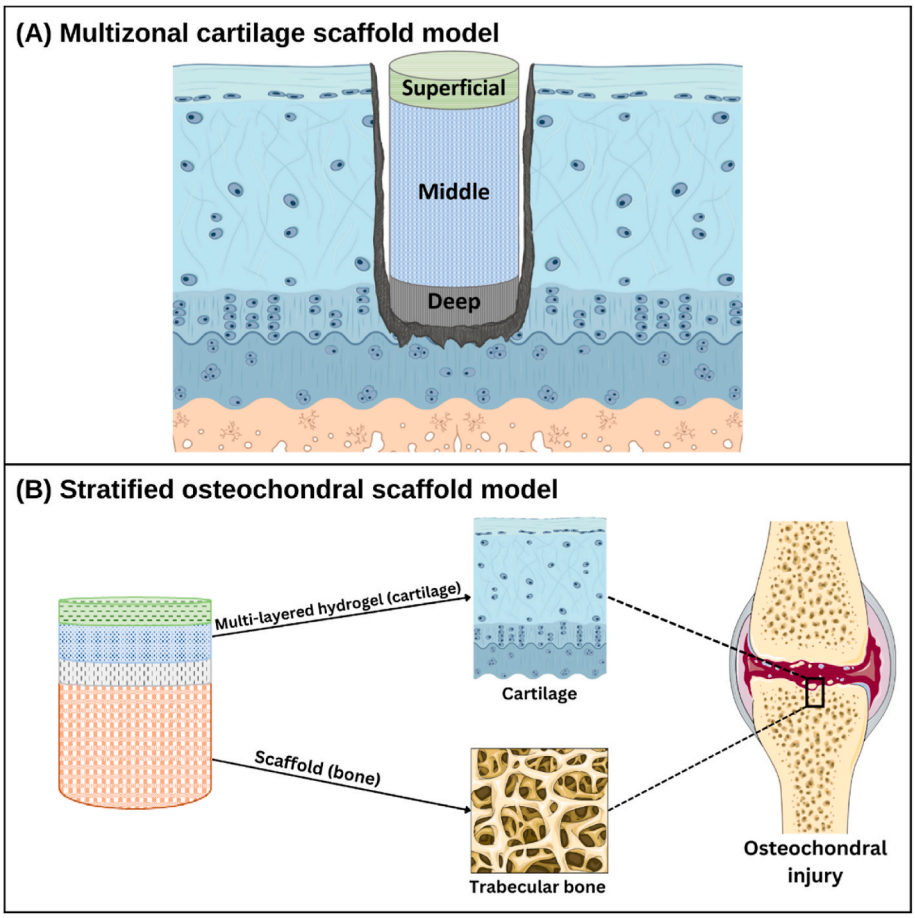

Fig. 3. Multizonal and stratified scaffold models. **(A)** A multizonal hydrogel model based on a 'full-thickness cartilage defect (grade 3)', replicating natural hierarchical structure of cartilage tissue. **(B)** A stratified osteochondral scaffold model combines a soft multilayered cartilaginous scaffold and a rigid subchondral bone scaffold. Figure created using Microsoft PowerPoint.

bone components. Because these are intended for repairing damaged or degenerated joints, particularly in weight-bearing joints such as the knee, scaffolds need to be designed to provide improved load distribution and seamless integration between cartilage and bone, and facilitate joint function under complex biomechanics. Multilayered and gradient architectures are the two most commonly considered scaffold designs, each with unique advantages and disadvantages.

3.1.1. *Multilayered scaffolds with discrete structure*

Multilayered scaffolds can contain three or more compartments with dissimilar architectures comprising different biomaterials to reconstruct the anatomical microstructure of articular cartilage, often with a concurrent transition layer facilitating integration with the subchondral bone. This design provides a relatively simple approach to recreating zonal variations in articular cartilage, as the different scaffold layers can be constructed separately and later integrated through various means. The scaffold hence provides greater tissue specificity in its different regions for matching native tissue characteristics. Particularly in osteochondral scaffolds where weight-bearing becomes increasingly important, the multilayered design can achieve higher mechanical properties by allowing wider materials selection that is not limited to hydrogels. Moreover, it is easier to create separation in the cartilage and bone regions of the scaffold through distinct layers, helping to prevent cell migration between the two tissue types and therefore enabling better maintenance of region-specific tissue phenotype. However, issues may arise due to inherent discontinuities in the multilayered structure, leading to mismatch of mechanical properties and biodegradation rates between adjacent layers. Resulting mechanical instability may result in poor tissue integration or even collapse of newly formed tissues [15]. In addition, weak interfacial mechanical properties and the risk of interlayer delamination may reduce long-term implant performance [23].

3.1.2. *Gradient scaffolds with continuous layers*

Gradient scaffolds exhibit a transition in material properties that varies gradually from one end to the other, creating a continuous gradient structure rather than having discrete layers. Gradient variation in scaffold architecture and/or properties allows seamless transition from one tissue region to another, which can effectively improve interfacial integration and minimise the risk of delamination [56]. The gradient design may also enable simpler and more reproducible fabrication, since often the same raw materials are used to create a continuous change in pore structure, biomaterial ratio, or the composition of biological agents [23]. Nevertheless, some common challenges are encountered in accurately modelling tissue specificity or precisely replicating the variation in properties seen in native zonal cartilage. Because a majority of gradient scaffolds is constructed by sequential layering and crosslinking of hydrogels, they often fail to provide the mechanical support necessary for cartilage and bone regeneration in weight-bearing regions or in a highly stressed joint environment.

3.2. *Zonal variations in mechanical properties and porous design*

Critical design factors that should be considered for zonal chondral and osteochondral scaffolds include the gradient variations in pore structure and mechanical characteristics of native cartilage and bone tissue, as shown in Table 1.

Table 1
Depth-dependent variation in pore structure, mechanical properties, and functional behaviour of human osteochondral tissue.

Tissue zone	Pore size/porosity	Mechanical properties	Functional behaviour
Superficial cartilage zone	Depth-dependent variations across zones [57,58] Pore sizes: 2–6 nm Porosity: 60–85 %	Tensile modulus: 10.1 MPa [10] Compressive modulus: 0.2 MPa [10] to 0.3 MPa [62]	Lubrication and load distribution. Responsible for the behaviour of cartilage under pressure at the weight-bearing site. Resistance against shear forces, reducing the risk of damage during joint movement.
Middle cartilage zone	Diameter of collagen fibrils: from thinnest 30–35 nm (superficial zone) to thickest 40–80 nm (deep zone)	Tensile modulus: 5.4 MPa [10]	Resistance against compressive forces.
Deep cartilage zone		Compressive modulus: 6.4 MPa [10] to 9.8 MPa [62]	Perpendicular collagen fibres and the resulting arcadic structure support the overlying load. Greatest resistance to compressive forces.
Calcified cartilage	Pore size: 10.71 ± 6.45 nm [63]	Indentation modulus: ~19 GPa [64]	Shock absorption. Interlocked tightly with the upper articular cartilage and the lower subchondral bone plate, resisting shear forces and preventing detachment from the underlying bone.
Cortical bone	Pore size: 30–50 μm Porosity: 3–5% [65], 5–10 % [59,60]	Average values from literature [65]: Tension strength: longitudinal 135 ± 15.6 MPa, transverse 53 ± 10.7 MPa; Compression strength: longitudinal 205 ± 17.3 MPa, transverse 131 ± 20.7 MPa Compressive modulus: 18–22 GPa [16]	Protective bone covering with a high degree of bending and twisting resistance, supporting the weight of the body.
Trabecular bone	Non-homogeneous anisotropic properties Pore size: 300–500 μm [61] Porosity: 50–90 % [59,60]	Average values from literature [65]: Vertebra 2.4 ± 1.6 MPa; Tibia 5.3 ± 2.9 MPa; Femur 6.8 ± 2.9 MPa Subchondral bone ultimate strength: 10–40 MPa (varies with medial/lateral region and depth below surface) [66] Compressive modulus: 0.1–0.9 GPa [16]	Sponge-like geometric arrangement can withstand localised forces transmitted through the bone while porous structure provides light weighted-ness.

Adult articular cartilage responds in a depth-dependent manner to compressive weight bearing, due to its zonal variations in collagen and GAG distribution. In the cartilage region of osteochondral tissue, mesopores range in sizes of 2–6 nm with porosity of 60–85 %, with gradual increase in pore size from the superficial to deep zone [57,58]. Calcified cartilage is present in the transition region between hyaline cartilage and subchondral bone, where collagen fibres are immobilised in the subchondral bone to anchor the cartilage layer [27], and hydroxyapatite becomes more abundant with increasing depth down to the bone. The subchondral bone serves as the bottom support platform with the highest load-bearing resistance. Morphologically, the porosity of cortical bone is usually between 5 and 10 %, while the porosity of cancellous bone ranges from 50 to 90 % [59,60]. Pore sizes in cortical bone are smaller compared to cancellous bone, with diameters of 30–50 μm (typically lower than 100 μm). The interconnected pores in the trabeculae form a network of varying pore sizes, typically 300–500 μm in diameter [61].

Mechanical properties of the designed scaffold are expected to match the load-bearing nature of the cartilage and restore its function to support joint movement, which includes replicating the mechanical variation seen in distinct cartilage zones. It is worth noting that the compressive modulus of the cartilage compartment is depth-dependent, increasing from the superficial to the deep zone from 0.2 to 6.44 MPa [16]. In the superficial zone, the tensile modulus is higher than in other zones, at 10.1 MPa, while this decreases to 5.4 MPa in the intermediate zone [10]. This mechanical gradient is created by depth-dependent variation in the ratio of collagen to GAG in the articular cartilage. Meanwhile, the subchondral bone is covered by a layer of cortical bone, characterised by Young's modulus of 15–20 GPa, with more porous cancellous bone underneath that has Young's modulus ranging between 0.1 and 2 GPa, contributing to its lighter and more flexible nature [67]. The mechanical variations along the osteochondral unit provide a combination of strength, resilience, flexibility, and adaptability to skeletal loads, creating a unique functional gradient that constitutes an important goal of biomimetic scaffold design.

Porosity and pore size are primary factors influencing the mechanical stiffness and biological properties of osteochondral scaffolds, while other secondary factors such as pore geometry are also of interest [61,68]. In biomaterial-based osteochondral tissue engineering, the biological properties of the scaffold are often correlated with how closely the scaffold matches the mechanical properties of surrounding tissues [69]. While high porosity is useful for avoiding stress shielding and stimulating cartilage and bone ingrowth [61], a balance needs to be maintained as this also reduces mechanical strength and may impact the scaffold's load-bearing capacity. Particularly in full-thickness osteochondral defects, adequate mechanical stability of the subchondral bone region is important for anchoring the scaffold within host tissue and protecting the regenerating cartilage from damage due to overloading. In the cartilage region, scaffold layers are often not designed to replicate the mesopore structure of surrounding chondral tissue, as tiny, tightly interconnected pores are not conducive to chondrocyte survival and growth. Instead, larger pore sizes of 100–200 μm [70] are employed to allow adequate space for cell adhesion, migration, and nutrient exchange. In deeper layers, the scaffold design often mimics highly porous cancellous bone with a large specific surface area to facilitate tissue integration. For instance, the optimal pore size for achieving osteogenesis and bone ingrowth ranges from 300 to 800 μm with approximately 60 % porosity [71–73], closely matching the cancellous bone and resulting in improved bone ingrowth and osseointegration [74].

Pore geometry [75,76] is an emerging factor being increasingly considered in biomimetic scaffold design due to its role in providing extracellular cues, and precise control over this parameter can now be realised through computer-aided design coupled with additive manufacturing methods. Recent evidence suggests that cells respond to physical cues in the microenvironment through alterations in cell shape and movement, which can lead to changes in cell activity and fate, and further direct the morphogenesis, pathology, and repair of many tissues [77]. Variations in pore geometry can influence both surface topography and mechanical characteristics of the scaffold, thereby impacting cell behaviour and regenerative processes. For instance, irregular pore structure in bioceramic scaffolds can improve biocompatibility by resembling the irregular order of bone trabeculae [78]. With advances in fabrication technologies, unique topological designs with high geometrical complexity and small dimensions can now be created, such as 3D printed cellular metals [68], ceramic cellular materials [79], and polymeric cellular materials [80] with deliberately integrated voids, as well as lattice structures [81,82] including strut-based lattice structures [83] and lattice sandwich structures [84]. Modulating pore geometry can augment regional variations in biomimetic osteochondral scaffolds by introducing changes in mass, surface area-to-volume ratio, porosity, mechanical properties, and surface curvature, all of which influence the spatiotemporal arrangement of cells and hence the outcomes of tissue

regeneration.

In the design of multizonal cartilage scaffolds, it is essential to not only consider the pore structure and mechanical properties, but also the functional behaviour of articular cartilage. The most important function of cartilage in providing wear resistance and constant lubrication in articulating joints should be a design consideration in biomimetic cartilage scaffolds [85]. Recent advances in biomedical research have shed light on the frictional behaviour and lubrication mechanisms underlying cartilage wear and degradation, inspiring new therapeutic strategies for cartilage repair and regeneration [86]. The significance of wear resistance and friction reduction is beginning to emerge in some current designs of cartilage scaffolds [87,88]. For instance, the integration of a top lubrication layer may help to augment the functional properties of the cartilage scaffold, where hydrogels or natural polymeric materials stand out due to their ability to provide low surface friction and exceptional lubrication, as well as remarkable biocompatibility [89,90].

It is notable that the regeneration rate of articular cartilage varies across its different zones, forming a gradient of healing speed [57]. This variation is attributed to the distinct structural, compositional, and cellular characteristics of each zone. The superficial zone has the highest regeneration capacity due to its higher cell density and proximity to the synovial fluid, which provides easier access to nutrients and bioactive factors. The regeneration rate becomes slower transitioning from the middle to deep zone, due to reduced cell density and limited nutrient supply. Besides a depth-dependent gradient in regenerative capacity, articular cartilage exhibits very limited healing potential overall, compared to the highly metabolically active subchondral bone that demonstrates fast and efficient regeneration after injury [16]. Meanwhile, the regeneration of calcified cartilage that anchors the articular cartilage to subchondral bone is also very limited due to the dense, calcified nature of the matrix, which impedes healing due to the lack of vascularisation and cellular presence [63]. Moreover, cartilage regeneration can be influenced by several factors, including age, mechanical loading, anatomical location, and injuries or disease conditions that can impair cartilage regrowth [57]. Although complex and highly variable, the regeneration rate of cartilage is an important design consideration for scaffolding strategies, as the biomaterials used are expected to achieve a degradation rate synchronised with the rate of new tissue formation. This is crucial for restoring cartilage function and supporting physiological weight-bearing without re-injury at the regeneration site.

3.3. Biomaterials selection

Biomaterials selection is the first step and a key factor in composing an osteochondral scaffold [23]. Other than meeting the essential criteria for a tissue engineering scaffold, including bioactivity, biodegradability, processability, and mechanical stability, biomaterials used for osteochondral repair also need to be conducive to cartilage and bone formation, and be amenable to providing region-specific properties. Natural and synthetic polymers, alone or in blends are mainly used to formulate the cartilage region and help induce zonal cartilage regeneration, which may be supported by hard materials such as bioceramics and metals used to recreate the subchondral bone region.

Each class of material has its advantages and drawbacks as candidates for osteochondral scaffolds, and combining different types of materials increases the likelihood of producing better region-specific biomimetic properties, although this also raises the complexity of fabrication and may reduce reproducibility. The biodegradability of different material components in a scaffold should be considered, as a scaffold that degrades too quickly may not provide sufficient support for the migrating cells and newly formed tissue, while one that degrades too slowly may impede tissue remodelling and integration [91]. Polymeric materials including natural and synthetic polymers, and decellularised matrix are usually chosen for creating multizonal cartilage scaffolds (Fig. 4). Polymers offer good biocompatibility and biodegradability, high water content, and good control over physicochemical characteristics, although they may have low stiffness and weak mechanical properties [92]. Bioceramics have poor elasticity but high stiffness, providing bioactivity and osteoconductive properties, and are usually used for creating the porous bone region. Metallic materials are widely used in orthopaedic implants because of their excellent mechanical support, which makes them possible candidates for replacing the subchondral bone. However, despite some applications as the bone part of osteochondral scaffolds, they are not considered tissue engineering materials due to biological inertness and non-biodegradability [9]. Newer developments in bioactive and biodegradable metal scaffolds sit at the interface of orthopaedic implants and tissue engineering [93–96]. Currently, multilayered osteochondral scaffolds usually comprise a bioactive polymer scaffold or hydrogel as the cartilage region, joined to a mechanically robust polymer/ceramic scaffold as the bone region, while gradient scaffolds are largely hydrogel constructs with regional variations in composition and/or properties. This section will briefly describe the classes of materials used for osteochondral scaffolds, as they have been extensively covered in other reviews [15,16]. Example studies on natural and synthetic polymers, and decellularised matrix illustrate the potential of these materials in promoting zonal cartilage regeneration. Bioceramics and metals are discussed in their capacity to be used as part of a ready-made subchondral support for zonal cartilage scaffolds.

3.3.1. Natural polymers

Natural polymers share structural similarities with ECM and typically have minimal risk of inducing immunological or inflammatory reactions within the body [100]. Biocompatible naturally derived polymers such as alginate, chitosan, gelatin, collagen, cellulose, and silk fibroin are widely used in tissue engineering of articular cartilage [96]. Due to their natural biomimetic properties, natural polymers can be layered to generate a bioactive environment for osteochondral repair, while also providing reasonable mechanical support for regenerating tissues. Natural polymers have been particularly useful in constructing bioinspired gradient scaffolds to mimic the stratified layers in osteochondral tissue, such as through gradient variations in pore structure, composition, and factors that induce osteochondrogenesis [101].

Alginate, derived from brown seaweed, is a natural polysaccharide frequently used to fabricate cartilage layers in the form of hydrogels, which can also facilitate the delivery of cells and therapeutic drugs [102]. They can be easily manufactured through cationic crosslinking such as by using divalent cations (e.g., Ca^{2+}, Cu^{2+}, Ba^{2+}, Sr^{2+}, Zn^{2+}, Co^{2+}) [102–107], trivalent cations (e.g., Fe^{3+}, Nd^{3+}, Tb^{3+}), and the combination of multiple cations [108–110]. Alginate hydrogels can provide a 3D environment for zonal cartilage regeneration and enable zone-specific chondrocyte density and growth [111]. Versatile processing options allow alginate hydrogels to be printed as a bioink, and used to construct multilayered zonal cartilage scaffolds embedding a gradient of cell densities to mimic the superficial, middle, and deep cartilage zones [112]. Alginate methacrylate hydrogels have also been used as cell encapsulation vehicles for infiltrating 3D printed synthetic polymer scaffolds with gradient pore structure designed for zonal cartilage repair [113].

Chitosan, derived from chitin in crustacean shells, is a polysaccharide that exhibits excellent biodegradability and structural similarity to GAGs [114]. The bioactivity of chitosan, reflected in its antimicrobial, antitumour, and antioxidant activities, contributes to reducing inflammation when chitosan scaffolds are used for cartilage defect repair [115]. Admittedly, chitosan itself has weak mechanical strength, and is often modified or enhanced by incorporating other materials to improve mechanical properties for cartilage regeneration, such as by short fibre segments [116] or blending with other materials [117]. Hyaluronic acid is another polysaccharide, and being a natural component of synovial fluid and cartilage, is often used in chondral hydrogel formulations because of its lubricating and viscoelastic

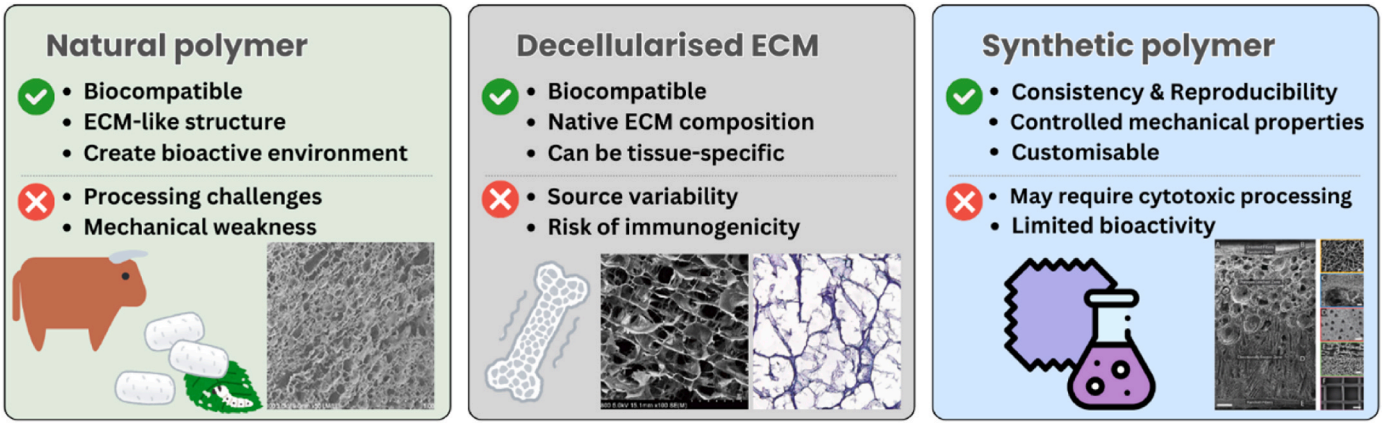

Fig. 4. For zonal cartilage regeneration, scaffolds are often constructed using polymeric materials, including naturally-derived (left), decellularised ECM (middle), and synthetic (right). Examples: Natural polymer scaffold (left) made from collagen/silk fibroin composites for chondrogenic differentiation, image adapted with permission from Ref. [97]. Decellularised ECM scaffold derived from human articular cartilage (middle) used in conjunction with microfracture for cartilage regeneration, image adapted with permission from Ref. [98]. Synthetic polymer scaffold (right) produced from PCL using multiple fabrication methods, with zonal microstructure for stratified cartilage repair, image adapted with permission from Ref. [99]. Figure created using Canva.

properties [118,119]. An emerging design approach for biomimetic cartilage scaffolds is to blend different types of natural polymers to achieve combinational properties. For example, one study used combinations of chitosan, collagen, hyaluronic acid, and silk fibroin to construct a bilayered chondral scaffold by freeze-drying, with different material composition and porous structure in the surface and transitional layers [20].

Other natural polymers commonly chosen to fabricate cartilaginous scaffolds include naturally derived proteins such as collagen and silk fibroin, partly due to their natural ability to enhance cell adhesion. Collagen, including the frequently used types I and II, is an abundant protein in mammals that can be derived from bovine, porcine, or even human tissues. Collagen is applied extensively in cartilage and bone tissue engineering, where one method to modulate region-specific properties is by varying the content of different types of collagens [120–122]. Silk fibroin, most commonly extracted from *Bombyx mori* cocoons, is a potent and newer type of natural polymer used for regenerating cartilage and bone tissues [123]. Silk scaffolds often possess superior mechanical strength, accompanied by a tailorable chemical structure and good bioactivity, elasticity, and degradability [124]. For scaffold fabrication, silk fibroin is usually dissolved in water-based solvents and can be easily reconstructed into a variety of formats, including films, mats, hydrogels, and sponges, through a range of techniques such as self-assembly, ultrasonication, pH adjustment, freeze-drying, and physical or chemical crosslinking [125]. Interestingly, one study reported that a nanoengineered silk surface with nanopillar arrays could regulate stem cell morphology, leading to a flattened ellipsoidal shape consistent with the appearance of chondrocytes in the superficial zone of articular cartilage [124]. A combination of collagen and silk fibroin could produce scaffolds with improved biological and mechanical properties compared to individual materials, for example, a hybrid scaffold with optimised ratio of 7:3 collagen/silk fibroin was shown to achieve efficient repair in a rabbit model of full-thickness cartilage defects [97].

3.3.2. *Decellularised extracellular matrix*

Decellularised extracellular matrix (dECM) has recently gained increasing interest as a new type of scaffolding material that is naturally derived from the ECM produced by cells and subsequently have the cells removed. dECM retains the intrinsic biochemical and biophysical cues of native ECM, providing structural and chemical signals that regulate cellular behaviour, such as adhesion, migration, proliferation, and differentiation [126–128]. Biochemical cues may include structural proteins, peptides, cytokines, and growth factors, while biophysical properties are conveyed by 3D structure, porosity, and mechanical properties akin to native tissue [126,129].

Several studies have demonstrated the potential of dECM materials in cartilage tissue engineering, although they have not yet been utilised for constructing cartilage scaffolds with zone-specific structure. Peng et al. [98] fabricated a human articular cartilage-derived ECM scaffold, validating its capacity to support the survival, proliferation, migration, and maintenance of the human chondrocyte phenotype *in vitro*. *In vivo* experiments showcased the ability of the scaffold to independently repair articular cartilage in a large animal (sheep) model when combined with microfracture technique. When combined with injection of IL-4 to induce M2 macrophage polarisation, Tian et al. [130] showed that a decellularised cartilage matrix scaffold could induce cartilage regeneration as well as provide immunomodulatory effects in a rat osteochondral defect model. Browe et al. [131] developed decellularised cartilage ECM-derived scaffolds crosslinked using glyoxal and dehydrothermal treatment. These scaffolds supported cartilage ECM synthesis when seeded with fat pad-derived stromal cells and displayed high elastic properties in compression tests. Another group [132] also showed that the mechanical properties of dECM scaffolds could be significantly enhanced through the integration of electrospun nanofibers. Li et al. [133] developed an injectable hydrogel composed of cartilage dECM and hyaluronic acid methacrylate (HAMA). This hydrogel demonstrated robust adhesion strength to cartilage and significantly enhanced mechanical performance compared to cartilage dECM or HAMA alone. *In vitro* cultures showed that the hybrid hydrogel promoted chondrogenic differentiation of encapsulated porcine bone marrow MSCs after 21 days. *In vivo* subcutaneous implantation in a mouse model further illustrated improved biocompatibility of the hybrid hydrogel compared to HAMA alone. Li et al. [134] developed a bioinspired hydrogel scaffold produced by 3D printing with cartilage and bone dECM. When constructed as a bilayer hydrogel with tissue-specific dECM in the respective layers and supplemented with human MSC-derived exosomes, these hydrogel scaffolds accelerated the simultaneous regeneration of cartilage and subchondral bone tissues in rat osteochondral defects.

3.3.3. *Synthetic polymers*

A wide range of synthetic polymers can be used for osteochondral tissue engineering, sometimes with highly customised composition, but mostly involve polyethylene glycol (PEG), polyvinyl alcohol (PVA), polycaprolactone (PCL), and polylactic acid and its co-polymers (PLA, PLLA, PLGA) [100,135]. In particular, PCL has been a popular choice for fabricating the scaffold frame to realise various zonal cartilage designs, mainly due to its mechanical integrity and compatibility with 3D

printing fabrication techniques for producing customisable structures [99,136,137]. In general, due to their reproducible and tailorable chemical structure, synthetic polymers offer more precise control over scaffold characteristics compared to naturally derived materials, including mechanical stiffness, porosity, and degradation rate. However, their drawbacks include poor cell adhesion, potential immune response or adverse reactions upon implantation, and lack of inherent bioactive cues that facilitate cell signalling, ECM production, and tissue integration. Due to the substantially different properties required of materials for constructing chondral and osteochondral scaffolds, polymeric blends or co-polymers, as well as composites or hybrid materials formed through combination with other biomaterial classes, are commonly employed to fabricate biomimetic scaffold layers [96,138]. In combination with advanced manufacturing techniques such as digital light processing (DLP), scaffolds with specially designed mechanical property gradients can be constructed using synthetic polymers. For example, a photopolymerisable PEG diacrylate (PEGDA) hydrogel printed into a micro-truss structure and infiltrated with PEG-norbornene hydrogel to form composite trusses could exhibit regional stiffness variations within the scaffold ranging from 0.3 to 1.1 MPa, which is potentially useful for mimicking the differing mechanical properties between cartilage and bone in osteochondral tissue [139].

3.3.4. Bioceramics

Bioceramics are renowned for their excellent wear resistance, high stiffness, resistance to oxidation, and low friction coefficient, making them particularly suitable for bone tissue engineering [140]. Various modifications and fabrication processes can be applied to enhance the properties of bioceramics for use as the bone component of an osteochondral scaffold, for example, a biomimetic bone scaffold with stress transfer capability can be constructed by creating a biopolymer-bioceramic composite, using a coupling agent that serves as a 'molecular bridge' to establish interfacial reinforcement between materials [141]. With recent advances in additive manufacturing, 3D-printed bioceramic scaffolds can be constructed with diverse compositions and hierarchical structures, allowing precise control over their mechanical, degradation, permeability, and biological properties [142]. Through composite processing to modulate their elastic and other mechanical properties, bioceramics can also be applied in cartilage tissue regeneration, such as through the construction of a collagen/nano-β-tricalcium phosphate scaffold [143]. Although the majority of bioceramics used in osteochondral scaffolds are artificially made, emerging approaches have also considered naturally-derived bioceramics derived from marine organisms such as sponges, corals, or seashells [144].

Hydroxyapatite, $Ca_{10}(PO_4)_6(OH)_2$, which has the same composition as the mineral component of bone, is a popular bioceramic used as bone grafts or coatings on orthopaedic implants due to its excellent biocompatibility and osteoconductivity [145]. Recent research has explored new methods to enhance the mechanical properties of this material towards load-bearing bone regeneration, for example, an interesting study generated 3D-printed hydroxyapatite scaffolds with greatly improved compressive strength through a triply periodic minimum surfaces (TPMS) design, characterised by unique non-self-intersecting, 3D periodic surface structures [146].

Bioactive glasses, composed mainly of silicon oxide, sodium oxide, calcium oxide, and phosphate, offer both osteoconductivity and osteoinductivity due to their ability to bond with both hard and soft tissues. A recent study has highlighted the applicability of bioactive glass-ceramic particles in long-term cartilage repair and promoting progressive bone growth, providing durable mechanical support to prevent late-stage cartilage collapse [147]. Other formulations of silicate-based bioceramics also exhibit excellent bioactivity and possible applications in subchondral bone and osteochondral tissue engineering [148,149].

3.3.5. Metallic scaffolds

Metal materials and their alloys are widely used in bone implants, with a long history of clinical application due to their biocompatibility, excellent corrosion resistance, and exceptional mechanical strength. In osteochondral tissue engineering, adopting a metallic subchondral bone scaffold can easily provide the essential mechanical support for articular cartilage repair to proceed under load-bearing conditions [61,150]. Titanium scaffolds were among the first metallic scaffolds considered for repairing osteochondral tissues, which can be made to match the properties of trabecular bone and provide sufficient space for bone ingrowth by altering their geometric structures [74] and porosities [151]. One interesting study designed a functionally graded porous lattice structure for a titanium bone scaffold with varying stiffness and density, providing spatial control of scaffold properties, which was fabricated using selective laser sintering (SLS) [152], as shown in Fig. 5A. The flexible chondral phase was a homogenous thin layer sponge fabricated through a sugar-leaching process, using a PDMS matrix and sugar as porogen, which was interlocked to the titanium scaffold during PDMS polymerisation. Although the assembled construct was able to support MSC growth and cellular communication, the distinct cartilage and bone layers were not well integrated. Addressing this problem, another study designed a tri-layered integrated osteochondral scaffold containing a titanium mesh cage as the bone scaffold [153]. Using 3D printing, PLGA hydrogel was directed printed on the titanium mesh to form a 30 μm dense layer, followed by porous PLGA layers with 100 μm pore size to form the cartilage region, as shown in Fig. 5B. Chondrocytes were then seeded into the cartilage scaffold, while autologous cancellous bone was filled into the titanium mesh to form the bone scaffold. This created an integrated scaffold structure, where the interfacial dense layer between cartilage and bone regions could inhibit the growth of new cartilage into the subchondral bone, and also shield the cartilage from excessive compression-related damage. *In vivo* study in a goat cartilage defect demonstrated the scaffold's ability to reconstruct a homogeneous and smooth articular surface. Additionally, the tidemark area between native cartilage and subchondral bone was observed to coincide with the location of the intermediate dense layer in the scaffold. Other approaches have been used to create bionic osteochondral scaffolds featuring a dense interfacial layer and a titanium base scaffold [72,154], as presented in Fig. 5C. The dense layer was shown in sheep osteochondral models to prevent bone marrow from flowing into the cartilage region or synovial components from flowing into the bone region, ensuring separate osteogenesis and chondrogenesis.

Recent studies have demonstrated heightened interest in metallic materials as tissue engineering scaffolds by shifting from non-biodegradable to biodegradable metals, which include three main types: magnesium (Mg), iron (Fe), and zinc (Zn) [73]. Magnesium-based materials are susceptible to excessively high degradation rates, and hydrogen emissions from the degradation process can alter the peri-implant pH, potentially interfering with osteoblast survival and bone formation [93]. Iron-based materials have a longer degradation time than natural tissues, potentially hindering complete tissue repair [155]. Zinc-based materials exhibit a reasonable degradation rate, potential to provide essential trace elements, and minimal effect on changing environmental pH during degradation [94]. A recent study designed a biodegradable bilayered scaffold comprising a porous zinc scaffold and chondroitin sulphate hydrogel for full-thickness osteochondral tissue reconstruction [156], as presented in Fig. 5D. The zinc scaffold provided a favourable degradation rate, offering long-lasting mechanical support as well as eventual complete degradation. In a porcine osteochondral defect model, the bilayered scaffold achieved reconstruction of a smooth hyaline-like cartilage surface and superior integration with surrounding host tissues.

3.4. Fabrication strategy

Fabrication strategies to create biomimetic osteochondral scaffolds

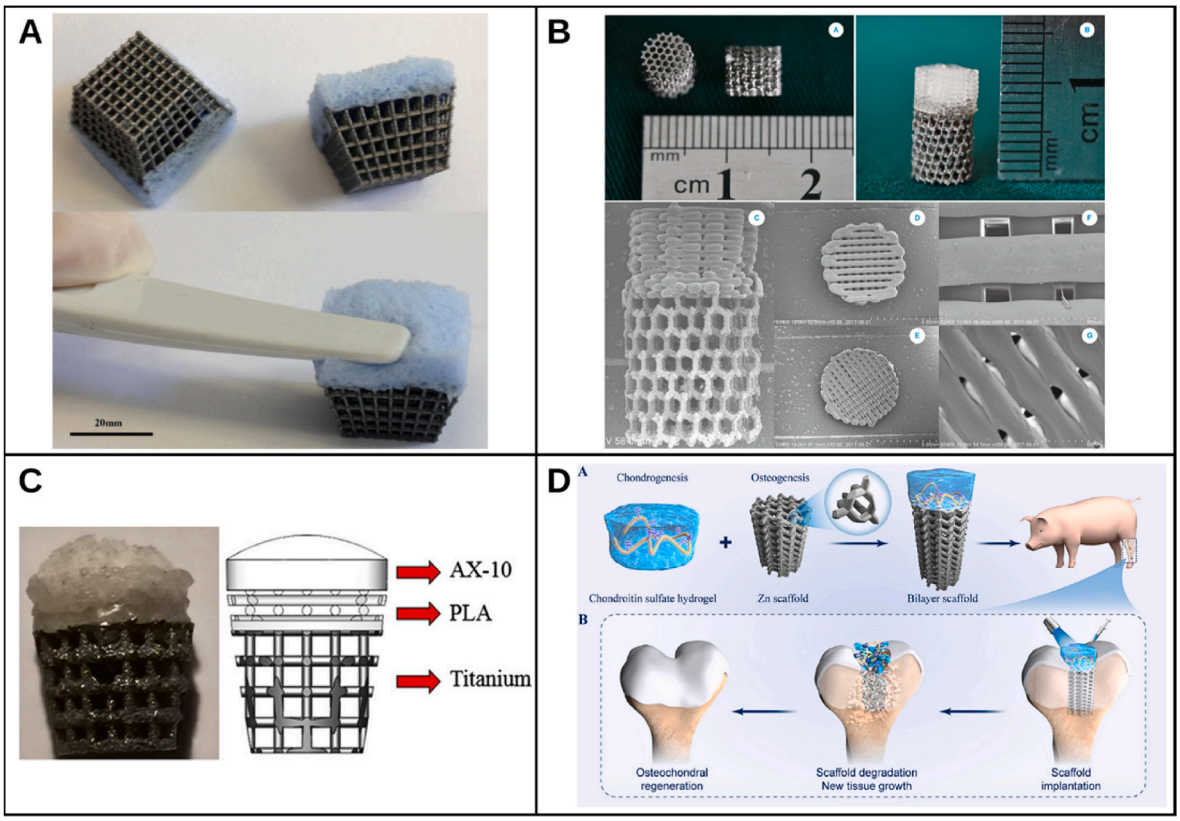

Fig. 5. Composite osteochondral scaffolds with a metallic bone component. **(A)** Bilayer osteochondral scaffold combining gradient titanium lattice scaffold and PDMS sponge, adapted with permission from Ref. [152]. **(B)** Tri-layered scaffold comprising a base titanium mesh cage and PLGA hydrogel, adapted with permission from Ref. [153]. **(C)** Multi-layer gradient osteochondral scaffold with titanium base, PLA intermediate layer and PLGA top layer, adapted with permission from Ref. [154]. **(D)** Biodegradable bilayered scaffold comprising porous zinc scaffold and chondroitin sulphate hydrogel, adapted with permission from Ref. [156].

have mainly involved the generation of fibrous or hydrogel structures for the articular cartilage compartment, which may or may not be reinforced with a subchondral bone compartment that provides higher stiffness and mechanical support. A variety of techniques may be used alone or in combination to realise scaffold designs that faithfully mimic the different components of osteochondral tissue, including the articular cartilage with zonal structure, interfacial calcified cartilage, and subchondral bone with high mechanical strength. Particularly for the cartilage component, fabrication methods have focused on precisely controlling fibre orientation in fibrous scaffolds or constructing compositional gradients in hydrogel scaffolds to produce zonal architecture and properties.

Traditionally, osteochondral and other types of tissue engineering scaffolds were fabricated using methods such as sol-gel [157,158], gas foaming [159,160], and emulsion freeze drying [161]. However, these methods were typically complex and time-consuming, providing low efficiency of tissue regeneration as well as inconsistent repair outcomes in osteochondral injuries. This was due to the lack of precise and spatial control over scaffold geometry, including porosity, pore size, and pore shape/distribution, leading to the inability to faithfully mimic original tissue structure, such as the depth-dependent zonal layers within articular cartilage, and the highly porous and interconnected but mechanically robust structure of subchondral bone.

Mould casting is a simple and versatile method compared to other approaches, which involves pouring a mixture of materials into a mould followed by gelling to create a wholesome scaffold. This method can create multi-layered scaffolds by sequentially casting the layers and adjusting the material composition of each layer [56,162]. Mould casting allows a high degree of control over the scaffold's final shape and dimensions. However, drawbacks include limited precision in the control of gradients, porosities, material properties, and manufacturing details.

Electrospinning involves charging a polymer solution and directly writing the scaffold by depositing micro- or nano-scale fibres [163,164]. A fibrous mesh can hence be created that mimics the topography of native ECM, with adjustable porosity, pore interconnectivity, mechanical characteristics, and surface area. The fibrous sheets can also be layered to form multi-layered scaffolds with spatial variation in structure or material composition.

3D printing, a form of additive manufacturing, is commonly employed in current osteochondral scaffolds due to its high precision, enabling biomimetic and patient-specific designs through layer-by-layer printing [165]. Integrated with computer-aided design, it enables the fabrication of complex and customisable structures with potential to closely mimic the multizonal and hierarchical nature of osteochondral tissue [166–169]. However, several limitations remain including equipment cost, printing speed, and frequent need for post-processing to enhance mechanical or biological characteristics. Moreover, material selection may be limited, particularly in extrusion-based approaches due to problems with nozzle clogging, as well as in 3D bioprinting that involves the simultaneous incorporation of cells or biomolecules, essentially limiting choices to hydrogel materials [170,171].

Other fabrication strategies are defined by the unique properties of certain materials, such as freeze-thaw physical crosslinking [172–175] and freeze-casting [176] for PVA hydrogels. To create region-specific properties, fabrication techniques may also be combined with approaches involving self-assembly and response to external stimuli such as magnetism, light, pH, and temperature [177]. While attempting to create a biomimetic, stratified structure, the selection of manufacturing method for osteochondral scaffolds should also consider processing complexity and reproducibility in sight of scale-up applications.

3.5. Biomimetic bilayered osteochondral scaffolds and the push towards biomimetic multizonal cartilage scaffolds

Conventional scaffolds with single-layer structure and homogeneous properties are generally insufficient in meeting the functional requirements for restoring the osteochondral tissue unit. Bilayered scaffolds first evolved to address varying requirements of regeneration for interfacial tissues, comprising two distinct but integrated layers that can respectively support different types of tissue formation such as cartilage and bone [178]. From earlier designs largely involving the integration of two separately fabricated homogeneous layers, biomimetic bilayered scaffolds have evolved to incorporate sophisticated designs that more closely mimic the stratified structure of native osteochondral tissue. For example, Zhu et al. [179] developed an injectable bilayer osteochondral scaffold with stratified biomimetic structure, comprising a thermosensitive sodium alginate/agarose composite hydrogel as the cartilage layer and a sodium alginate/bioglass composite hydrogel as the bone layer, which encapsulated different cell types. This was found to induce region-specific cartilage and bone formation in a rat osteochondral model while maintaining integration between layers and benefitting from a minimally invasive approach for scaffold implantation. Similarly addressing interlayer integration challenges, Gan et al. [180] produced a mussel-inspired osteochondral scaffold comprising a bilayered gelatine methacryloyl-polydopamine hydrogel. The cartilage and bone layers were seamlessly integrated through simultaneous polymerisation, respectively containing immobilised TGF-β3 and bone morphogenetic protein 2 (BMP-2), together with mineralised hydroxyapatite reinforcement in the bone layer. This biomimetic design was seen to promote osteochondral repair in a rabbit full-thickness cartilage defect. Also tested in rabbits, Zhou et al. [181] developed a biphasic scaffold using fish collagen to enable simultaneous cartilage and bone repair, where the cartilage layer comprised chondroitin sulphate-incorporated fish collagen with 128 μm pores and the bone layer was a fish collagen-hydroxyapatite scaffold with 326 μm pores.

Newer bilayered scaffolds have built on hydrogel-based strategies to address specific challenges in osteochondral tissue repair. For instance, one notable challenge is the integration of newly formed cartilage within the scaffold with surrounding native cartilage. In this space, Wu et al. [182] developed a methacrylated silk fibroin (Sil-MA) sealant containing TGF-β3, with adhesive properties and the ability to chondrocyte migration and differentiation. This was used to provide 'marginal sealing' around a bilayer silk scaffold in rabbit osteochondral defects, which together achieved regeneration with superior lateral tissue integration. Jiang et al. [183] also used Sil-MA in their bilayered scaffold design, creating two integrated Sil-MA hydrogel layers through stratified photocuring, which served as a base matrix for the incorporation of silk fibroin microspheres. By loading the microspheres with kartogenin and berberine and anchoring them within the respective cartilage and bone layers, this all-silk bilayered scaffold achieved osteochondral repair in a rat model after 8 weeks of implantation. Another notable challenge lies in the generally insufficient mechanical properties of osteochondral scaffolds for promoting tissue regeneration in load-bearing regions. To achieve better mechanical reinforcement, Liu et al. [184] employed a 3D-printed porous hydroxyapatite ceramic platform that releases alendronate for promoting bone regeneration. This was integrated with a mechanically enhanced hyaluronic acid methacryloyl hydrogel that releases kartogenin as the cartilage layer, through a semi-immersion approach. This scaffold was found to encourage region-specific cartilage and bone formation during rat subcutaneous implantation, although tissue regeneration under load-bearing conditions remains to be tested. Also using 3D printing, Gao et al. [185] fabricated a high-strength supramolecular polymer hydrogel as the basis for a bilayered osteochondral scaffold. The hydrogel mechanical properties were significantly enhanced by photo-initiated polymerisation to combine poly (N-acryloyl 2-glycine) (PACG) with gelatin methacrylate (GelMA), greatly superceding the ranges achievable with conventional GelMA hydrogels. A bilayered gradient structure was created by doping the cartilage layer with Mn^{2+} ions and the bone layer with bioactive glass, which was found to enhance osteochondral repair after 12 weeks of implantation in a rat model.

Biomimetic bilayered osteochondral scaffolds have generally demonstrated the ability to facilitate differential chondrogenesis and osteogenesis in the respective layers, and have provided important insights into the significance of scaffold microenvironment on lineage-specific tissue differentiation during osteochondral regeneration. However, the bilayered design encounters key challenges in recreating physiologically meaningful biomimetic structure, particularly in the articular cartilage compartment. Firstly, there is a lack of biomimetic transition between the hyaline cartilage and subchondral bone regions due to the absence of a calcified cartilage layer, leading to an increased risk of fracture between discrete scaffold regions [186]. Secondly, bilayered scaffolds have a homogeneous cartilage region that does not mimic zonal variations in the chondral matrix, including its depth-dependent gradient in collagen fibre organisation, GAG composition, pore size, and mechanical strength, as well as differences in chondrocyte morphology and arrangement. Recently, a variety of innovative approaches have emerged for creating biomimetic multizonal cartilage scaffolds to address these challenges.

4. Biomimetic multizonal cartilage scaffolds with zone-specific variation in scaffold properties

Biomimetic multizonal scaffolds are designed to reflect the anatomical microstructure of articular cartilage and its stratified regions, ideally comprising three or more distinguishable but continuous layers. These scaffold designs may fulfil the unique zonal property requirements for faithful articular cartilage regeneration, through depth-dependent modifications in collagen fibril orientations, matrix architectures, biomechanical properties, cell properties and phenotypes, and zone-specific growth factors. Current studies reporting biomimetic zonal cartilage scaffolds have mainly adopted three types of stratification approaches: fibre orientation, composition or porous architecture, and cell types and growth factors, as summarised in Table 2.

4.1. Creating zonal cartilage structure by varying fibre orientation

A central feature of zonal variation in native articular cartilage is collagen fibril orientation. The alignment of collagen fibres is the primary determinant to the region-specific mechanical properties and functionality of hyaline cartilage, providing a smooth and wear-resistant surface in the superficial layer and changing to more randomly aligned and interwoven fibres in the transition zone to provide better load-bearing properties, as well as to vertical fibre orientation in the deep zone for anchoring the cartilage in underlying mineralised tissues. Because of its capability to easily produce nanofibrous sheets mimicking the structure of native ECM, electrospinning has been commonly explored as a fabrication technique for creating biomimetic osteochondral scaffolds, initially as bilayered structures replicating the cartilage-bone interface [187,188]. However, a typical electrospun fibre mat has randomly distributed and oriented polymer fibres that may resemble the transition zone of articular cartilage but do not include characteristics of the superficial or deep zones, and also do not provide good adherence to the bone component scaffold. To create a more functionally graded scaffold resembling osteochondral tissue layers, including zonal variations in articular cartilage, Hejazi et al. [189] used electrospinning to fabricate a nanofibrous scaffold with five layers comprising different ratios of raw materials: PCL/gelatin and chitosan/PVA for the chondral layers, and PCL/gelatin with incorporated nanohydroxyapatite for the bony layers. The scaffold showed variation in fibre composition and porosity accompanied by smooth transition between layers, mimicking to some extent the change in matrix composition along the

Table 2
Summary of studies on multizonal cartilage scaffolds, broadly categorised by variations in fibre orientation, composition or pore architecture, and cell types or growth factors.

Type	Scaffold name	Fabrication method	Zonal structure		Main findings		Reference
			Cartilage scaffold features	Other features (e.g., bone)	Structural & mechanical characterisations	*In vitro* and *in vivo* study	
Fibre orientation	Bi-layered micro-fibre reinforced hydrogels	Melt electrospinning writing (MEW)	**Materials**: Soft gelatine-methacrylamide (GelMA) hydrogel embedded, melt electrospun written polycaprolactone (PCL) fibre scaffold **Bi-layered structure:** •Superficial tangential zone (STZ): Densely distributed crossed fibre mat, with tightly packed and tangentially oriented fibres (alternating angles: 0–45–90–135°) •Middle and deep zone (MDZ): A uniform box structure fibre organisation (cross-shaped 0–90° lay-down pattern)	N/A	**Pore size (fibre spacing):** •STZ: ~50 mm •MDZ: ~800 mm •Fibre diameter ~20 mm **Mechanical properties:** •Composite constructs with a thin STZ layer exhibited significantly higher peak modulus under incongruent and congruent loading conditions than hydrogels reinforced solely with a uniform MDZ structure. •The bi-layered composite constructs demonstrated a stress relaxation response similar to that of native cartilage tissue. •The STZ layer notably influenced the mechanical behaviour of the composite constructs under incongruent loading. •Capable of simulating native cartilage and supporting neo-cartilage formation upon physiologically relevant mechanical stimulation. •The STZ layer might play a more critical role under dynamic compression.	***In vitro* study** **Cells:** Chondrocytes from cartilage of equine metacarpophalangeal joints **Time period of *in vitro* culture:** 28 days **Findings:** •STMDZ-reinforced hydrogels can support cartilaginous tissue formation upon physiologically relevant mechanical stimulation. •Hydrogel mechanical failure under dynamic loading indicates limited dynamic mechanical properties.	(Castilho et al., 2018; Castilho et al., 2019) [192,193]
	3D anisotropic tri-layered fibrous scaffolds	Electrospinning Layer-by-layer assembly	**Materials**: PCL-GO-collagen scaffold •Electrospun layers: Polycaprolactone (PCL) •Framework: Graphene oxide-collagen (GO-collagen) **Tri-layered structure:** •Superficial Layer: Fibres aligned parallel to the top surface of the scaffold. •Middle Layer: Random orientation of collagen fibres, the transition zone between the superficial and deep zones. •Deep Layer: Spiral-shaped, electrospun mesh rectangles, cut and rolled into cylinders, formed a vertically oriented fibrous network akin to natural cartilage tissue.	N/A	**Morphology:** •Superficial layer: fibre diameter of 1.20 ± 0.51 μm, 68 % of pores with diameters between 5 and 10 μm and 16 % of pores with sizes superior to 10 μm; •Middle layer: larger fibre diameter (2.00 ± 0.63 μm) and bigger pores as 53 % of pores between 5 and 10 μm and 31 % of pores with a diameter superior to 10 μm •Deep layer: larger pores to facilitate nutrient and oxygen transport, waste removal, and cell attachment. **Mechanical properties:** •The compression modulus varied with the direction of	N/A	(Girão et al., 2018) [194]

(*continued on next page*)

Table 2 (*continued*)

Type	Scaffold name	Fabrication method	Zonal structure		Main findings		Reference
			Cartilage scaffold features	Other features (e.g., bone)	Structural & mechanical characterisations	*In vitro* and *in vivo* study	
					fibre arrangement, decreasing from vertical to random to horizontal. •When the direction of the force was perpendicular to the direction of the fibres/ pores, the resistance to deformation was low.		
	Multizone scaffold	Electrospinning and Cryo-printing	**Materials**: Polycaprolactone (PCL) as base scaffold. **Tri-layered structure:** •Top layer (aligned fibres): Highly aligned fibres resembling cartilage's superficial zone. •Middle layer (randomly oriented fibres): Randomly deposited fibres on cryo-printed helix scaffolds. •Bottom layer (helix structure): PCL, providing interconnected architecture and compressive support, mimicking cartilage's deep zone.	N/A	**Fibre diameter & pore size:** •Top zone aligned fibre diameter: 1.57 ± 0.50 μm •Middle zone random fibre diameter: 1.94 ± 0.51 μm •Bottom zone helix scaffold pore size: 3.62 ± 2.46 μm **Mechanical Properties:** •The multizone scaffolds showed slightly higher compressive properties than the electrospun control scaffolds. •Compressive properties remained consistent over the 4-week culture period and were similar to acellular controls across all tested strains.	***In vitro* study** **Cells:** Primary human adult chondrocytes **Time period of *in vitro* culture:** 5 weeks **Time frame for culture:** 24 h, 1 week, 3 weeks, 5 weeks **Findings:** Multizone scaffolds maintained chondrocyte phenotype and function and demonstrated their potential in cartilage tissue engineering applications.	(Munir et al., 2020) [195]
	Microribbon (μRB) scaffold	Hydrogel: mould casting μRBs: wet-spinning	**Materials:** •Hydrogel: Gelatine (GEL) methacrylate, chondroitin sulphate (CS) methacrylate •μRBs: gelatine (GEL) μRBs **Spatially-patterned tri-layered scaffold:** •Superficial zone:100 % gelatin, aligned μRB •Middle zone: 90GEL:10CS Deep zone: 75GEL: 25CS	N/A	**Mechanical properties:** •Trilayer μRB scaffolds showed a significant increase in compressive modulus from superficial to deep zones, mirroring native cartilage. •Deep zones of μRB scaffolds exhibited a remarkable over 34-fold increase in compressive modulus, approaching values of native articular cartilage (464 kPa and 452 kPa for μRB and μRB + aligned cultures, respectively). •Trilayer hydrogel (HG) scaffolds displayed only a marginal increase in compressive modulus in deep zones after 21 days, remaining significantly lower than native cartilage. •Interfacial shear strength of trilayer μRB scaffolds significantly surpassed that of trilayer HG scaffolds.	***In vitro* study** **Cell/scaffold type:** MSC-seeded trilayer microribbon (μRB) **Cells:** Human MSCs **Time period of *in vitro* culture:** 21 days **Findings:** Trilayer μRB scaffolds maintained high cell viability throughout the culture. •Trilayer μRB scaffolds promoted significant cartilaginous ECM deposition by MSCs, with increasing sGAG production from superficial to deep zones. •Aligned μRB scaffolds enhanced ECM deposition, with a notable increase in sGAG content and collagen production, particularly in the superficial zone. •Varying the ratio of gelatin to chondroitin sulphate μRBs within the scaffold could impact MSC chondrogenesis, guiding zonal-specific differentiation. Trilayer μRB scaffolds enabled MSCs to produce zonal-specific	(Gegg & Yang, 2020) [190]

(*continued on next page*)

Table 2 (*continued*)

Type	Scaffold name	Fabrication method	Zonal structure		Main findings		Reference
			Cartilage scaffold features	Other features (e.g., bone)	Structural & mechanical characterisations	*In vitro* and *in vivo* study	
					Both μRB groups (with and without aligned μRB layer) were able to withstand shear stress greater than 100 kPa before failure, whereas the HG groups fractured with just 7.5 kPa of shear stress applied.	cartilage with biochemical and morphological properties closely resembling native tissue. Observed in native cartilage.	
	Mesenchymal stem cells loaded 3D-printed gradient PCL/ALMA composite scaffold.	3D printing	**Materials:** •Poly (ε-caprolactone) (PCL) impregnated with methacrylate alginate (ALMA) •Embedded rat bone marrow mesenchymal stem cells (BMSCs), Cell density: 3×10^5 cells/ml **Tri-layered PCL/ALMA scaffolds:** Depth-dependent gradient, with 0°/90°, 0°/60°, and 0°/30° lay-down pattern respectively, mimicking chondral zonal layers	N/A	**Pores**: •Superficial layer: filament gap of 300 μm, 0°/90° lay-down pattern •Middle layer: filament gap of 500 μm, 0°/60° lay-down pattern •Deep layer: filament gap of 700 μm, 0°/30° lay-down pattern **Mechanical properties gradient:** •SL: tensile modulus 61.57 ± 2.05 MPa and compressive modulus 20.44 ± 1.32 MPa •Compressive modulus were SL-PMA > PCL/ALMA-gradient > ML-PMA > DL-PMA •The compressive modulus of the entire PCL/ALMA gradient scaffold was 9.52 ± 1.79 MPa	***In vitro* study** **Cells:** BMSCs from bone marrow extracted from the femora and tibiae of 6-week-old male Sprague-Dawley rats **Time period of *in vitro* culture:** Day 1, 3, 7 for cell proliferation assessment, 3 weeks of chondrogenic culture for gene expression analysis **Findings:** •PCL/ALMA hybrid scaffolds exhibited excellent compatibility with rat BMSCs. ALMA furnished an appropriate cartilage-growth microenvironment, with evidence of some larger cell masses and homogeneous distribution.	(Cao et al., 2021) [113]
	Bio-inspired cellulose-reinforced anisotropic composite hydrogel	Mould casting, sequential hydrogel layering	**Materials:** •Polyethylene glycol diacrylate (PEGDA): Primary polymer matrix for hydrogel •Cellulose fibres: Structural reinforcement **Three-zone structure:** •Superficial zone: Cellulose fabric fibres, oriented parallel to the surface •Middle zone: Cellulose nanofibres, randomly distributed •Deep Zone: Wood cellulose fibres, oriented perpendicular to the surface .	N/A	**Pores:** •No numerical values for pore size in the superficial and middle zones •Deep zone has distinct microstructures depending on whether they are cut from hardwood or softwood: -Softwood: Square interlaced hollow channels, with widths 10–40 μm and average lengths 3–5 mm -Hardwood: Aligned hollow cellulose channels with gradient circular apertures, from a few to several tens of microns **Mechanical properties:** Zone-dependent complex mechanical adaptability •Superficial zone: Resists shear forces. Compressive modulus ~298 kPa. Modulus	***In vitro* study** **Cells:** BMSCs **Time period of *in vitro* culture:** 3 days (cell morphology), 7 days (cell proliferation assessment), 14 days (chondrogenic differentiation evaluation) **Findings:** •BMSCs showed alignment along the cellulose channels, indicating that anisotropic hydrogel structure could guide cell orientation. BMSCs showed good adhesion and growth on hydrogel surfaces. •Hydrogel could promote chondrogenic differentiation of BMSCs, where cells in the superficial zone produced significantly higher levels of collagen II compared to the deep zone.	(Wang et al., 2020) [62]

(*continued on next page*)

Table 2 (*continued*)

Type	Scaffold name	Fabrication method	Zonal structure		Main findings		Reference
			Cartilage scaffold features	Other features (e.g., bone)	Structural & mechanical characterisations	*In vitro* and *in vivo* study	
					and stress increase with adding more layers of cellulose fabric. •Middle zone: Cushion to absorb forces from superficial zone. Compressive modulus ~182 kPa. Exhibits clear nonlinear compression behaviour, with modulus increasing slowly at low strain and rapidly at high strain. •Deep zone: Transfers force to subchondral bone. Compressive modulus significantly higher at ~9.8 MPa due to reinforcement by cellulose network. Anisotropic mechanical properties with higher compressive modulus and stress in longitudinal compared to radial direction.		
	Hypotrochoidal scaffolds	Fused Deposition Modelling (FDM) technology through a bioprinter.	**Material**: Poly (ε-caprolactone) (PCL) **Arch-like Structure:** •Hypotrochoidal Design: Mimicked collagen fibres in cartilage using curved patterns generated by smaller circles rolling inside larger ones. •Zone Division: Divided the scaffold into superficial, middle, and deep zones, replicating cartilage composition and cell density variations. •Pore Structure: Created gradient pores, with the smallest in the superficial zone and the largest in the deep zone, mimicking cartilage heterogeneity for nutrient transport.	N/A	**Mechanical Properties** •Scaffold with r = 0.17 showed Young's modulus similar to native cartilage, making it less stiff than the 0–90 woodpile design (14.1 MPa). •Yield strain and strength of r = 0.17 scaffold ranged from 7.9 ± 0.0 % to 11.0 ± 2.6 %, indicating its ability to withstand deformation. •r = 0.17 design exhibited significantly higher toughness (0.035 ± 0.001 N mm^2) than other designs, crucial for load-bearing tissues like cartilage.	***In vitro* study** **Cells:** ATDC5, a teratocarcinoma-derived chondrogenic cell line **Time period of *in vitro* culture:** 28 days **Findings:** •r = 0.17 scaffold in dynamic culture showed increased collagen type II deposition, promoting cartilage-specific protein synthesis. •Reduced expression of collagen type X suggests that the design may prevent hypertrophic changes detrimental to cartilage regeneration. •Higher stress areas in the scaffold exhibited increased glycosaminoglycan (GAG) synthesis, essential for cartilage function. •Enhanced cell proliferation and potential tissue regeneration indicated by increased DNA content per pore volume in r = 0.17 samples under dynamic stimulation.	(van Kampen et al., 2023) [137]
	Biomimetic arch-like 3D bioprinted construct	3D bioprinting, directed printing, photo-crosslinking	**Materials:** Gelatine Methacryloyl (GelMA) and Silk Fibroin-Gelatine (SF-G) bioinks **Arch-like structures:**	N/A	**No information about pore size** **Mechanical properties:** (no details about mechanical	***In vitro* study** **Cells:** Human bone marrow MSCs **Time period of *in vitro* culture:** 21 days	(Chakraborty et al., 2023) [208]

(*continued on next page*)

Table 2 (*continued*)

Type	Scaffold name	Fabrication method	Zonal structure		Main findings		Reference
			Cartilage scaffold features	Other features (e.g., bone)	Structural & mechanical characterisations	*In vitro* and *in vivo* study	
			•Arch-like Structure: Mimicked collagen II arrangement in native cartilage, replicating its layered characteristics: superficial, middle, and deep zones. •Layered Design: Varying porosities and fibre orientations in each layer simulate cartilage's natural structure and function. •Biomimetic Approach: Imitating cartilage's microstructure and biochemistry created a natural environment for chondrocytes, enhancing proliferation and differentiation.		properties values): •The selection of bioinks (GelMA and SF-G) and the arch-like scaffold design, aimed to mimic the mechanical properties of native cartilage. •The arch-like architecture likely enhanced organised and anisotropic mechanical behaviour, resembling natural cartilage.	**Time frame for culture:** 1, 7, and 21 days (gene expression analysis); 7 and 21 days (immunofluorescence, histological analysis) **Findings:** •SF-G constructs exhibited higher encapsulation efficiency and proliferation rates, along with a more uniform distribution of human bone marrow-derived mesenchymal stem cells (BM-MSCs) compared to GelMA constructs. •SF-G demonstrated superiority in forming a fibrous collagen network, promoting chondrogenesis, and facilitating the production of cartilage-specific extracellular matrix. •SF-G enabled the creation of 3D bioprinted arch-like structures for cartilage regeneration and regulation of the Wnt/β-catenin and TGF-β signaling pathways.	
Composition or porous architecture	A biomimetic cartilage gradient hybrid scaffold	Mould-casting, freeze-drying	**Materials:** A combination of chitosan (Cs), sodium β-glycerophosphate (GP), and gelatin (Gel) **Zonal porous design:** Gradient porous scaffolds were designed with varying pore sizes along the longitudinal dimension, smaller in the superficial zone and larger in the deep zone.	N/A	**Porosity:** Optimal cartilage defect repair was observed with a Cs:GP:Gel ratio of 9:1:5 with porosity at 95.2 %. **No information about mechanical properties**	***In vitro* study** **Cells:** BMSCs from Tibia and femur of Sprague-Dawley (SD) rats **Time period of *in vitro* culture:** 14 days **Findings:** •Gradient scaffolds with a Cs/GP/Gel ratio of 9:1:5 exhibited good biocompatibility, supporting BMSCs survival, distribution, and extension. •This suggestd that the scaffold's physical properties, including its gradient structure, were conducive to cell attachment. •The pore size gradient did not significantly influence cell proliferation. •The BMSCs showed potential for differentiation into osteoblasts and chondrocytes when cultured in specific induction media.	(Hu et al., 2019) [201]
	Dual-layer scaffold with orientated porous structure	Surface layer: freeze-drying method Transitional layer: unidirectional freeze-drying technique	**Materials:** A combination of collagen, chitosan, hyaluronic acid, and silk fibroin **Bi-layered structure:** •The surface layer comprised collagen (COL), chitosan (CS), and hyaluronic acid sodium (HAS), with polylactic	N/A	Morphology: The double structure resembled natural cartilage, featuring larger pores in the surface layer and a microtubule array structure in the transitional layer. This	***In vitro* study** **Cells:** BMSCs from bone marrow of a 4-week-old male SD rat **Time frame for culture:** 1, 3, 5, 7 days (cell proliferation assessment); 3, 5, and 7 days of incubation (cell viability	(Wang et al., 2019) [20]

(*continued on next page*)

Table 2 (*continued*)

Type	Scaffold name	Fabrication method	Zonal structure		Main findings		Reference
			Cartilage scaffold features	Other features (e.g., bone)	Structural & mechanical characterisations	*In vitro* and *in vivo* study	
			acid-glycolic acid (PLGA) microspheres (MPs) containing Kartogenin (KGN) embedded within. •The transitional layer incorporated collagen (COL), chitosan (CS), silk fibroin (SF), and polylysine-heparin sodium nanoparticles loaded with transforming growth factor-β1 (TGF-β1).		design aimd to guide bone marrow stromal cells (BMSCs) along the microtubule walls to the surface layer, promoting their differentiation into chondrocytes. Porosity: The ideal ratio of 1:1:0.1 (COL/CS/HAS) yielded favourable porosity at 50 %, promoting cell proliferation and tissue regeneration. COL/CS/0.5SF exhibited a porosity of up to 92 % Mechanical Properties: Wet biomimetic cartilage scaffolds demonstrated a compressive strength of 0.051 MPa, surpassing dry scaffolds (0.033 MPa), with an elastic modulus of 1.2 KPa.	assessment) **Findings:** The biomimetic cartilage scaffold promoted cell proliferation, maintained cell viability, and had the potential to regenerate damaged cartilage tissue. ***In vivo* study** **Animal model**: Male New Zealand white rabbits aged 16 weeks **Time period/time frame of *in vivo* test:** 4, 8, 12, 16 weeks post-operation **Findings:** The biomimetic cartilage scaffold effectively guided cartilage tissue regeneration in a knee osteoarthritis model. Its bi-layered structure with specific orientations and materials supported BMSCs' proliferation, migration, and differentiation, resulting in the formation of new cartilage tissue closely resembling normal cartilage.	
	Porous zonal microstructured scaffold	**Multiple fabrication strategies:** Electrospinning (aligned and random fibres), spherical porogen leaching (intermediate zone), directional freezing (deep zone), melt electrowetting (osteochondral interface).	**Materials:** Poly (ε-caprolactone) (PCL) **Zonal design:** •Superficial Zone: Features aligned electrospun fibres, mirroring the collagen alignment on the cartilage surface. •Intermediate Zone: Utilised a porogen-leached structure to provide an isotropic framework, facilitating the transition between superficial and deep zones. •Deep Zone: Exhibited a directionally frozen structure, imparting greater stiffness and vertical pore morphology akin to deeper cartilage layers. •Osteochondral Interface: Comprised of a fibrous layer facilitating the transition to the subchondral bone, fostering seamless integration.	Osteo component consisted of 20 μm diameter fibres stacked at 200 μm intervals in a 90-degree lay-down pattern	**Pore Sizes:** •The fibrous zone presented a median major axis pore size of 2.1 μm and 123.3 μm, fostering optimal cell attachment and proliferation. •The porogen-leached zone (PLZ) showcased a median major axis pore size of 44.4 μm, emulating the intermediate cartilage zone with a more isotropic structure. •The directional frozen zone (DFZ) featured larger pores to enhance compressive stiffness, mimicking deeper cartilage regions. Pore geometries in the DFZ and fibrous zones were anisotropic, with smaller pores in the orthogonal direction. **Porosity**: •The microstructured scaffolds possessed an overall porosity of 97 ± 1 %, critical for enabling cell	***In vitro* study** **Cells:** Bovine chondrocytes from stifle joints of approximately 1-year-old calves **Time period of *in vitro* culture:** 4 weeks **Findings:** The designed zonal microstructured scaffold can mimic the regional characteristics of articular cartilage and support the growth of chondrocytes and accumulation of ECM *in vitro* ***In vivo* study** **Animal model**: Female skeletally mature pigs (60–97 kg, mean 78 kg) with osteochondral defects **Time period/time frame of *in vivo* test:** 6 months **Findings:** •New bone formation was observed in the subchondral repair site, with evidence of osteointegration. •Microstructured scaffolds did not demonstrate superior repair quality based on histological scoring at six months. •The study suggested that at	(Steele et al., 2022) [99]

(*continued on next page*)

Table 2 (*continued*)

Type	Scaffold name	Fabrication method	Zonal structure		Main findings		Reference
			Cartilage scaffold features	Other features (e.g., bone)	Structural & mechanical characterisations	*In vitro* and *in vivo* study	
					infiltration, nutrient and oxygen diffusion, as well as waste removal. **Mechanical properties** •Compressive Modulus: DFZ: 1974 kPa PLZ: 38 kPa Combined DFZ and PLZ: 64 kPa •Mechanical Anisotropy: Exhibited different mechanical responses in different directions, resembling natural cartilage. •Strain Stiffening and Frequency Dependence: The modulus increased with strain during compression and varied with the frequency of loading. •Cyclic Loading Stability: Underwent a 28 kPa stress at 1 Hz for 12 h, demonstrating long-term stability under physiological loading conditions.	longer time points, further scaffold biodegradation may lead to increased matrix deposition and improved repair outcomes.	
	Functionally graded multilayer scaffolds	**Top layer:** Photo-polymerisation under UV light (hydrogel encapsulating the hMSC) **Bottom and middle layers**: created as a single bilayer system using a cryogelation process	**Materials:** Poly (ethylene glycol)-diacrylate (PEGDA) and N-acryloyl 6-aminocaproic acid (A6ACA) **Trilayer scaffold:** •Top layer: chondrocytes encapsulated hydrogel to facilitate cartilage tissue formation (PEGDA). •Middle layer: cryogel with an anisotropic, columnar pore architecture to support cartilage tissue formation (PEGDA), hMSCs and chondrocyte-laden layer	Biomineralisation of the bottom layer to mimic the calcium phosphate (CaP)-rich bone micro-environment, designed to support bone formation.	**Pore sizes:** Bottom layer: interconnected macroporous structures, approximately 33.6 ± 13.2 μm and 27.4 ± 11.1 μm Middle layer: column pore architecture, pore sizes approximately 132.6 ± 24.2 μm, and the minor axis pore sizes being around 37.5 ± 8.6 μm. **No information about the mechanical study**	***In vitro* study** **Cell/scaffold type:** Human mesenchymal stem cells (hMSCs) & bovine chondrocytes laden scaffold (middle layer) **Medium:** Chondrogenic-inducing medium **Cells:** Primary human adult MSCs, chondrocytes from articular cartilage of 8-week-old bovine legs **Time period of *in vitro* culture:** 9 weeks **Time frame for culture:** 3 days, 1 week, 5 weeks, and 9 weeks **Findings:** The designed trilayer scaffold was capable of supporting the formation of stratified cartilage-like tissue *in vitro*. ***In vivo* study** **Animal model:** Immunodeficient mice (3-month-old) **Time period/time frame of *in vivo* test:** 0, 4, and 8 weeks post-implantation **Findings:** The scaffold's design, integrating biomaterials with spatially	(Kang et al., 2018) [162]

(*continued on next page*)

Table 2 (*continued*)

Type	Scaffold name	Fabrication method	Zonal structure		Main findings		Reference
			Cartilage scaffold features	Other features (e.g., bone)	Structural & mechanical characterisations	*In vitro* and *in vivo* study	
						controlled cell differentiation and tissue formation, effectively supported osteochondral tissue regeneration. It integrated with host tissues, promoting the formation of both bone and cartilage components.	
	Biomimetic soft network composites (SNC)	Melt electrospinning writing (MEW), Numerical model-based approach	**Materials**: The multiphasic SNC was combined with a mPCL and nHA architecture to mimic the cartilage calcified zone. **Multiphasic structure:** Structurally graded medical grade poly (ε-caprolactone) (mPCL) fibers •Superficial zone: 800 μm pore •Transitional zone: 400 μm pore •Deep zone: 200 μm •Calcified: 10 layers of mPCL/nHA composite fibers The biomimetic SNC comprised a water-swollen hydrogel matrix and a reinforced fibrous network optimised using an *in silico* design library-based numerical model.	N/A	**Pore size (fibre spacing):** •Superficial zone: 800 μm •Transitional zone: 400 μm •Deep zone: 200 μm **Fibre diameter** •Superficial zone: 25 μm •Transitional zone: 25 μm •Deep zone: 20 μm **Mechanical Properties (E_{SNC})** •Superficial zone: 491.7 ± 103.0 kPa •Transitional zone: 1340.4 ± 143.7 kPa •Deep zone: 2425.8 ± 574.6 kPa •The printed fibrous networks were used to reinforce the GelMA hydrogel with $E_{Matrix} = 39.8 \pm 3.8$ kPa The zonal mechanical differences in articular cartilage were highly associated with the variations in the organisation and density of the fibre network	N/A	(Bas et al., 2018) [199]
	3D printing multiphasic osteochondral tissue constructs Novelty: Nano hydroxyapatite	Fused deposition modelling (FDM) 3D printing, computer-aided design (CAD) and fused	**Materials:** Primary component: Polycaprolactone (PCL)-based shape memory material, polycaprolactone-triol, castor oil, and poly (hexamethylene diisocyanate) **Multiphasic constructs (articular cartilage):** •Superficial region: horizontal pattern •Intermediate region: randomly oriented hexagonal pore structure •Deep region: orthogonal pattern •The upper half of the constructs: without nHA, was soaked in a dopamine hydrochloride solution to polymerise polydopamine (PDA) on the structs surface and in bovine serum protein (BSA) to protect the activity of growth factor TGF-β1	Polycaprolactone (PCL)-based orthogonal pattern scaffold layer: Nanocrystalline hydroxyapatite (nHA) was synthesised and printed into the subchondral bone layers	**No information about the Pore sizes** **Mechanical Properties**: The addition of nHA and polymerised polydopamine (PDA) coating was shown to improve the compressive strength and Young's modulus of the scaffold, making it suitable for load-bearing applications.	***In vitro* study** **Cells:** human bone marrow MSCs **Chondrogenic factors:** including TGF-β1 **Time frame of *in vitro* culture:** 1, 2, and 3 weeks (differentiation/ chondrogenic studies) **Findings:** •Enhanced hMSC differentiation in cartilage constructs and osteochondral constructs •constructs with nHA and those with nHA, PDA, and TGF-β1 significantly outperformed all other constructs in terms of total collagen production in the upper portion •3D printed constructs containing nHA and bioactive cues had better	(Nowicki et al., 2020) [200]

(*continued on next page*)

Table 2 (*continued*)

Type	Scaffold name	Fabrication method	Zonal structure		Main findings		Reference
			Cartilage scaffold features	Other features (e.g., bone)	Structural & mechanical characterisations	*In vitro* and *in vivo* study	
						mechanical properties and enhanced hMSC adhesion, growth, and differentiation	
	Bone marrow stromal cell (BMSC)-laden anisotropic hydrogels	3D-bioprinting	**Materials:** Poly (ε-caprolactone) (PCL) **Structure (micropattern):** Gradient scaffolds (Gradient group: 150, 350, 550, 750 μm pore layers)	N/A	**Pore sizes:** •Non-gradient scaffolds Small pore size (SPZ): 150 μm Transitional pore sizes: 350 μm, 550 μm Large pore size (LPS): 750 μm **No information about mechanical properties**	***In vitro* study** **Cells:** BMSCs from rabbit bone marrow aspirates **Time period of *in vitro* culture:** 6 weeks **Findings:** Pore size-dependent chondrogenesis of BMSCs in the SPZ scaffold was modulated by the HIF1α-regulated cell adhesion signalling pathway. ***In vivo* study** **Animal model:** Adult male New Zealand white rabbits weighing 3.0–3.5 kg, knee full-thickness cartilage defect model **Time period of *in vivo* test:** 24 weeks post-implantation period **Findings:** The gradient anisotropic scaffolds had a better cartilage-repairing effect and joint protection function after transplantation compared to Non-gradient scaffolds	(Sun et al., 2021) [21]
	Biomimetic multidirectional scaffolds	Freeze-casting, Lyophilization bonding	**Materials**: Superficial zone (SZ) scaffold: collagen-hyaluronic acid Transitional zone: collagen-hyaluronic acid suspension **Structure (zone-specific fibre orientation)**: Matrices contained a thin, highly aligned superficial zone that interfaced with a cellular transition zone (TZ) vertically oriented calcified cartilage (OCZ) and osseous zones (OZ).	Lamellar Osseous Zone (OZ) scaffold: collagen-hydroxyapatite-containing suspensions	**Zone pore size:** SZ: 48 ± 5 μm TZ: 105 ± 16 μm OCZ: 88 ± 16 μm OZ: 98 ± 15 μm **Porosity (%):** SZ: 75 TZ: 89 OCZ: 92 OZ: 92 **Mechanical properties**: Compressive testing of hydrated scaffold zones confirmed an increase in stiffness with scaffold depth, where compressive moduli of chondral and osseous zones fell within or near ranges conducive for chondrogenesis or osteogenesis of mesenchymal stem cells.	N/A	(Clearfield et al., 2018) [205]
	Collagen–Hyaluronic Acid Cryogels	Directional freezing and cryogelation (CollGTA first network), UV light crosslinking (MeHA second network)	**Material:** Collagen glutaraldehyde–hyaluronic acid methacryloyl (CollGTA-MeHA) **Arcade-like structure:** •Arcade-like structure: the growth of	N/A	**No information about pore size** **Mechanical properties:** •CollGTA first network exhibited a very low Young's	***In vitro* study** **Cells**: Human chondrocytes from femoral head of an osteoarthritic patient **Time period of *in vitro* culture:**	(Yamamoto et al., 2022) [210]

(*continued on next page*)

Table 2 (*continued*)

Type	Scaffold name	Fabrication method	Zonal structure		Main findings		Reference
			Cartilage scaffold features	Other features (e.g., bone)	Structural & mechanical characterisations	*In vitro* and *in vivo* study	
			ice crystals from copper pins at cryogenic temperatures •The directional cryogel formation enabled the organised growth of ice crystals over a large distance (>4 mm).		modulus (1.6 Pa). MeHA alone exhibited a higher elastic modulus (233 kPa) and stress at break (260 kPa). •MeHA-CollGTA DNs network •exhibited a high early elastic modulus (~200 kPa) and a stress at break of ~184 kPa.	24 h **Finding:** •No evident toxicity effect on human chondrocytes in contact with CollGTA-MeHA DN was found.	
Cell types & growth factors	Zonal-Specific Cell Density Scaffold	3D bioprint	**Material:** Alginate-based bioink containing human articular chondrocytes. **Structure (three cell densities):** 3D print a PCL-reinforced alginate-based scaffold containing human chondrocytes with clinically relevant thicknesses and zone-specific cell densities: •Superficial zone: 20 × 10^6 cells/mL. •Middle zone: 10 × 10^6 cells/mL •Deep zone: 5 × 10^6 cells/mL	N/A	No information about pore size **Mechanical properties:** PCL frame design significantly increased the bulk mechanical properties compared to the bioink alone.	***In vitro* study** **Cell/scaffold type:** Human articular chondrocytes from hyaline cartilage in the knee **Time period of *in vitro* culture:** 25 days **Findings:** •Generated a zonal cell density with high viability. •A smooth transition between the zones in terms of cell distribution and a higher sulphated glycosaminoglycan deposition in the highest cell density zone.	(Dimaraki et al., 2021) [112]
	Bilayered fibrin hydrogel Scaffold integrated with dynamic microcarrier expanded zonal chondrocytes	N/A	**Material:** •Autologous chondrocytes extracted from articular cartilage in the non-weight bearing (NWB) cartilage region of the knee. Large/DZ chondrocytes (S3) 40 %; Medium size/MZ (S2) 40 %; Small/SZ chondrocytes (S1) 20 % •Fibrin hydrogel **Structure (zonal chondrocytes):** •Bilayered fibrin hydrogel construct	N/A	**No information about pore size** **Mechanical properties:** S2S3 chondrocytes from both weight bearing (WB) and NWB regions generated tissue constructs with comparable Young's Modulus, with significantly higher strength than their respective S1 constructs.	**Cell source for scaffold:** Chondrocytes from femoral condyle and trochlea of articular cartilage in 11–13 months old micropigs ***In vivo* study** **Animal model:** Porcine knee chondral defect mode **Time period of *in vivo* test:** 6 months post-implantation **Findings:** •Zonal phenotype of regenerated tissues •Bilayered implantation of dynamic microcarrier-expanded zonal chondrocytes resulted in substantial recapitulation of zonal architecture, including chondrocyte arrangement, specific Proteoglycan 4 distribution, and collagen alignment, that was accompanied by healthier underlying subchondral bone.	(Tee et al., 2022; Tee et al., 2023) [202, 203]
	Tri-layered PCEC scaffolds, fibre-reinforced GelMA Hydrogels with the incorporation of growth factor-loaded PLGA microspheres	Melt electrowetting (MEW) for microfibre fabrication. UV cross-linking casting method, infiltration and crosslinking procedures for the injection of	**Materials:** •Poly (ε-caprolactone)-poly (ethylene glycol) (PCEC) fibres with depth-dependent fibre organisation •Gelatine methacrylamide (GelMA) hydrogel incorporating rabbit bone-derived MSCs (BMSCs)	Subchondral Bone layer (B): 10 mg BMP-2@PLGA microspheres/ml	**Pores size:** •S layer: 100 μm •D layer: 200 μm •B layer: 600 μm **Lay-down patterns:** •S layer: 0°–30° •D and B layer: 0°–90°	***In vitro* study** **Cells:** Bone marrow MSCs from male New Zealand white rabbits (4 weeks old) **Medium:** Cell-incorporating constructs were incubated in the chondrogenic and osteogenic	(Qiao et al., 2021) [22]

(*continued on next page*)

Table 2 (*continued*)

Type	Scaffold name	Fabrication method	Zonal structure		Main findings		Reference
			Cartilage scaffold features	Other features (e.g., bone)	Structural & mechanical characterisations	*In vitro* and *in vivo* study	
		hydrogels into fibre networks	•Zone-specific growth factor (GF)-loaded poly (lactic-co-glycolic acid) (PLGA) microspheres •Scaffold: Spatially varying PCEC microfibre configuration (diameters, spacings, and interweaving angle) and biomaterial composition (PCEC-HA fibre for bone layer): PCEC microfibre and PCEC-HA fibre scaffolds •Hydrogel: spatial distribution of the bioactive factors of the transforming growth factor-β (TGF-β) and bone morphological protein (BMP) **Zone-specific growth factors:** •Superficial cartilage (S) layer: 6 mg BMP-7@PLGA microspheres/ml + 2 mg TGF-β1@PLGA microspheres/ml (growth factors: TGF-β1 + BMP-7) •Deep cartilage (D) layer: 8 mg TGF-β1@PLGA microspheres/ml (growth factor: TGF-β1)		**Scaffold porosities:** •S layer 86.89 %, •D layer 92.27 % •B layer 60.46 %. **Thickness of *in vivo* implanted scaffold:** •S layer 150 μm, •D layer 450 μm •B layer 2.5 mm **Spherical PLGA microspheres average diameter:** 3.12 ± 0.87 μm. **Compressive mechanical properties (*E*):** •GelMA hydrogel: 28.4 ± 2.3 kPa •Fibrous networks: •S layer alone: 46.1 ± 3.8 kPa, •D layer alone: 34.8 ± 2.7 kPa •SD layer alone: 165.8 ± 27.6 kPa (significantly low compared with that of human articular cartilage, which is ≈ 1 MPa) •S layer-reinforced construct: 283.6 ± 22.3 kPa •D layer-reinforced construct: 256.6 ± 24.9 kPa •SD layer reinforcement: 964.2 ± 56.8 kPa. •B layer (scaffold alone): 46.1 ± 4.2 MPa •B layer (PCEC/hydrogel composite): 55.8 ± 5.4 MPa	induction medium. **Time frame of *in vitro* culture:** 7, 14, and 21 days (chondrogenic induction and osteogenesis test); 14 days (cell viability); 21 days (protein expression analysis & immunofluorescence) **Findings:** •The infilled hydrogels and PLGA microspheres did not negatively affect the cell viability. •Differential mRNA expression of osteochondral-related zonal markers in three layers (S, D, and B constructs) confirmed chondrogenesis and osteogenesis. •S layer constructs were more aligned along the fibrous networks; cytoskeletons were elongated and mainly oriented parallel to the fibres in the S layer, while in the deeper zones, the cytoskeletons were oriented more randomly. •Stratified osteochondral tissue function in guiding native-like cell orientation and zonal marker protein deposition. ***In vivo* study** **Animal model:** New Zealand white rabbits, three-month-old, weighting 2.5–3.0 kg **Time period of *in vivo* test:** 24 weeks post-surgery **Findings:** •The S layer in the defect region enabled lubrication (lower roughness), which endowed the regenerated cartilage with a smoother surface. (compared between B + D and B + D + S groups) •Tri-layered B + D + S group acquired a more lubricating and wear-resistant repair surface. •The stratified structure enabled the entire osteochondral tissue repair	
	Cytokine-containing microsphere-loaded scaffold	Melt electro-writing (MEW) and Inkjet printing technology (microsphere)	**Scaffold materials:** Polycaprolactone (PCL) or PCL/hydroxyapatite (HA) scaffolds **Multilayer scaffolds (zone-specific growth factors):** •Surface layer (SL): PCL scaffold	N/A	**Microsphere particle size** •83.6 % of 1–5 μm diameter •30.2 % of 3–4 μm diameter **Pore structures** •SL: 100 μm; ML & DL: 200 μm	***In vitro* study** **Cells**: Bone marrow MSCs from New Zealand rabbits (male, 2–4 weeks) **Time period of *in vitro* culture:** 21 days	(Han et al., 2020) [136]

(*continued on next page*)

Table 2 (*continued*)

Type	Scaffold name	Fabrication method	Zonal structure		Main findings		Reference
			Cartilage scaffold features	Other features (e.g., bone)	Structural & mechanical characterisations	*In vitro* and *in vivo* study	
			containing PLGA microsphere encapsulating transforming growth factor-β1 and bone morphogenetic protein-7 (TGF β1+BMP-7) •Middle layer (ML): PCL scaffold containing PLGA microsphere encapsulating transforming growth factor-β1 and insulin-like growth factor-1 (TGF β1+IGF-1) •Deep layer: PCL/10 % hydroxyapatite (HA) scaffold with PLGA microsphere incorporating transforming growth factor-β1 (TGF β1+HA)		•Even fibre shape and smooth surface. **Mechanical properties:** Mixing HA with PCL improves the scaffold's compressive strength, which is suitable for the performance of the cartilage calcification layer while reducing the tensile strength.	**Time frame for culture:** 7, 14, 21 days (gene expression analysis) **Findings:** •The composite biological scaffold was conducive to adhesion, proliferation, and differentiation of mesenchymal stem cells. •The environmental differences between the scaffold's layers contributed to the regional heterogeneity of chondrocytes and secreted proteins to promote functional cartilage regeneration. ***In vivo* study** **Animal model**: Six-month-old male New Zealand rabbits weighing about 3–4 kg **Time frame of *in vivo* test:** 3 weeks, 6 weeks, 12 weeks, and 24 weeks **Findings:** •The composite cartilage group formed smooth cartilage on the surface at 12 w, and the cross-section showed that the scaffold was well integrated with the surrounding tissue. •Adding cytokine-loaded microspheres significantly enhanced the scaffold's biological activity.	

osteochondral unit. However, the scaffold is constructed by iterative layering of numerous electrospun fibre mats, which is relatively tedious and the random fibre orientations within each layer also do not reflect the natural arrangement of collagen fibres in articular cartilage, progressing from parallel to random and then perpendicular. Another approach might be to simply incorporate directionally oriented polymer fibres, such as in the form of microribbons [190], into a hydrogel matrix to create zonal variation within the scaffold, but hydrogels typically exhibit insufficient mechanical properties for applications in load-bearing osteochondral regions. Continued advances in electrospinning technology will enable the construction of nanofibres with specialised designs, and their assembly into sophisticated 3D morphologies that may have versatile applications in the fabrication of multizonal cartilage scaffolds [191].

To create more biomimetic cartilage zones while ensuring load-bearing capability, Castilho et al. [192,193] employed the melt electrospinning (MEW) technique, where the PCL is melted and extruded through a spinneret connected to a high-voltage source to fabricate a bilayered microfibre-reinforced chondral scaffold, comprising a superficial tangential zone (STZ) and a middle and deep zone (MDZ) with varying fibre orientations, as shown in Fig. 6A. The STZ contains densely distributed cross-fibres along the tangential direction, with the fibres laid at alternating angles (0-45-90-135°). This fibre orientation is designed to resist shear forces and provide a smooth, low-friction surface for joint movement. The MDZ contains cross-fibres with a cross-shaped laying pattern of 0–90°, creating a uniform box structure with more randomly oriented fibres, designed to withstand compressive loads, maintain tissue integrity, and provide structural support. The fibrous scaffold is then created by integrating the fibres into a GelMA solution and setting the mixture by UV crosslinking to form a stable hydrogel matrix that encapsulates the fibres. When cultured with chondrocytes, the scaffold showed ability to support the maintenance of chondrogenic phenotype and the continued synthesis of cartilage-specific ECM components such as collagen type II and GAG. However, the different layers did not necessarily produce region-specific mechanical properties, in fact, the hydrogel showed signs of mechanical failure under dynamic loading. This highlights the need for further improvements in the hydrogel system to enhance its fracture toughness and durability under cyclic loading conditions.

Also through electrospinning, Girão et al. [194] developed a tri-layered chondral scaffold using PCL as the bulk material combined with a graphene-oxide (GO)-collagen microporous network, with depth-dependent control over fibre orientation through the generation of horizontally, randomly, and vertically aligned fibres in the corresponding layers, as shown in Fig. 6B. Fibres were first electrospun onto a rotating drum to form a mesh. Cylindrical sheets were then cut from this mesh to serve as the superficial zone. For the deep zone, a small rectangular piece of the electrospun mesh was rolled and embedded within a GO-collagen hydrogel. The middle zone was created by electrospinning fibres into an ethanol-water bath, resulting in a distribution of randomly loosened fibres. This multilayered scaffold showed variation in fibre diameter and pore size among layers, which was considered beneficial for offering topographical cues that could improve cellular organisation and zonal ECM production, although this was not tested in the study. Mechanical testing results suggested that the compressive modulus varied with the direction of fibre arrangement, increasing from the superficial to deep scaffold layers. Moreover, the scaffold exhibited a linear stress-strain curve at low strains, suggesting that the fibres remained straight during compression and the scaffold could maintain its structural integrity.

Another tri-layered scaffold was produced by Munir et al. [195] using a novel combination of cryo-printing and electrospinning, as presented in Fig. 6C. The scaffold design aimed to mimic the zonal structure of articular cartilage through variations in fibre orientation and mechanical properties. PCL was used as the base material throughout the scaffold, first to fabricate a printed helix structure through cryo-printing that represents the deep zone of cartilage. Electrospinning was then used to deposit PCL on the helix as randomly oriented fibres mimicking the middle zone, followed by highly aligned fibres on the top mimicking the superficial zone. *In vitro* tests confirmed that the multizone scaffold facilitated chondrocyte attachment, survival, and chondrogenic differentiation, as well as promoted the production of cartilage-specific ECM components while maintaining structural and mechanical integrity over the 4-week culture period, providing a potentially effective platform for cartilage tissue engineering.

Using 3D printing, Cao et al. [113] fabricated a tri-layer zonal cartilage scaffold with each layer characterised by unique pore structure and filament gaps. All layers were constructed using PCL impregnated with methacrylate alginate (ALMA). The superficial layer had an orthogonal architecture with a 0°/90° lay-down pattern and filament gap of 300 μm, the middle layer comprised a 0°/60° diagonal pattern with filament gap of 500 μm, and the deep layer had a denser diagonal pattern exhibiting smaller pores and a 0°/30° lay-down pattern with filament gap of 700 μm. These design elements were used to provide structural integrity and mechanical stability for the scaffold when used in areas subjected to high pressures. PCL was used to create the primary scaffold framework, while the ALMA hydrogel was used for encapsulating MSCs and integrated into the scaffold through photo-crosslinking. Subsequent *in vitro* culture showed the ability of the scaffold to promote MSC survival, proliferation, and chondrogenic differentiation over 3 weeks, although differential cell activity within the three layers in the integrated scaffold was not separately assessed.

Using unique naturally-derived materials, Wang et al. [62] constructed a bioinspired three-zone hydrogel scaffold with anisotropic pores and zone-dependent, non-linear viscoelastic mechanical properties, as presented in Fig. 6D. The hydrogel layers comprised a PEGDA polymer matrix combined with cellulose fabric, cellulose nanofibres, and wood cellulose fibres respectively to form the superficial, middle, and deep zones, mimicking the native structure of articular cartilage. Moreover, fibre orientations were made to exhibit zonal variations, with parallel alignment in the superficial zone to resist shear forces, transitioning to random distribution in the middle zone, and perpendicular alignment in the deep zone to enable force transfer to the subchondral bone. This also led to regional variation in mechanical properties, where the compressive modulus of layers changed from 298 kPa to 182 kPa respectively in the superficial and middle zones, to 9.8 MPa in the deep zone. A very interesting observation arising from the study was that the wood cellulose fibres used to construct the deep zone had capillary channel-like structure, which could aid the transport of nutrients and cells. Moreover, cellulose fibres from softwood and hardwood showed distinct structural differences that could be utilised to enhance cartilage regeneration. The softwood fibres exhibited uniformly oriented square channels in the longitudinal direction and interlaced hollow channels in the radial direction, compared to hardwood fibres which showed aligned hollow channels with gradient circular openings longitudinally and orthogonally arranged fibres radially. These aligned anisotropic properties were thought to enhance liquid transport and mechanical performance in the deep zone, and be beneficial for cartilage regeneration. The scaffold showed ability to support the proliferation, migration, and chondrogenic differentiation of MSCs during *in vitro* experiments. Although its performance in aiding *in vivo* cartilage repair remains to be verified, this scaffold provides interesting design ideas for biomimetic multizonal scaffolds, deriving inspirations from nature to recreate the zone-specific structural and mechanical features of articular cartilage.

4.2. Creating zonal cartilage structure by gradient composition or porous architecture

Incorporating gradient composition or depth-dependent porous architecture in multizonal scaffolds is a widely applied strategy for recreating the unique structural features of articular cartilage. A gradient

composition can be achieved through several strategies such as by blending different materials, adjusting mineral concentration, and creating continuous transitions using techniques such as 3D printing. Levingstone et al. [196] provided one of the earlier examples of combining compositional and structural gradients for osteochondral repair by fabricating a tri-layer scaffold through an 'iterative layering' freeze-drying method. Each layer contained a different material composition, with collagen types I and II in the cartilage layer, collagen types I and II together with hydroxyapatite in the intermediate layer, and collagen I and hydroxyapatite in the bone layer. The layers were integrated seamlessly by sequentially depositing subsequent layers and iterative freeze-drying, leading to a three-layer gradient structure with high porosity and pore interconnectivity as well as some variation in pore structure between layers. Employing a similar compositional gradient, Cao et al. [197] designed a tri-layered biomimetic scaffold containing collagen type II and chondroitin sulphate in the cartilage layer, collagen type II and hydroxyapatite in the calcified cartilage layer, and collagen type I and hydroxyapatite in the bone layer. This scaffold was seen to promote region-specific tissue repair in rabbit osteochondral defects after 4 months of implantation. Camarero-Espinosa et al. [198] instead focused on changing pore orientation in different scaffold layers to mimic articular cartilage zones. The tri-layered scaffold contained polylactic acid (PLA) in the superficial layer with tubular pores parallel to the surface, an isotropic porous middle layer comprising PLA and sulphated cellulose nanocrystals (CNCs), and a deep layer composed of PLA and phosphate CNCs with tubular pores oriented perpendicular to the subchondral bone. To reduce the risk of mismatch between layers, Parisi et al. [56] created a multilayered scaffold comprising a collagen matrix throughout with depth-dependent distribution of hydroxyapatite particles, ensuring a smooth transitional gradient from the superficial cartilage layer to the bone layer.

In an attempt to satisfy the differing structural, compositional, and biochemical requirements for regeneration of zonal articular cartilage, Wang et al. [20] designed a dual-layer biomimetic scaffold with orientated porous structure resembling the superficial and transitional cartilage zones, as shown in Fig. 7A. The surface layer contained larger pores, while the transitional layer contained a microtubular array structure, which were fabricated through freeze-drying. To match the varying ECM composition of cartilage, the scaffold contained collagen and chitosan in both layers, together with hyaluronic acid in the surface layer or silk fibroin in the transitional layer. Moreover, to provide adequate biochemical cues in different layers, PLGA microspheres loaded with kartogenin and TGF-β1 were respectively incorporated into the surface and transitional layers. *In vitro* experiments showed that the scaffold structure enhanced the adhesion and proliferation of bone marrow MSCs, while *in vivo* testing in a rabbit knee osteoarthritis model demonstrated the scaffold's ability to achieve defect filling and cartilage repair, with the repair tissue exhibiting cell morphologies almost matching the normal cartilage after 16 weeks.

Bas et al. [199] introduced a systematic, modelling-based approach to designing biomimetic soft network composites (SNC) as cartilage scaffolds, as presented in Fig. 7B. This approach combined MEW, numerical modelling, injection moulding, and photo-crosslinking to enable precise control over the structure and properties of the engineered constructs. The scaffold design process involved using an *in silico* design library and numerical modelling to simulate the mechanical properties of SNCs, based on hydrogel matrix properties and fibre network structure, under various conditions to mimic the responses of articular cartilage. This allowed selection of the most promising designs for proceeding to fabrication. The scaffold structure was fabricated by MEW using medical grade PCL to create a reinforced fibrous network containing the desired porous structure, with depth-dependent variations in fibre diameter and pore size. Subsequently, injection moulding was combined with photo-crosslinking to infiltrate the GelMA hydrogel matrix into the pores of the printed fibrous network. The resulting scaffold constructs exhibited a zonal architecture with distinct differences in compressive modulus values between zones, which were highly associated with variations in the organisation and density of the fibre network. The impact of this design on chondrogenic behaviour remains to be confirmed.

Nowicki et al. [200] integrated fused deposition modelling (FDM) as a form of 3D printing with a casting technique to produce a gradient osteochondral scaffold using a novel bioink, as shown in Fig. 7C. The scaffold structure was printed using a PCL-based shape memory material, incorporated with nanohydroxyapatite in the bone part and chondrogenic growth factors in the cartilage part. The gradient structure featured depth-dependent variation in pore distribution and geometry, transitioning from a horizontally aligned superficial zone to a randomly oriented middle zone with a hexagonal pattern, and finally to a stacked orthogonal pattern in the bottom region including the deep zone, calcified zone, and subchondral bone area. The scaffold was found to enhance the adhesion, growth, and chondrogenic differentiation of human MSCs.

Kang et al. [162] created a tri-layer scaffold with depth-varying pore architecture using a poly (ethylene glycol)-diacrylate (PEGDA)-based polymer hydrogel for osteochondral tissue engineering, as shown in Fig. 7D. Initially, the porous bottom and middle layers were fabricated as a single bilayer system using cryogelation. The bottom layer featured an interconnected macroporous structure with pore sizes along the major and minor axes measuring approximately 33.6 ± 13.2 μm and 27.4 ± 11.1 μm, respectively. These pore sizes were designed to facilitate cell infiltration and provide a supportive environment for bone formation. The middle layer had a columnar pore architecture with much larger pore sizes of approximately 132.6 ± 24.2 μm along the major axis and 37.5 ± 8.6 μm along the minor axis. The anisotropic pore structure in this layer was designed to guide cell alignment and nutrient transport for cartilage repair. Prior to fabricating the top layer, the bilayer scaffold was subjected to biomineralisation in the bottom layer to provide an environment rich in calcium phosphate that is conducive to bone regeneration. The top layer consisted of a hydrogel without interconnected pores formed by photopolymerisation. For *in vitro* testing, the scaffold was cultured in chondrogenic medium with human MSCs and bovine chondrocytes in the middle layer, together with human MSC aggregates in the top layer and an acellular bottom layer. The cells were capable of chondrogenic differentiation without concurrent osteogenic differentiation, evidenced by minimal collagen type I and osteocalcin staining in the top and middle layers. The scaffold also supported tissue formation resembling osteochondral tissue structure when implanted subcutaneously in mice.

Through mould casting and freeze-drying, Hu et al. [201] fabricated a gradient scaffold comprising chitosan/β-glycerophosphate/gelatin with gradual variation in pore size, as shown in Fig. 7E. Preliminary experiments identified an optimal mass ratio of materials at 9:1:5 for use in scaffold fabrication, which provided the highest porosity and water absorption rate. Through a gravity-aided mixing and casting process followed by freeze-drying, the resulting scaffolds exhibited a gradient of pore sizes along the longitudinal dimension, with smaller pores in the superficial zone and larger pores in the deep zone. *In vitro* tests using bone marrow MSCs showed the scaffold's ability to support cell survival and distribution, as well as chondrogenic and osteogenic differentiation when cultured in specific induction media, although the pore size gradient was not observed to significantly influence cell proliferation compared to non-gradient scaffolds.

Using a 3D bioprinting technique, Sun et al. [21] constructed a four-layered cartilage scaffold with an anisotropic gradient in pore structure, comprising a PCL framework with varying fibre spacing and a natural polymer composite hydrogel encapsulating bone marrow MSCs that was printed into the microchannels between PCL fibres, as shown in Fig. 7F. The spacing between PCL fibres varied from 150 μm in the top layer to 350, 550, and 750 μm in the subsequent layers to create the gradient structure. This resulted in smaller pore size in the top layer, designed to mimic the superficial cartilage zone, which would restrict

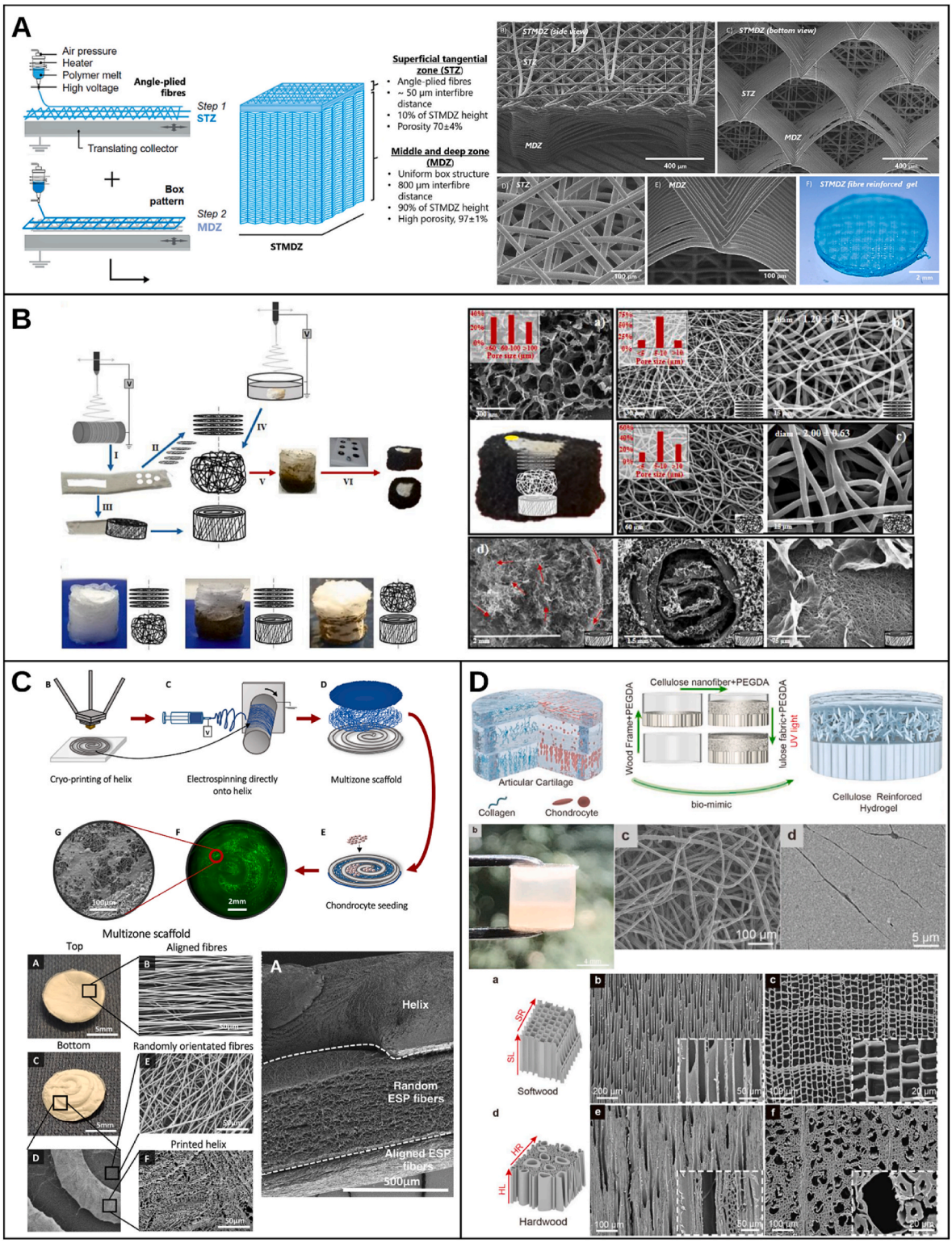

Fig. 6. Examples of zonal cartilage scaffolds based on varying fibre orientation. **(A)** Bilayered microfibre-reinforced chondral scaffold obtained by melt-electrospinning (MEW) with superficial tangential zone (STZ) and middle-deep zone (MDZ) simulated the structure of articular cartilage, adapted with permission from Ref. [193]. **(B)** Tri-layered anisotropic fibrous scaffold fabricated by electrospinning and modifying the electrospun mesh to mimic the three distinct cartilage zones, adapted with permission from Ref. [194]. **(C)** Tri-layered scaffold fabricated by integrating cryo-printing and electrospinning to precisely mimic the superficial cartilage zone with aligned fibres, the middle zone with random fibres, and the deep zone with a printed porous structure, adapted with permission from Ref. [195]. **(D)** Scaffold with zone-dependent variation in fibre diameter and orientation, and mechanical properties to closely replicate the stratified structure of articular cartilage, composed with cellulose nanofibres and a wood cellulose frame reinforced by polyethylene glycol-based anisotropic composite hydrogel, adapted with permission from Ref. [62].

vascularisation and provide a conducive microenvironment for chondrogenic differentiation while also enhancing scaffold strength. In the bottom layer, the large pore size was designed for maximising the penetration of nutrients and oxygen to promote angiogenesis, which would support cartilage maturation, tissue calcification, and scaffold integration with surrounding tissues. When tested separately, the scaffold layers with different pore sizes were seen to influence chondrogenic differentiation and cartilage ECM formation by MSCs. Specifically, scaffold layers with smaller pores upregulated genes associated with superficial hyaline chondrocytes, such as HIF1α, ACAN, and COL2A1, while layers with larger pores upregulated genes associated with deep hypertrophic chondrocytes, such as COL10A1 and RUNX2. Interestingly, the study revealed that the pore size-dependent chondrogenic behaviour of MSCs was modulated by the HIF1α/FAK signalling axis. When tested in full-thickness cartilage defects in the rabbit knee, the gradient scaffold was shown to achieve better cartilage repair and joint protection compared to single-layer scaffolds with small or large pore sizes, with faithful reconstruction of hyaline-like cartilage that exhibited zone-specific cell morphology and ECM formation approximating the structure of native tissue.

Steele et al. [99] employed multiple fabrication strategies to produce a porous zonal microstructured scaffold closely mimicking the variation in architecture, ECM composition, and mechanical properties within the osteochondral tissue unit, as shown in Fig. 7G. Uniquely, the scaffold was fabricated from PCL as the only material constituent, with various gradients created through different processing techniques. Electrospinning was used to fabricate the uppermost layer with aligned fibres for the superficial zone, as well as the bottommost layer with random fibres for the osteochondral interface. The intermediate zone was formed using thermoset gelatin microspheres as porogens, which were subsequently removed by lyophilisation. The deep zone was constructed by directional freezing, involving phase separation of the polymer solution to form longitudinal pore orientations with large pore diameters. MEW was used to print the bone component with a grid-like structure, comprising 20 μm fibres spaced at 200 μm intervals. This study possibly represented the most biomimetic scaffold design for osteochondral tissue, providing not only architectural and pore size gradients but also transition in mechanical properties between layers that faithfully replicated many of the zonal features of articular cartilage as well as the region-specific properties of cartilage and bone. Notably, the scaffold exhibited dynamic loading response, where the modulus increased with strain during compression and varied with the frequency of loading. Long-term mechanical stability was also observed with cyclic loading under physiologically relevant conditions. This was one of the few studies where detailed mechanical characterisation was performed and showed that the scaffold replicated many of the mechanical features of native osteochondral tissue. When tested *in vitro*, the scaffold supported chondrocyte growth and ECM deposition that mimicked the zonal characteristics of articular cartilage. Uniquely, the scaffold was then tested *in vivo* using a clinically relevant large animal model, and assessed for its capacity to induce osteochondral repair in skeletally mature pigs over 6 months. The zonal scaffold showed mechanical stability and reproducible repair quality within the defect, with clear osseointegration and restoration of a flush articular surface. However, the repair quality did not exceed the control based on histological scoring. The thorough investigations in this study have also underlined the difficulty of relating outcomes obtained in smaller animals to larger animals and clinical application due to inherent differences in physiology and tissue repair capacity between species.

4.3. Creating zonal cartilage structure by incorporating cells or growth factors

In addition to providing architectural or compositional gradients, biomimetic scaffolds may be augmented in their capacity to induce zonal cartilage formation through the incorporation of zone-specific cell populations and/or growth factors, which can help to create stratified variations in the regenerative microenvironment. Variation in cell population alone within the same base scaffold material has been shown to help with recapitulating the zonal architecture of articular cartilage. For instance, Tee et al. [202,203] isolated chondrocytes from the non-weight-bearing femoral condyle and trochlea regions of porcine articular cartilage and sorted them by size-based strategies. The superficial zone (SZ) chondrocytes were smaller and more elongated compared to cells in other zones, and produced high amounts of PRG4 crucial for lubrication. Middle zone (MZ) chondrocytes had intermediate size, and were primarily responsible for producing cartilage ECM components such as collagen type II and aggrecan. Deep zone (DZ) chondrocytes were larger and responsible for producing a robust ECM that could withstand high compressive forces. Autologous zonal chondrocytes were isolated and expanded, then sorted by size and incorporated into fibrin hydrogels for implantation into porcine knee cartilage defects. When evaluated at 6 months after implantation, bilayered fibrin hydrogels containing SZ and MZ/DZ chondrocytes respectively in the top and bottom layers outperformed the same hydrogels containing a homogeneous chondrocyte population with mixed zonal phenotypes. The bilayered constructs formed cartilage tissues with zone-specific biochemical and biomechanical properties, including variations in chondrocyte arrangement, PRG4 distribution, and collagen alignment between the two layers accompanied by elevated subchondral bone health.

To mimic the zone-specific variations in cell density observed in articular cartilage, Dimaraki et al. [112] constructed a zonal scaffold comprising a PCL outer skeleton and 3D bioprinted cellular layers built using an alginate-based bioink, as shown in Fig. 8A. Human articular chondrocytes were embedded in the scaffold layers at different densities, with the cell distribution controlled to reflect a natural zonal gradient: 20×10^6 cells/mL in the superficial zone, 10×10^6 cells/mL in the middle zone, and 5×10^6 cells/mL in the deep zone. The scaffold was structured as a cube with dimensions of 7.2 mm × 7.2 mm × 3 mm, and divided into 15 layers distributed among the three zones. *In vitro* culture in chondrogenic medium for 25 days showed that the bioprinted zonal scaffold with gradient variation in cell densities could maintain its structure and promote the formation of cartilage-like tissue. A smooth transition in cell distribution was noted between zones, and increased GAG deposition was found in the zone with the highest cell density.

Other studies have augmented biomimetic zonal scaffold designs with zone-specific variation in growth factors. For example, a study by Wang et al. [20] discussed earlier produced a dual-layer scaffold with orientated porous structure, which was supplemented by the incorporation of PLGA microspheres encapsulating kartogenin and TGF-β1 in the surface and transitional scaffold layers, respectively. Through a somewhat similar approach that combined gradients in scaffold architecture and distribution of growth factors, Qiao et al. [22] developed a bioinspired tri-layered scaffold based on a MEW poly (ε-caprolactone) and poly (ethylene glycol) (PCEC) network that provided depth-dependent variation in fibre structure according to diameter, spacing, and interweaving angle, as shown in Fig. 8B. In addition to this architectural gradient, a biochemical gradient was created by polymerising GelMA hydrogels loaded with MSCs and zone-varying growth factors. The selection of growth factors was based on their abilities for guiding MSC differentiation in different zones to induce specific tissue formation corresponding to the stratified morphology of articular cartilage. Specifically, the superficial cartilage layer contained TGF-β1 and BMP-7 for inducing chondrogenic differentiation and enhancing the expression of superficial zone protein (SZP) to improve the lubricating and wear-resistant properties of the cartilage surface. Meanwhile, the deep cartilage layer contained TGF-β1 to promote the formation of a proteoglycan-rich, interconnected cartilaginous matrix, and the subchondral bone layer was loaded with BMP-2 to stimulate osteogenic differentiation and the formation of a mineralised bone-like matrix. Through targeted delivery of growth factors, the scaffold enabled

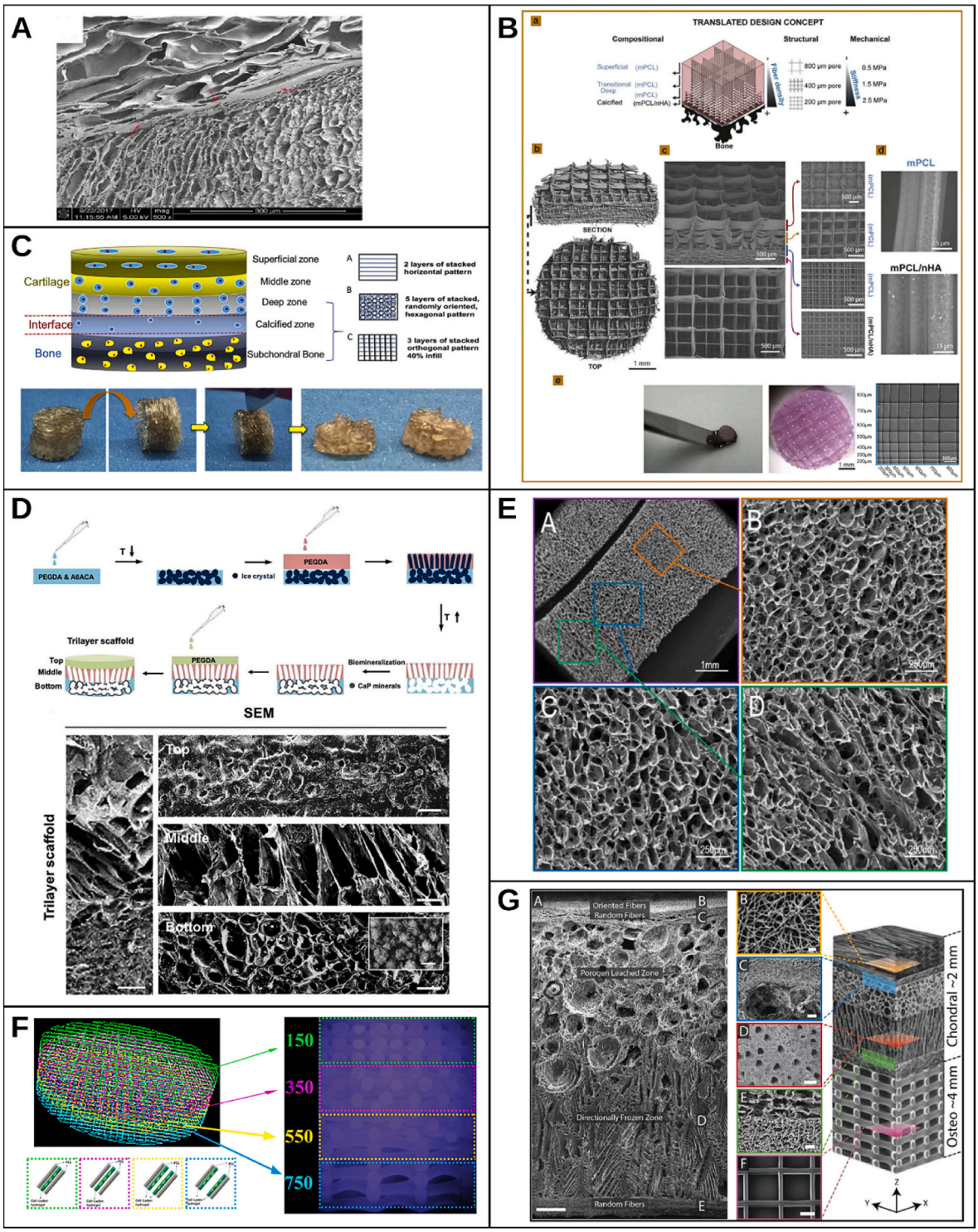

Fig. 7. Examples of zonal cartilage scaffolds based on gradient composition and porous architecture. **(A)** Dual-layer biomimetic cartilage scaffold resembling the surface and transition layers of articular cartilage (SEM image indicates the distinct microstructure between layers), adapted with permission from Ref. [20]. **(B)** Multilayered soft network composites with spatial stratification of structural fibre spaces, compositional differences, and gradient mechanical stiffness, adapted with permission from Ref. [199]. **(C)** Gradient osteochondral scaffold produced by FDM with change in pore distribution and geometry, adapted with permission from Ref. [200]. **(D)** Tri-layer scaffold with depth-varying porous design and biomineralised environment, adapted with permission from Ref. [162]. **(E)** Gradient scaffold with gradual variation in pore size, adapted with permission from Ref. [201]. **(F)** 3D-bioprinted four-layered scaffold with a pore structure gradient, adapted with permission from Ref. [21]. **(G)** Porous zonal microstructured scaffold with gradient variation in architecture, composition, and mechanical properties, adapted with permission from Ref. [99].

zone-specific deposition of protein markers related to chondrogenesis and osteogenesis by MSCs after *in vitro* culture for 28 days, including SZP in the superficial layer, aggrecan in the deep layer, collagen type II in both superficial and deep layers, and collagen type I in the bone layer. When implanted into rabbit osteochondral defects for 24 weeks, the tri-layer scaffold achieved osteochondral tissue repair throughout the defect region, particularly noting a lubricating and wear-resistant repair surface. It should be mentioned that the *in vivo* study compared the tri-layer scaffold to other scaffold variations with fewer layers, rather than between scaffolds loaded with or without growth factors.

Through a different selection of growth factor distribution, Han et al. [136] produced a multilayer scaffold through MEW, comprising a network of PCL fibres and PCL + hydroxyapatite fibres in the respective cartilage and bone regions, as shown in Fig. 8C. PLGA microspheres containing different types of growth factors were inkjet printed onto the scaffold layers during fabrication to create a zone-specific distribution, characterised by TGF-β1 throughout the surface, middle, and deep scaffold layers, BMP-7 only in the surface layer, and IGF-1 only in the middle layer. The deep layer comprising the bone region hence contained TGF-β1 and hydroxyapatite in addition to PCL. After culturing with bone marrow MSCs for 21 days, the scaffold induced zone-specific expression of mRNA and proteins associated with chondrogenesis, including higher levels of PRG4 in the surface layer and CILP in the middle layer, as well as COLII and SOX9 in all three layers. When implanted in a rabbit osteochondral defect for 12 weeks, the scaffold loaded with growth factors achieved significantly better repair compared to a scaffold control group not containing growth factors, demonstrated by the formation of a smooth cartilage surface, strong integration with surrounding tissue, and greatly increased deposition of collagen type II and compressive modulus of the repair tissue towards functional cartilage regeneration. Multizonal cartilage scaffolds based on spatial variation in growth factors may also benefit from having 'dynamically adaptive' properties, for instance, scaffolds can be designed to dynamically release different types of growth factors in response to physiological or mechanical changes in the environment during the healing process [204].

4.4. Other special zonal scaffold designs

Other interesting designs of zonal cartilage scaffolds have been generated by specific modulation of oriented pore structures through freezing and controlling the direction of heat transfer [169,205–207]. It is also possible to generate biomimetic arcade-like structures within the scaffold through various methods including 3D printing [137,208,209] and directional freezing [210]. By modifying freeze-drying kinetics with the aid of a mould, scaffolds can be made into either an isotropic porous structure containing random pores or an anisotropically aligned porous structure, depending on the direction of heat transfer. For example, Clearfield et al. [205] developed an osteochondral scaffold with multi-directional layers through directional freezing, as shown in Fig. 9A. The superficial cartilage layer and subchondral bone layer were respectively created by unidirectional freeze casting of collagen-hyaluronic acid and collagen-hydroxyapatite solutions, utilising a temperature gradient to allow for directional solidification. The two layers were then joined through a lyophilisation bonding process involving a collagen-hyaluronic acid suspension to mimic the transition zone. This led to the formation of an integrated scaffold with pores aligned in different directions within the superficial, transition, and osseous zones. Cellular responses to this biomimetic scaffold remain to be verified.

The arcade-like structure is a new type of scaffold architecture design that directly resembles the collagen fibre orientation within the articular cartilage region. In an example study, Yamamoto et al. [210] fabricated such structures through a relatively simple method of directional cryogel formation from collagen and hyaluronic acid derivatives, by inducing the growth of ice crystals from copper pins, as shown in Fig. 9B. The scaffolds exhibited an anisotropic structure with pores and polymer fibres aligned in specific directions, guided by the growth direction of ice crystals, forming distinct zones with different fibre orientations and packing densities mimicking the zonal architecture of articular cartilage.

An interesting concept of 'hypotrochoidal scaffolds' was recently demonstrated by van Kampen et al. [137] who used FDM to build up a PCL construct layer by layer, as shown in Fig. 9C. This scaffold featured a unique architecture comprising a hypotrochoidal pore network mimicking the arch-like organisation of collagen type II fibres in articular cartilage. The hypotrochoidal curve was generated by tracing a point linked to a smaller circle rolling inside a larger circle. This hypotrochoidal scaffold design exhibited a gradient in pore size, with the smallest pores in the superficial zone and the most prominent pores in the deep zone, replicating the heterogeneous structure of articular cartilage. A specific design with radius (r) of the smaller circle $r = 0.17$ was found to result in optimal scaffold mechanical properties approaching native cartilage in Young's modulus, as well as provide high toughness and ability to withstand deformation. The same design also enhanced chondrogenic behaviour by a commonly used cell line, evidenced by increased collagen type II and GAG deposition accompanied by reduced expression of collagen type X.

5. Outlook and perspectives

Satisfactory treatment of osteochondral defects has been a long-standing clinical challenge due to the intricate structure of the chondral region and its limited self-healing capacity. The last few years have seen growing research interest in scaffold-based approaches for engineering stratified cartilage and osteochondral tissues [15,211]. Scaffold designs have attempted to address the distinct, region-specific regenerative requirements of osteochondral tissue by introducing various architectures, material compositions, and fabrication methods [9,212]. Multizonal or zone-specific scaffolds are now emerging as an innovative concept for osteochondral repair, with the aim of specifically replicating the unique spatial organisation of articular cartilage to achieve functional tissue restoration. The recapitulation of native tissue characteristics may be considered from several aspects to achieve a biomimetic microenvironment, including zone-specific matrix composition, collagen fibre orientation, mechanical properties, cellular phenotypes, and bioactive factors [213,214].

As seen through the example studies discussed in this review, biomimetic multizonal cartilage scaffolds hold great promise in restoring the physical and biochemical properties necessary for recreating the stratified structure seen in native articular cartilage. However, a few factors need to be considered for translating the outcomes of current studies towards clinical applications. For instance, many of the studies discussed in the review have focused on recreating the zonal architecture or composition of articular cartilage, but did not actually verify the ability of the scaffold design to induce zone-specific cellular behaviour *in vitro* or better cartilage repair outcomes *in vivo*. Moreover, it is relatively easier to create separate scaffold layers for satisfying the disparate requirements of zonal cartilage and subchondral bone regeneration, imposing challenges for seamless integration at the layer interfaces. In particular, the transition in properties from one layer to the next can introduce a mismatch in mechanical properties and degradation rates, leading to increased shear stress between layers and a risk of non-integration or scaffold failure when used in load-bearing regions. This risk increases with the number of distinct layers within a single scaffold, which may also hinder the rate of integration with host tissues [10]. The greater processing complexity of zonal compared to homogeneous chondral scaffolds may pose another issue, as this reduces the reproducibility of fabrication and scale-up potential. This issue may be exacerbated by the popular selection of naturally-derived materials for constructing chondral scaffolds, which often present batch-to-batch variability in composition or properties [215]. Hence, despite the apparent advantages of biomimetic multizonal scaffold designs for cartilage regeneration, current limitations in materials selection and

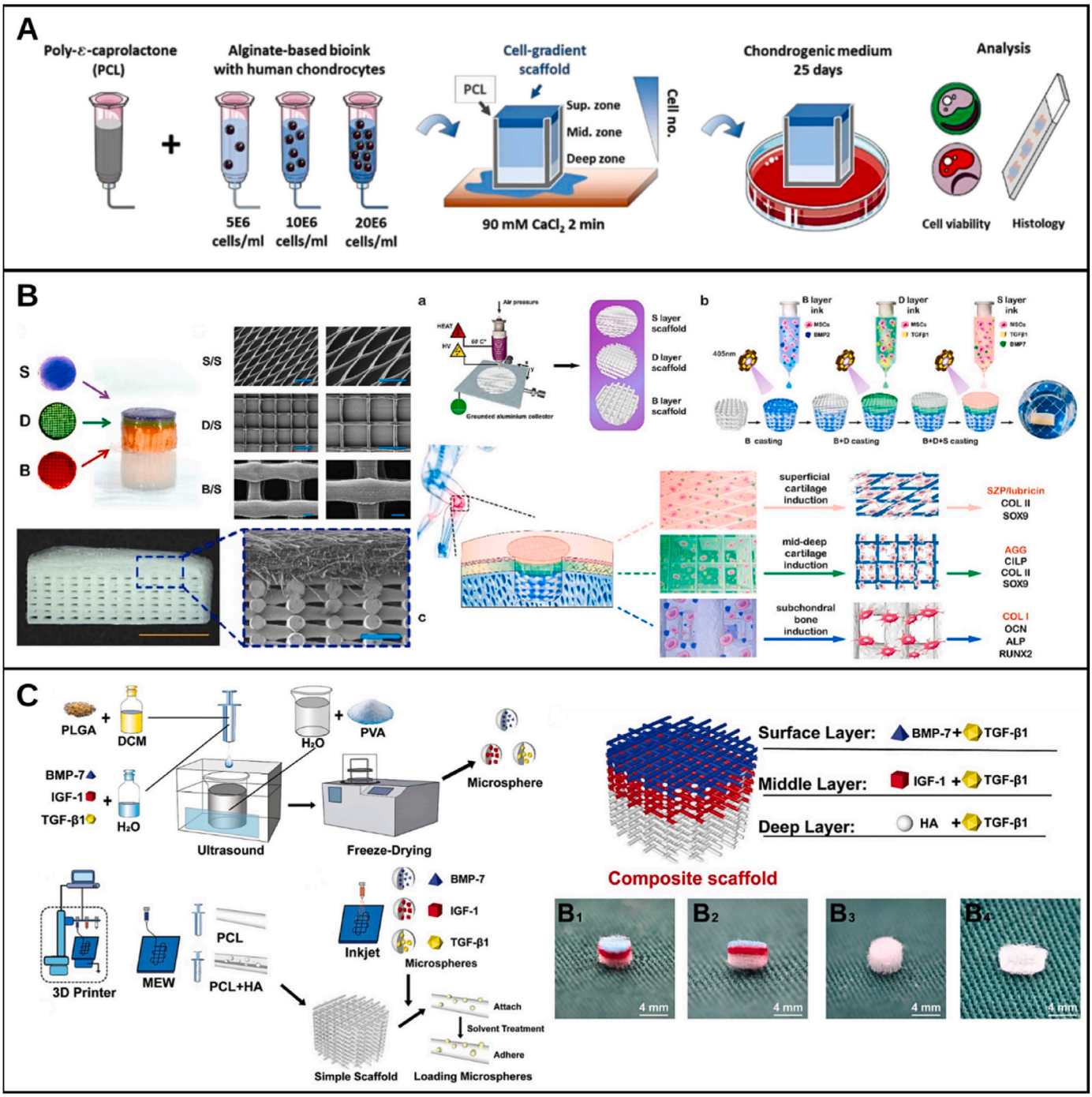

Fig. 8. Examples of zonal cartilage scaffolds based on variations in cell type or growth factors. **(A)** Zonal-specific cell density scaffold mimicking the natural cell concentrations across superficial, middle and deep cartilage zones, adapted with permission from Ref. [112]. **(B)** Bioinspired stratified electrowritten fibre-reinforced hydrogel constructs with zone-specific variation in the growth factors BMP-2, TGF-β1 and BMP-7 across the subchondral bone, middle-deep cartilage zone, and superficial cartilage zone, adapted with permission from Ref. [22]. **(C)** High-precision multilayer scaffolds with zone-specific variation in the growth factors BMP-7 and IGF-1 to resemble the depth-dependent microenvironment of articular cartilage, adapted with permission from Ref. [136].

manufacturing techniques may pose some practical hurdles for generating complex scaffolds that are suitable for real-world applications. While these limitations are beginning to be addressed by continuous advances in biomaterials and biomanufacturing technologies, further research on cartilage scaffolds should aim to strike a balance between the benefits and limitations of employing a biomimetic multizonal design.

5.1. *Future directions in designing multizonal cartilage scaffolds*

Some of the abovementioned issues for creating practically-relevant, biomimetic multizonal scaffolds may be addressed through advances in biomanufacturing to achieve greater precision and control over scaffold characteristics, including fabrication techniques such as 3D bioprinting [168,216] and direct writing electrospinning [163], and imaging techniques such as MRI to guide the design of patient-specific biometric scaffolds that incorporate details about the morphology and

composition of native tissue [217]. Through the integration of new fabrication technologies and biomaterial selections, scaffold designs can be generated with tailored geometries and material properties that closely mimic the native tissue environment [218]. Moreover, multi-modal approaches incorporating stem cells, growth factors, and other bioactive molecules hold promise for improving patient-specific tissue regeneration and scaffold-tissue integration [219]. Ongoing research into biomimetic materials with tunable mechanical properties and degradation rates may help to address the challenges of mismatched mechanical properties and variability in biodegradation rates between scaffold layers [22,192,220]. Meanwhile, advanced computational modelling will further aid in scaffold design optimisation, enabling the prediction of scaffold-tissue interactions based on scaffold architecture and mechanical behaviour [221,222]. Artificial intelligence (AI) can be leveraged to optimise cell populations and deliver zone-specific growth factors, thereby streamlining the research process and reducing costs and time associated with experimentation [223]. The advancement of biomimetic scaffolds into bionic scaffolds that simultaneously deliver

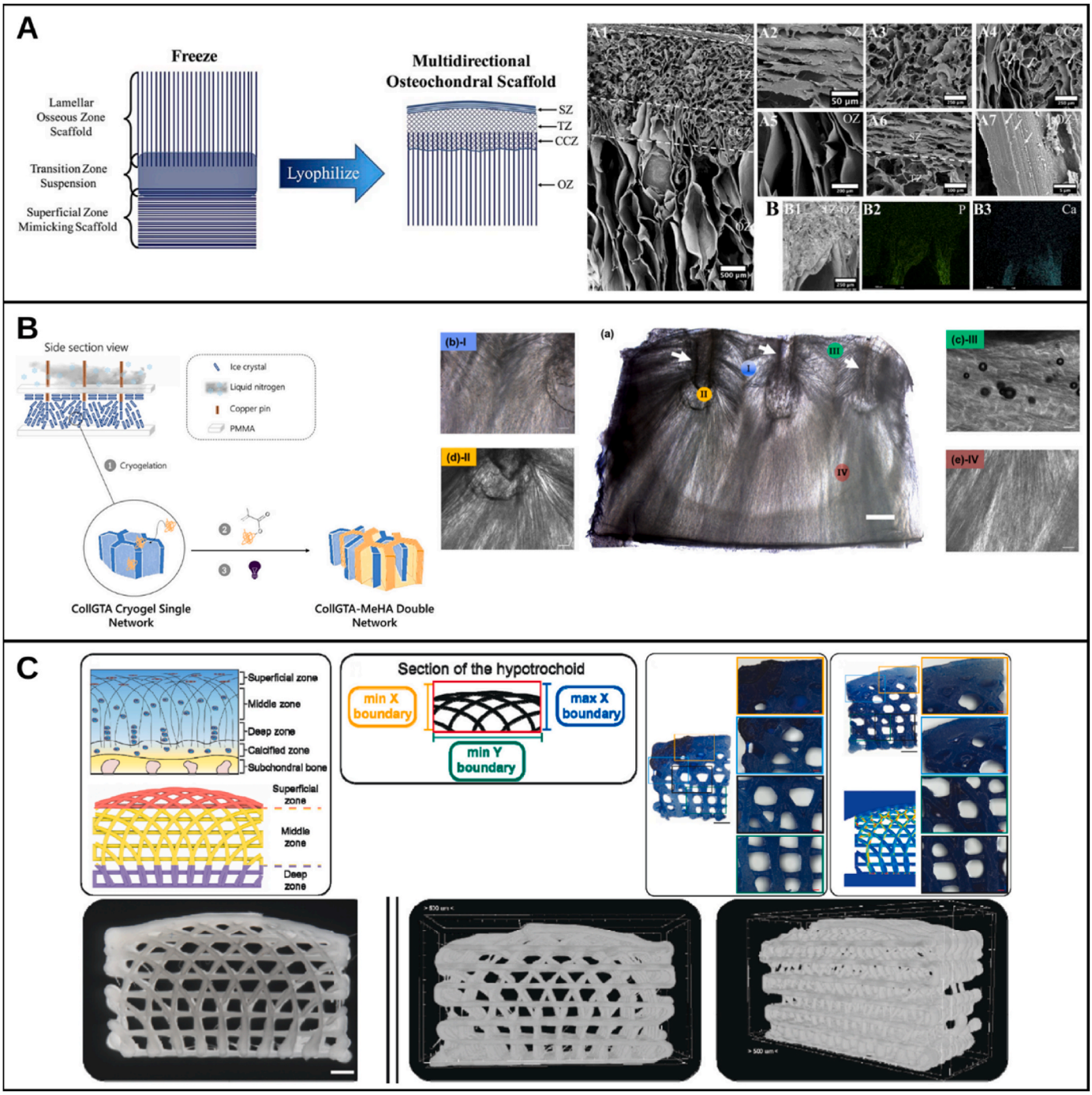

Fig. 9. Other types of special designs for zonal cartilage scaffolds. **(A)** Multidirectional osteochondral scaffolds generated by directional freezing formed three different pore orientations simulating the collagen fibre spacing of articular cartilage zones, adapted with permission from Ref. [205]. **(B)** Collagen–hyaluronic acid cryogels with arcade-like structure mimicking continuous variations in articular cartilage collagen fibre orientation and force distribution, adapted with permission from Ref. [210]. **(C)** Hypotrochoidal scaffolds resembling the arch-like organisation of collagen type II along the entire depth of articular cartilage, adapted with permission from Ref. [137].

therapeutic effects while enabling in-situ real-time monitoring of tissue repair may lead to a new era of multizonal cartilage scaffolds. For instance, utilising electroactive nature of living organisms, smart nanoengineered electronic scaffolds may be developed to stimulate cartilage repair while also providing timely assessment of disease progression and treatment effects [224].

As an alternative to creating distinct scaffold layers for representing the zone-specific properties of articular cartilage, emerging one-pot strategies based on innovative fabrication techniques may provide new food for thought. For example, a new light-based biofabrication method known as Filamented Light (FLight) can be applied to photosensitive bioresins to efficiently create macroporous anisotropic scaffolds, composed of hydrogels containing microchannels of 14 ± 5 μm and microfilaments of 8 ± 2 μm [225]. This scaffold was found to be effective in instructing anisotropic cell growth and directional deposition of collagen, resulting in improved maturation of cartilage-like tissues that mimicked the ECM architecture and mechanical properties of native deep zone cartilage. Another study utilised laser micro-patterning technology (LMPT) to directly modify the surface of native porcine osteochondral grafts [226]. By optimising LMPT parameters to create the most suitable density and morphology of pores on the graft surface, the osteochondral grafts demonstrated improved permeability while maintaining mechanical stability, enabling more efficient decellularisation and subsequent recellularisation for use as osteochondral transplants. *In vivo* implantation in a goat model showed significant regeneration of both cartilage and subchondral bone at 6 and 12 months. While these examples did not specifically attempt to recreate the zonal cartilage structure, they provided a simple approach for generating biomimetic osteochondral tissue that could potentially include zonal variations in the chondral region.

Other exciting advances in scaffold biomanufacturing for tissue engineering include 4D bioprinting, which has evolved from 3D bioprinting but with the addition of a fourth dimension – time [227]. This allows the construction of smart or stimuli-responsive dynamic scaffolds that exhibit programmable variation in structure, properties, and functionality over time or when exposed to specific external stimuli, such as pH, light, temperature, water, and electric or magnetic fields. The programmable dynamic structures of 4D printed scaffolds can be achieved by using smart bioinks, comprising specialised materials capable of altering their shape or characteristics when exposed to external cues. Current biomaterials employed as smart bioinks include shape memory polymers (SMPs), shape-morphing hydrogels (SMHs), and their composite materials. Based on some limited evidence of applying 4D bioprinting in cartilage tissue engineering [228], SMHs may be more favourable than SMPs for this purpose, due to their ability to undergo reversible shape deformation in response to external stimuli [229]. SMHs may therefore mimic the dynamic and functional properties of native cartilage, by adapting their structure over time to better integrate with the surrounding tissue or respond to physiological changes. Some examples of SMHs used as bioinks in 4D bioprinting to generate cartilage-like tissue constructs include silk fibroin [230], oxidized methacrylate alginate (OMA) without [231] or with GelMA [232], and tyramine-functionalised hyaluronan (HAT) without or with alginate [233].

Future strategies in using bioprinting to construct multizonal cartilage scaffolds may also benefit from the integration of nanoparticles, to create nanocomposite scaffolds with enhanced control over their structural, physicochemical, mechanical, and biological properties, stemming from the shape, size, surface chemistry, concentration, and/or source material of the nanoparticles [234]. A diverse array of nanomaterials have been integrated into bioinks for scaffold biopirinting, including carbon-based nanoparticles such as graphene and graphene oxide, carbon nanotubes, and carbon nanofibers; ceramic nanoparticles such as silica-based bioceramics, calcium phosphates, various oxides, and bioactive glasses; natural and synthetic biopolymeric nanoparticles; and a variety of metallic nanoparticles. Excitingly, the incorporation of nanomaterials may help with 4D bioprinting of cartilage scaffolds. In addition to conferring improved mechanical strength to the polymeric matrix, nanoparticles may be stimuli-responsive, thereby allowing the bioprinted nanocomposite scaffold to respond with changes in properties under exogenous cues. For example, Ricotti's group used 4D printing to create a nanocomposite bioactive hydrogel that incorporated piezoelectric barium titanate nanoparticles and graphene oxide nanoflakes [235]. This was the first study to explore the synergistic use of piezoelectric nanomaterials with ultrasound stimulation for enhancing cartilage regeneration. Adipose-derived MSCs embedded within the hydrogel were stimulated with dose-controlled ultrasound waves at a range of frequencies and intensities. The optimal stimulation regimen at 1 MHz frequency and 250 mW/cm^2 intensity once every two days over ten days resulted in significantly increased expression of chondrogenic genes such as COL2A1, ACAN, and SOX9 with simultaneous reduction of fibrotic and catabolic markers such as COL1A1 and MMP13. The improved anti-inflammatory and chondrogenic responses of MSCs were thought to be enabled by stimulus-responsive changes in the nanocomposite hydrogel, leading to an electric field that modulated mechanotransduction pathways in cells and consequent alterations in gene and protein expression. It should be noted that the type of approach and technology used in this study is still in the very early stages of development, and further *in vivo* studies are needed to demonstrate proof-of-concept. Nevertheless, the emergence of 4D bioprinting and continued innovations in nanocomposite materials may be partnered to help with the design of a new generation of multizonal cartilage scaffolds.

5.2. Preclinical evaluation of multizonal cartilage scaffolds

To evaluate the potential efficacy of new multizonal cartilage scaffolds, their biological performance needs to be rigorously assessed *in vitro* and *in vivo* using physiologically relevant preclinical models. The evaluation of tissue repair outcomes should be conducted through comprehensive and comparable analytical methods. However, there is significant heterogeneity among studies reporting new chondral and osteochondral scaffolds in their use of *in vitro* and *in vivo* evaluation methods [236], which is also reflected in the example studies listed in Table 2. This makes it extremely difficult to meaningfully compare outcomes among studies, or identify 'optimal' scaffold designs.

The majority of studies in Table 2 conducted *in vitro* evaluation of the reported scaffolds, mainly using chondrocytes and/or MSCs derived from humans or other species such as murine, leporine, and bovine. To assess biocompatibility, cell viability or proliferation was usually measured over 1–7 days after seeding onto scaffolds, while chondrogenic differentiation was measured at 3–5 weeks usually by gene expression or immunofluorescence staining of cartilage markers. A few studies also conducted long-term *in vitro* cultures to assess cartilage-like tissue maturation within the scaffolds, such as over 6 weeks [21] or 9 weeks [162]. For multizonal cartilage scaffolds, their ability to generate or maintain zone-specific cellular or ECM properties from the superficial to deep layers should be an essential part of the *in vitro* evaluation, although this was only performed in some of the studies [21,22,62,99,112,136]. Considering the possible influences of a chronic injury or osteoarthritic joint environment on resident cells [7], it would also be relevant to test the cartilage regeneration capacity of scaffolds using cells derived from diseased joint tissues, although this was only attempted in one of the discussed studies [210].

Only ~30 % of studies in Table 2 performed *in vivo* evaluation using a preclinical animal model, the majority of which employed chondral or osteochondral defects in small animals such as rats or rabbits. Only two studies evaluated the scaffold in larger animals, one in micropigs [203] and another in skeletally mature pigs [99], both over a 6 month period. Steele et al.'s study in mature pigs with average weight of 78 kg was one of the very few in the broader field of osteochondral scaffolds to have used a physiologically and clinically relevant animal model with weight,

skeletal structure and maturity, and injury type mimicking those of humans. Interestingly, they found that the multizonal scaffold could support *in vitro* chondrogenesis with zone-specific properties, but the same scaffold did not produce better cartilage repair quality compared to the commercially available MaioRegen® control scaffold (without zonal architecture in the chondral layer). This comprehensive study highlighted the translational challenges associated with heterogeneous regeneration outcomes for scaffold-based approaches when scaling up from *in vitro* and small animal models. In the broader field of osteochondral scaffolds without zonal cartilage architecture, limited studies have investigated various types of single- or bi-layered scaffolds in large animals, using caprine and ovine [72,237–242] or equine [243] models. While the scientific community concurs that large animal models are more clinically relevant due to their skeletal similarities to humans, including anatomical size, cartilage thickness, and tissue regeneration potential, the use of these models remains restricted by complex logistical, financial, and ethical challenges [244]. In light of this, there is a need for better standardisation of *in vivo* evaluation methods to enable more meaningful comparisons among studies which used different types and sizes of animal models for scaffold testing,

To evaluate whether multizonal cartilage scaffolds can induce physiologically relevant tissue regeneration and functional recovery of the cartilage injury in animal models, rather than simply filling the defect with an anatomically similar but functionally futile implant, preclinical assessments should involve detailed analysis of the macroscopic, microscopic, and functional characteristics of the regenerated tissue. Macroscopic evaluation is conducted in the majority of *in vivo* studies testing osteochondral scaffolds, where gross morphological inspection of the implantation site can serve as a first-line screening tool to rule out ineffective designs, and allow straightforward comparison between studies. For example, it gives direct visual information on scaffold integration with the surrounding tissue, and the level or quality of cartilage repair, noting that a yellow or brownish tissue may be an indication of undesirable fibrocartilage formation. There is some consensus in the macroscopic scoring systems used in the literature for scaffold-based osteochondral repair, with >50 % of studies published since 2015 using the International Cartilage Repair Society (ICRS) scoring system [236] that evaluates the degree of defect repair, integration of the border zone, and macroscopic cartilage appearance. Other studies have used alternative scoring systems such as the Wayne score [245], which is based on tissue coverage, colour, surface, and defect margins.

For microscopic evaluation of repair tissue quality, studies on osteochondral scaffolds have used heterogeneous analysis methods such as histological staining using general and cartilage-specific stains, as well as immunofluorescence or immunohistochemical staining for cartilage matrix components [246]. A comprehensive evaluation of microscopic cartilage repair quality can be derived by combining the observations of different stains, including: i) haematoxylin and eosin (H&E) for overall cellular organisation and morphology, tissue integration, ECM formation, surface smoothness, any inflammatory infiltration and scaffold degradation; ii) Masson's trichrome or picosirius red for collagen expression and fibre orientation; iii) safranin O/fast green or toluidine blue for cartilage matrix components such as glycosaminoglycans (GAGs), mineralisation of subchondral bone, and tidemark formation. A variety of histological scoring systems have been used, each considering different aspects of the repair tissue quality, including ICRS [247], OARSI [248], Wakitani [249], O'Driscoll [250], and the newer modified O'Driscoll [251] scoring systems. To confirm whether the repair tissue is hyaline cartilage or fibrocartilage, histological findings can be coupled with immunohistochemistry to identify the presence of different collagens. The vast majority of studies that conducted immunohistochemical analysis examined collagen type II as an essential ECM component of hyaline cartilage, followed by collagen type I as an indication of fibrocartilage. The examination of other relevant markers is more limited, such as aggrecan and Sox9 for cartilage, collagen type X for calcified cartilage, and osteocalcin for subchondral bone [236,246].

As a final point, functional evaluation of implanted osteochondral scaffolds should be an essential component of scaffold testing in preclinical studies, to ensure that the scaffold can help sustain physiological loads. This is often a challenge in translating new scaffold designs, as they may achieve favourable macroscopic and histological repair outcomes but fall short of the requirements for restoring normal joint biomechanics. However, mechanical testing has only been conducted in <20 % of preclinical studies on osteochondral scaffolds [236]. Among the analytical techniques used, indentation test was the most common followed by compression loading, while push-out test was rarely performed. Considering the patterns of physiological loading in native osteochondral tissues, a combination of nanoindentation, compression, and push-out or shear testing would give the best indication of the functional biomechanical properties of the osteochondral scaffold or repair tissues, by providing information on tissue stiffness, compressive strength, stress relaxation, strain at failure, and interfacial strength [252,253]. As new designs of multizonal cartilage scaffolds evolve, the use of comprehensive and standardised *in vitro* and *in vivo* evaluation methods for their biological performance would accelerate the journey of translation into clinical applications.

5.3. Towards clinical applications of multizonal cartilage scaffolds

Currently, there are no multizonal cartilage scaffolds with zonal cartilage design that have become commercially available or been tested in clinical studies. All current scaffolds have only been tested *in vitro* or in preclinical *in vivo* models. Nevertheless, a few multiphasic osteochondral scaffolds containing a bulk cartilage compartment are commercially available and have been tested in early-stage clinical studies, such as MaioRegen® (Finceramica, Italy), Agili-C™ (CartiHeal, Israel), and Chondrotissue® (BioTissue, Switzerland) [15]. While the early results are promising, their longer-term performance in achieving physiologically relevant osteochondral repair and preventing injury-related progression of degenerative joint diseases require continuous monitoring. The successful progression of osteochondral scaffolds from preclinical testing to clinical studies demonstrates the future potential to apply multizonal cartilage scaffolds in the clinical repair of chondral and osteochondral injuries. However, as noted with commercially available osteochondral scaffolds [15], the scaffold design as well as incorporation of cellular or biologically active components may be critical influences to long-term repair outcomes using multizonal cartilage scaffolds.

The transformation of multizonal osteochondral scaffolds from experimental research into clinical applications presents a myriad of regulatory challenges. A primary hurdle is the stringent approval process required for innovative biomedical devices and tissue-engineered products. Regulatory bodies such as the U.S. Food and Drug Administration (FDA) and the European Medicines Agency (EMA) have established rigorous frameworks to ensure the safety, efficacy, and quality of complex medical products. These frameworks require comprehensive preclinical studies demonstrating biocompatibility, mechanical integrity, and biological functionality, followed by phased clinical trials to assess therapeutic outcomes in humans. The pathway of scaffold-based tissue engineering therapy from experimental design to clinical application can take three routes: a traditional pathway of clinical trials designed to collect research evidence; the non-research innovative therapy pathway of improving patient accessibility such as off-label use, compassionate use, and hospital exemption; and unproven commercial interventions that are ready to be marketed prior to completion of proof of efficacy and safety [254]. The first key challenge in this process is the demonstration of consistent manufacturing practices for multizonal scaffolds, which often involve intricate biomaterial compositions and multi-step fabrication processes [255]. The reproducibility and scalability of scaffold production must meet Good Manufacturing Practice (GMP) standards to ensure product reliability and safety [256]. This

requirement poses challenges for many types of complex scaffold designs in scaling from small-batch laboratory production to large-scale clinical manufacturing.

The second key challenge is the diverse regulatory classification schemes applied to novel multilayered scaffold products, each with distinct regulatory pathways and requirements, impacting the time and resources required for market approval [257]. Depending on the product composition, regulatory agencies such as the FDA and EMA may categorise the same product differently. Currently, there is no dedicated regulatory framework for tissue engineering products, resulting in the combined use of regulations for both medical devices and biological products. Cell-based products are typically classified as biological products or drugs, while cell-free strategies are often categorised as medical devices. In clinical practice, tissue engineered scaffolds with a cellular component may be assessed as combination products, with the primary focus on the drug or biological component and the device considered secondary. This dual classification often results in extended and costly regulatory approval processes. The stringent requirements for biological or combination products, which entail more rigorous testing and longer timelines, have led to increased interest in developing cell-free materials for cartilage repair [257,258]. Moreover, the same tissue engineered product may be categorised differently depending on the jurisdiction responsible for its oversight. For example, in the European Union, it may be classified as a Tissue Engineered Product or Combined Advanced Therapy Medicinal Product (TEP/CATMP); in the United States, as human cells, tissues, and cellular and tissue-based products (HCT/Ps); in Canada, as a biologic drug; in Australia, biologicals; in Japan, as a regenerative medicine product; and in South Korea, as a biological cell therapy product. Each country has its own specific authorisation process, with varying requirements and timelines, leading to significant differences in regulatory compliance, which may favour the market translation of one particular type of product to some countries [257,259].

Another regulatory challenge is the definition and standardisation of clinical endpoints in trials involving multizonal scaffolds [258]. Stratified chondral and osteochondral defects encompass a wide range of severity and patient-specific factors, complicating the establishment of universally accepted outcome measures. Regulatory bodies require clear demonstration of clinical benefit, which necessitates rigorous and often lengthy clinical trials with appropriate control groups and long-term follow-up. To boost bench to bedside translation, a global initiative aimed at standardising the international classification and regulatory evaluation pathways of multizonal osteochondral scaffold products is in progress [257,259].

Despite the significant need to develop biomimetic osteochondral scaffolds in orthopaedic medicine, very few scaffolds have proceeded to evaluation in clinical studies. Currently, the commercially available osteochondral scaffolds such as MaioRegen® and Agili-C™ contain a homogenous cartilage layer which does not account for zone-specific variations in native articular cartilage [14,15]. Global research effort into biomimetic multizonal scaffolds will hopefully bring us closer to a clinical solution for chondral and osteochondral defects, through innovations in materials science, fabrication technologies, design methods, and collaborations across disciplines to enable the creation of bioactive, functionally mimetic, personalisable, and smart scaffolds.

CRediT authorship contribution statement

Xiaoqi Lin: Writing – review & editing, Writing – original draft, Methodology, Investigation, Formal analysis, Conceptualization. **Ye Zhang:** Writing – review & editing, Writing – original draft, Investigation, Formal analysis. **Jiarong Li:** Writing – review & editing, Writing – original draft, Investigation, Formal analysis. **Brian G. Oliver:** Writing – review & editing, Formal analysis. **Bin Wang:** Writing – review & editing, Formal analysis. **Haiyan Li:** Writing – review & editing, Supervision, Formal analysis. **Ken-Tye Yong:** Writing – review & editing, Supervision, Formal analysis. **Jiao Jiao Li:** Writing – review & editing, Writing – original draft, Supervision, Methodology, Investigation, Formal analysis, Conceptualization.

Declaration of competing interest

There are no conflicts of interest to declare.

Acknowledgements

We acknowledge funding support from the National Stem Cell Foundation of Australia.

References

[1] L. Zhou, V.O. Gjvm, J. Malda, M.J. Stoddart, Y. Lai, R.G. Richards, K. Ki-Wai Ho, L. Qin, Innovative tissue-engineered strategies for osteochondral defect repair and regeneration: current progress and challenges, Adv. Healthcare Mater. 9 (2020) 2001008.
[2] D.C. Flanigan, J.D. Harris, T.Q. Trinh, R.A. Siston, R.H. Brophy, Prevalence of chondral defects in athletes' knees: a systematic review, Med. Sci. Sports Exerc. 42 (2010) 1795–1801.
[3] F. Accadbled, J. Vial, J. Sales de Gauzy, Osteochondritis dissecans of the knee, Orthop. Traumatol. Surg. Res. 104 (2018) S97–S105.
[4] A.J. Sophia Fox, A. Bedi, S.A. Rodeo, The basic science of articular cartilage: structure, composition, and function, Sport Health 1 (2009) 461–468.
[5] D. Dehghan-Baniani, B. Mehrjou, P.K. Chu, W.Y.W. Lee, H. Wu, Recent advances in "functional engineering of articular cartilage zones by polymeric biomaterials mediated with physical, mechanical, and biological/chemical cues", Adv. Healthcare Mater. 12 (2023) e2202581.
[6] L.P. Yan, J.M. Oliveira, A.L. Oliveira, R.L. Reis, Current concepts and challenges in osteochondral tissue engineering and regenerative medicine, ACS Biomater. Sci. Eng. 1 (2015) 183–200.
[7] V. Shang, J. Li, C.B. Little, J.J. Li, Understanding the effects of mesenchymal stromal cell therapy for treating osteoarthritis using an in vitro co-culture model, Eur. cells mater 45 (2023) 143–157.
[8] M.T. Frassica, M.A. Grunlan, Perspectives on synthetic materials to guide tissue regeneration for osteochondral defect repair, ACS Biomater. Sci. Eng. 6 (2020) 4324–4336.
[9] W. Wei, H. Dai, Articular cartilage and osteochondral tissue engineering techniques: recent advances and challenges, Bioact. Mater. 6 (2021) 4830–4855.
[10] O. Urbanek, D. Kołbuk, M. Wróbel, Articular cartilage: new directions and barriers of scaffolds development – review, Int. J. Polym. Mater. 68 (2018) 396–410.
[11] T. Paatela, A. Vasara, H. Nurmi, H. Kautiainen, I. Kiviranta, Assessment of cartilage repair quality with the international cartilage repair society score and the oswestry arthroscopy score, J. Orthop. Res. 38 (2020) 555–562.
[12] M. Wasyleczko, W. Sikorska, A. Chwojnowski, Review of synthetic and hybrid scaffolds in cartilage tissue engineering, Membranes 10 (2020) 348.
[13] Z. Wang, H. Le, Y. Wang, H. Liu, Z. Li, X. Yang, C. Wang, J. Ding, X. Chen, Instructive cartilage regeneration modalities with advanced therapeutic implantations under abnormal conditions, Bioact. Mater. 11 (2022) 317–338.
[14] C. Ai, Y.H.D. Lee, X.H. Tan, S.H.S. Tan, J.H.P. Hui, J.C. Goh, Osteochondral tissue engineering: perspectives for clinical application and preclinical development, J. Orthop. Translat. 30 (2021) 93–102.
[15] R. Chen, J.S. Pye, J. Li, C.B. Little, J.J. Li, Multiphasic scaffolds for the repair of osteochondral defects: outcomes of preclinical studies, Bioact. Mater. 27 (2023) 505–545.
[16] B. Zhang, J. Huang, R.J. Narayan, Gradient scaffolds for osteochondral tissue engineering and regeneration, J. Mater. Chem. B 8 (2020) 8149–8170.
[17] J.J. Chung, H. Im, S.H. Kim, J.W. Park, Y. Jung, Toward biomimetic scaffolds for tissue engineering: 3D printing techniques in regenerative medicine, Front. Bioeng. Biotechnol. 8 (2020) 586406.
[18] S. Jiang, M. Wang, J. He, A review of biomimetic scaffolds for bone regeneration: toward a cell-free strategy, Bioeng. Transl. Med. 6 (2021) e10206.
[19] S. Wu, X. Liu, K.W.K. Yeung, C. Liu, X. Yang, Biomimetic porous scaffolds for bone tissue engineering, Mater. Sci. Eng., R 80 (2014) 1–36.
[20] J. Wang, Y. Wang, X. Sun, D. Liu, C. Huang, J. Wu, C. Yang, Q. Zhang, Biomimetic cartilage scaffold with orientated porous structure of two factors for cartilage repair of knee osteoarthritis, Artif. Cells, Nanomed. Biotechnol. 47 (2019) 1710–1721.
[21] Y. Sun, Q. Wu, Y. Zhang, K. Dai, Y. Wei, 3D-bioprinted gradient-structured scaffold generates anisotropic cartilage with vascularization by pore-size-dependent activation of HIF1α/FAK signaling axis, Nanomedicine. 37 (2021) 102426.
[22] Z. Qiao, M. Lian, Y. Han, B. Sun, X. Zhang, W. Jiang, H. Li, Y. Hao, K. Dai, Bioinspired stratified electrowritten fiber-reinforced hydrogel constructs with layer-specific induction capacity for functional osteochondral regeneration, Biomaterials 266 (2021) 120385.
[23] L. Yu, S. Cavelier, B. Hannon, M. Wei, Recent development in multizonal scaffolds for osteochondral regeneration, Bioact, Mater. 25 (2023) 122–159.

[24] L. Fu, Z. Yang, C. Gao, H. Li, Z. Yuan, F. Wang, X. Sui, S. Liu, Q. Guo, Advances and prospects in biomimetic multilayered scaffolds for articular cartilage regeneration, Regen. Biomater. 7 (2020) 527–542.
[25] S.E. Doyle, F. Snow, S. Duchi, C.D. O'Connell, C. Onofrillo, C. Di Bella, E. Pirogova, 3D printed multiphasic scaffolds for osteochondral repair: challenges and opportunities, Int. J. Mol. Sci. 22 (2021) 12420.
[26] J. Antons, M.G.M. Marascio, J. Nohava, R. Martin, L.A. Applegate, P.E. Bourban, D.P. Pioletti, Zone-dependent mechanical properties of human articular cartilage obtained by indentation measurements, J. Mater. Sci. Mater. Med. 29 (2018) 57.
[27] W. Wang, R. Ye, W. Xie, Y. Zhang, S. An, Y. Li, Y. Zhou, Roles of the calcified cartilage layer and its tissue engineering reconstruction in osteoarthritis treatment, Front. Bioeng. Biotechnol. 10 (2022) 911281.
[28] X. Wang, Z. Zhu, H. Xiao, C. Luo, X. Luo, F. Lv, J. Liao, W. Huang, Three-Dimensional, MultiScale, and interconnected trabecular bone mimic porous tantalum scaffold for bone tissue engineering, ACS Omega 5 (2020) 22520–22528.
[29] M. Tamaddon, L. Wang, Z. Liu, C. Liu, Osteochondral tissue repair in osteoarthritic joints: clinical challenges and opportunities in tissue engineering, Bio-Des, Man (Lond.) 1 (2018) 101–114.
[30] J.J. Li, D.L. Kaplan, H. Zreiqat, Scaffold-based regeneration of skeletal tissues to meet clinical challenges, J. Mater. Chem. B 2 (2014) 7272–7306.
[31] F. Buttgereit, G.R. Burmester, J.W. Bijlsma, Non-surgical management of knee osteoarthritis: where are we now and where do we need to go? RMD Open 1 (2015) e000027.
[32] K. Solanki, S. Shanmugasundaram, N. Shetty, S.J. Kim, Articular cartilage repair & joint preservation: a review of the current status of biological approach, J. Clin. Orthop. Trauma. 22 (2021) 101602.
[33] S.H. Edwards, Intra-articular drug delivery: the challenge to extend drug residence time within the joint, Vet. J. 190 (2011) 15–21.
[34] C. Cooper, R. Chapurlat, N. Al-Daghri, G. Herrero-Beaumont, O. Bruyere, F. Rannou, R. Roth, D. Uebelhart, J.Y. Reginster, Safety of oral non-selective non-steroidal anti-inflammatory drugs in osteoarthritis: what does the literature say? Drugs Aging 36 (2019) 15–24.
[35] B. Gallagher, F.P. Tjoumakaris, M.I. Harwood, R.P. Good, M.G. Ciccotti, K. B. Freedman, Chondroprotection and the prevention of osteoarthritis progression of the knee: a systematic review of treatment agents, Am. J. Sports Med. 43 (2015) 734–744.
[36] N. Garg, L. Perry, A. Deodhar, Intra-articular and soft tissue injections, a systematic review of relative efficacy of various corticosteroids, Clin. Rheumatol. 33 (2014) 1695–1706.
[37] M. Telikicherla, S.U. Kamath, Accuracy of needle placement into the intra-articular space of the knee in osteoarthritis patients for viscosupplementation, J. Clin. Diagn. Res. 10 (2016) RC15–R17.
[38] M.M. Richards, J.S. Maxwell, L. Weng, M.G. Angelos, J. Golzarian, Intra-articular treatment of knee osteoarthritis: from anti-inflammatories to products of regenerative medicine, Phys. Sportsmed. 44 (2016) 101–108.
[39] G.D. Abrams, R.M. Frank, L.A. Fortier, B.J. Cole, Platelet-rich plasma for articular cartilage repair, Sports Med. Arthrosc. Rev. 21 (2013) 213–219.
[40] S. Shanmugasundaram, A. Vaish, V. Chavada, W.D. Murrell, R. Vaishya, Assessment of safety and efficacy of intra-articular injection of stromal vascular fraction for the treatment of knee osteoarthritis-a systematic review, Int. Orthop. 45 (2021) 615–625.
[41] Y.H. Chang, H.W. Liu, K.C. Wu, D.C. Ding, Mesenchymal stem cells and their clinical applications in osteoarthritis, Cell Transplant. 25 (2016) 937–950.
[42] J.G. Kim, Y.A. Rim, J.H. Ju, The role of transforming growth factor beta in joint homeostasis and cartilage regeneration, Tissue Eng. C Methods 28 (2022) 570–587.
[43] D. Dallari, C. Stagni, N. Rani, G. Sabbioni, P. Pelotti, P. Torricelli, M. Tschon, G. Giavaresi, Ultrasound-guided injection of platelet-rich plasma and hyaluronic acid, separately and in combination, for hip osteoarthritis: a randomized controlled study, Am. J. Sports Med. 44 (2016) 664–671.
[44] G. Wang, D. Xing, W. Liu, Y. Zhu, H. Liu, L. Yan, K. Fan, P. Liu, B. Yu, J.J. Li, B. Wang, Preclinical studies and clinical trials on mesenchymal stem cell therapy for knee osteoarthritis: a systematic review on models and cell doses, Int. J. Rheum. Dis. 25 (2022) 532–562.
[45] R. Soler, L. Orozco, A. Munar, M. Huguet, R. Lopez, J. Vives, R. Coll, M. Codinach, J. Garcia-Lopez, Final results of a phase I-II trial using ex vivo expanded autologous Mesenchymal Stromal Cells for the treatment of osteoarthritis of the knee confirming safety and suggesting cartilage regeneration, Knee 23 (2016) 647–654.
[46] E. Estrada, J.L. Decima, M. Rodriguez, M. Di Tomaso, J. Roberti, Patient-reported outcomes after platelet-rich plasma, bone marrow aspirate, and adipose-derived mesenchymal stem cell injections for symptomatic knee osteoarthritis, Clin. Med. Insights Arthritis Musculoskelet. Disord. 13 (2020) 1–4.
[47] B.J. Sherman, J. Chahla, J. Glowney, R.M. Frank, The role of orthobiologics in the management of osteoarthritis and focal cartilage defects, Orthopedics 42 (2019) 66–73.
[48] K. Huebner, R.M. Frank, A. Getgood, Ortho-biologics for osteoarthritis, clin, Sports Med. 38 (2019) 123–141.
[49] Z. Shang, P. Wanyan, B. Zhang, M. Wang, X. Wang, A systematic review, umbrella review, and quality assessment on clinical translation of stem cell therapy for knee osteoarthritis: are we there yet? Stem Cell Res. Ther. 14 (2023) 91.
[50] J.M. Case, J.M. Scopp, Treatment of articular cartilage defects of the knee with microfracture and enhanced microfracture techniques, sports med, Arthrosc. Rev. 24 (2016) 63–68.
[51] D. Goyal, S. Keyhani, E.H. Lee, J.H. Hui, Evidence-based status of microfracture technique: a systematic review of level I and II studies, Arthroscopy 29 (2013) 1579–1588.
[52] R.L. Davies, N.J. Kuiper, Regenerative medicine: a review of the evolution of autologous chondrocyte implantation (ACI) therapy, Bioengineering 6 (2019) 22.
[53] G.H. Gou, F.J. Tseng, S.H. Wang, P.J. Chen, J.F. Shyu, C.F. Weng, R.Y. Pan, Autologous chondrocyte implantation versus microfracture in the knee: a meta-analysis and systematic review, Arthroscopy 36 (2020) 289–303.
[54] E.V. Medvedeva, E.A. Grebenik, S.N. Gornostaeva, V.I. Telpuhov, A.V. Lychagin, P.S. Timashev, A.S. Chagin, Repair of damaged articular cartilage: current approaches and future directions, Int. J. Mol. Sci. 19 (2018) 2366.
[55] K.R. Sochacki, K. Varshneya, J.G. Calcei, M.R. Safran, G.D. Abrams, J. Donahue, C. Chu, S.L. Sherman, Comparison of autologous chondrocyte implantation and osteochondral allograft transplantation of the knee in a large insurance database: reoperation rate, complications, and cost analysis, Cartilage 13 (2021) 1187S, 94S.
[56] C. Parisi, L. Salvatore, L. Veschini, M.P. Serra, C. Hobbs, M. Madaghiele, A. Sannino, L. Di Silvio, Biomimetic gradient scaffold of collagen-hydroxyapatite for osteochondral regeneration, J. Tissue Eng. 11 (2020) 1–13.
[57] S. Ansari, S. Khorshidi, A. Karkhaneh, Engineering of gradient osteochondral tissue: from nature to lab, Acta Biomater. 87 (2019) 41–54.
[58] D. Majda, A. Bhattarai, J. Riikonen, B.D. Napruszewska, M. Zimowska, A. Michalik-Zym, J. Töyräs, V.P. Lehto, New approach for determining cartilage pore size distribution: NaCl-thermoporometry, Microporous Mesoporous Mater. 241 (2017) 238–245.
[59] A. Di Luca, A. Longoni, G. Criscenti, C. Mota, C. van Blitterswijk, L. Moroni, Toward mimicking the bone structure: design of novel hierarchical scaffolds with a tailored radial porosity gradient, Biofabrication 8 (2016) 045007.
[60] I. Sahafnejad-Mohammadi, S. Rahmati, N. Najmoddin, M. Bodaghi, Biomimetic polycaprolactone-graphene oxide composites for 3D printing bone scaffolds, Macromol. Mater. Eng. 308 (2023) 2200558.
[61] J. Jiao, Q. Hong, D. Zhang, M. Wang, H. Tang, J. Yang, X. Qu, B. Yue, Influence of porosity on osteogenesis, bone growth and osteointegration in trabecular tantalum scaffolds fabricated by additive manufacturing, Front. Bioeng. Biotechnol. 11 (2023) 1117954.
[62] D. Wang, H. Xu, J. Liu, Z. Chen, Y. Li, B. Hu, D. Zhang, J. Li, H. Chu, Bio-inspired cellulose reinforced anisotropic composite hydrogel with zone-dependent complex mechanical adaptability and cell recruitment characteristics, Compos. B Eng. (2020) 202.
[63] B. Pouran, A. Raoof, D.A.M. de Winter, V. Arbabi, R. Bleys, F.J. Beekman, A. A. Zadpoor, J. Malda, H. Weinans, Topographic features of nano-pores within the osteochondral interface and their effects on transport properties -a 3D imaging and modeling study, J. Biomech. 123 (2021) 110504.
[64] V.L. Ferguson, A.J. Bushby, A. Boyde, Nanomechanical properties and mineral concentration in articular calcified cartilage and subchondral bone, J. Anat. 203 (2003) 191–202.
[65] X. Wang, S. Xu, S. Zhou, W. Xu, M. Leary, P. Choong, M. Qian, M. Brandt, Y. M. Xie, Topological design and additive manufacturing of porous metals for bone scaffolds and orthopaedic implants: a review, Biomaterials 83 (2016) 127–141.
[66] Y. Harada, H.W. Wevers, T.D.V. Cooke, Distribution of bone strength in the proximal tibia, J. Arthroplasty 3 (1988) 167–175.
[67] J. Scheinpflug, M. Pfeiffenberger, A. Damerau, F. Schwarz, M. Textor, A. Lang, F. Schulze, Journey into bone models: a review, Genes 9 (2018) 247.
[68] O. Al-Ketan, R. Rowshan, R.K. Abu Al-Rub, Topology-mechanical property relationship of 3D printed strut, skeletal, and sheet based periodic metallic cellular materials, Addit. Manuf. 19 (2018) 167–183.
[69] J. Zhou, H. Huang, L.-J. Wang, M. Tamaddon, C.-Z. Liu, Z.-Y. Liu, T.-B. Yu, Y.-Z. Zhang, Stable mechanical fixation in a bionic osteochondral scaffold considering bone growth, Rare Met. 41 (2022) 2711–2718.
[70] Y. Han, M. Lian, Q. Wu, Z. Qiao, B. Sun, K. Dai, Effect of pore size on cell behavior using melt electrowritten scaffolds, Front. Bioeng. Biotechnol. 9 (2021) 629270.
[71] N. Abbasi, S. Hamlet, R.M. Love, N.-T. Nguyen, Porous scaffolds for bone regeneration, JS: amd 5 (2020) 1–9.
[72] M. Tamaddon, G. Blunn, R. Tan, P. Yang, X. Sun, S.M. Chen, J. Luo, Z. Liu, L. Wang, D. Li, R. Donate, M. Monzon, C. Liu, In vivo evaluation of additively manufactured multi-layered scaffold for the repair of large osteochondral defects, Bio-Des. Manuf. 5 (2022) 481–496.
[73] Y. Qin, P. Wen, H. Guo, D. Xia, Y. Zheng, L. Jauer, R. Poprawe, M. Voshage, J. H. Schleifenbaum, Additive manufacturing of biodegradable metals: current research status and future perspectives, Acta Biomater. 98 (2019) 3–22.
[74] F. Deng, L. Liu, Z. Li, J. Liu, 3D printed Ti6Al4V bone scaffolds with different pore structure effects on bone ingrowth, J. Biol. Eng. 15 (2021) 4.
[75] S. Van Bael, Y.C. Chai, S. Truscello, M. Moesen, G. Kerckhofs, H. Van Oosterwyck, J.P. Kruth, J. Schrooten, The effect of pore geometry on the in vitro biological behavior of human periosteum-derived cells seeded on selective laser-melted Ti6Al4V bone scaffolds, Acta Biomater. 8 (2012) 2824–2834.
[76] P.F. Egan, Integrated design approaches for 3D printed tissue scaffolds: review and outlook, Materials 12 (2019) 2355.
[77] S.J.P. Callens, R.J.C. Uyttendaele, L.E. Fratila-Apachitei, A.A. Zadpoor, Substrate curvature as a cue to guide spatiotemporal cell and tissue organization, Biomaterials 232 (2020) 119739.
[78] C. Jiao, D. Xie, Z. He, H. Liang, L. Shen, Y. Yang, Z. Tian, G. Wu, C. Wang, Additive manufacturing of Bio-inspired ceramic bone Scaffolds: structural Design, mechanical properties and biocompatibility, Mater. Des. 217 (2022) 110610.

[79] M. Shen, W. Qin, B. Xing, W. Zhao, S. Gao, Y. Sun, T. Jiao, Z. Zhao, Mechanical properties of 3D printed ceramic cellular materials with triply periodic minimal surface architectures, J. Eur. Ceram. Soc. 41 (2021) 1481–1489.
[80] D.W. Abueidda, M. Bakir, R.K. Abu Al-Rub, J.S. Bergström, N.A. Sobh, I. Jasiuk, Mechanical properties of 3D printed polymeric cellular materials with triply periodic minimal surface architectures, Mater. Des. 122 (2017) 255–267.
[81] F. Teng, Y. Sun, S. Guo, B. Gao, G. Yu, Topological and mechanical properties of different lattice structures based on additive manufacturing, Micromachines 13 (2022) 1017.
[82] P. Bogusz, A. Poplawski, M. Stankiewicz, B. Kowalski, Experimental research of selected lattice structures developed with 3D printing technology, Materials 15 (2022) 378.
[83] H.M.A. Ali, M. Abdi, Y. Sun, Insight into the mechanical properties of 3D printed strut-based lattice structures, Prog. Addit. Manuf. 8 (2022) 919–931.
[84] N. Kladovasilakis, P. Charalampous, K. Tsongas, I. Kostavelis, D. Tzetzis, D. Tzovaras, Experimental and computational investigation of lattice sandwich structures constructed by additive manufacturing technologies, J. Manuf. Mater. Process. 5 (2021) 95.
[85] M. Parkes, F. Tallia, G.R. Young, P. Cann, J.R. Jones, J.R.T. Jeffers, Tribological evaluation of a novel hybrid for repair of articular cartilage defects, Mater. Sci. Eng., C 119 (2021) 111495.
[86] W. Lin, J. Klein, Recent progress in cartilage lubrication, Adv. Mater. 33 (2021) e2005513.
[87] W. Zhao, Y. Zhang, X. Zhao, Z. Ji, Z. Ma, X. Gao, S. Ma, X. Wang, F. Zhou, Bioinspired design of a cartilage-like lubricated composite with mechanical robustness, ACS Appl. Mater. Interfaces 14 (2022) 9899–9908.
[88] S. Affatato, D. Trucco, P. Taddei, L. Vannozzi, L. Ricotti, G.D. Nessim, G. Lisignoli, Wear behavior characterization of hydrogels constructs for cartilage tissue replacement, Materials 14 (2021).
[89] Y. Wu, X. Li, Y. Wang, Y. Shi, F. Wang, G. Lin, Research progress on mechanical properties and wear resistance of cartilage repair hydrogel, Mater. Des. 216 (2022) 110575.
[90] V. Adibnia, M. Mirbagheri, J. Faivre, J. Robert, J. Lee, K. Matyjaszewski, D. W. Lee, X. Banquy, Bioinspired polymers for lubrication and wear resistance, Prog. Polym. Sci. 110 (2020) 101298.
[91] A. Trengove, C. Di Bella, A.J. O'Connor, The challenge of cartilage integration: understanding a major barrier to chondral repair, Tissue Eng., Part B 28 (2022) 114–128.
[92] X. Yang, S. Li, Y. Ren, L. Qiang, Y. Liu, J. Wang, K. Dai, 3D printed hydrogel for articular cartilage regeneration, Compos. B Eng. 237 (2022) 109863.
[93] V. Manescu, I. Antoniac, A. Antoniac, D. Laptoiu, G. Paltanea, R. Ciocoiu, I. V. Nemoianu, L.G. Gruionu, H. Dura, Bone regeneration induced by patient-adapted Mg alloy-based scaffolds for bone defects: present and future perspectives, Biomimetics 8 (2023) 618.
[94] I. Cockerill, Y. Su, S. Sinha, Y.X. Qin, Y. Zheng, M.L. Young, D. Zhu, Porous zinc scaffolds for bone tissue engineering applications: a novel additive manufacturing and casting approach, Mater. Sci. Eng., C 110 (2020) 110738.
[95] L. Li, F. Yu, L. Zheng, R. Wang, W. Yan, Z. Wang, J. Xu, J. Wu, D. Shi, L. Zhu, X. Wang, Q. Jiang, Natural hydrogels for cartilage regeneration: modification, preparation and application, J. Orthop. Translat. 17 (2019) 26–41.
[96] X. Zhao, D.A. Hu, D. Wu, F. He, H. Wang, L. Huang, D. Shi, Q. Liu, N. Ni, M. Pakvasa, Y. Zhang, K. Fu, K.H. Qin, A.J. Li, O. Hagag, E.J. Wang, M. Sabharwal, W. Wagstaff, R.R. Reid, M.J. Lee, J.M. Wolf, M. El Dafrawy, K. Hynes, J. Strelzow, S.H. Ho, T.C. He, A. Athiviraham, Applications of biocompatible scaffold materials in stem cell-based cartilage tissue engineering, Front. Bioeng. Biotechnol. 9 (2021) 603444.
[97] S. Yu, X. Shu, L. Chen, C. Wang, X. Wang, J. Jing, G. Yan, Y. Zhang, C. Wu, Construction of ultrasonically treated collagen/silk fibroin composite scaffolds to induce cartilage regeneration, Sci. Rep. 13 (2023) 20168.
[98] L. Peng, H. Li, H. Deng, T. Gao, R. Li, Z. Xu, Q. Tian, T. Zhao, J. Li, Y. Yang, C. Wang, S. Liu, Q. Guo, Combination of a human articular cartilage-derived extracellular matrix scaffold and microfracture techniques for cartilage regeneration: a proof of concept in a sheep model, J. Orthop. Translat. 44 (2024) 72–87.
[99] J.A.M. Steele, A.C. Moore, J.P. St-Pierre, S.D. McCullen, A.J. Gormley, C. C. Horgan, C.R. Black, C. Meinert, T. Klein, S. Saifzadeh, R. Steck, J. Ren, M. A. Woodruff, M.M. Stevens, In vitro and in vivo investigation of a zonal microstructured scaffold for osteochondral defect repair, Biomaterials 286 (2022) 121548.
[100] X. Bai, M. Gao, S. Syed, J. Zhuang, X. Xu, X.Q. Zhang, Bioactive hydrogels for bone regeneration, Bioact. Mater. 3 (2018) 401–417.
[101] Y. Peng, Y. Zhuang, Y. Liu, H. Le, D. Li, M. Zhang, K. Liu, Y. Zhang, J. Zuo, J. Ding, Bioinspired gradient scaffolds for osteochondral tissue engineering, Explorations 3 (2023) 20210043.
[102] H. Zhang, Y. Lu, L. Huang, P. Liu, J. Ni, T. Yang, Y. Li, Y. Zhong, X. He, X. Xia, J. Zhou, Scalable and versatile metal ion solidificated alginate hydrogel for skin wound infection therapy, Adv. Healthcare Mater. 12 (2024) 2303688.
[103] A. Sergeeva, A.S. Vikulina, D. Volodkin, Porous alginate scaffolds assembled using vaterite CaCO3 crystals, Micromachines 10 (2019) 357.
[104] K. Mikula, D. Skrzypczak, B. Ligas, A. Witek-Krowiak, Preparation of hydrogel composites using Ca2+ and Cu2+ ions as crosslinking agents, SN Appl. Sci. 1 (2019) 643.
[105] Y. Chen, J. Feng, M. Fang, X. Wang, Y. Liu, S. Li, L. Wen, Y. Zhu, L. Jiang, Large-scale, ultrastrong Cu2+ cross-linked sodium alginate membrane for effective salinity gradient power conversion, ACS Appl. Polym. Mater. 3 (2021) 3902–3910.
[106] Z. Cai, Y. Li, W. Song, Y. He, H. Li, X. Liu, Anti-inflammatory and prochondrogenic in situ-formed injectable hydrogel crosslinked by strontium-doped bioglass for cartilage regeneration, ACS Appl. Mater. Interfaces 13 (2021) 59772–59786.
[107] M. Sarker, M. Izadifar, D. Schreyer, X. Chen, Influence of ionic crosslinkers (Ca2+/Ba2+/Zn2+) on the mechanical and biological properties of 3D Bioplotted Hydrogel Scaffolds, J. Biomater. Sci. Polym. Ed. 29 (2018) 1126–1154.
[108] H. Malektaj, A.D. Drozdov, J. deClaville Christiansen, Mechanical properties of alginate hydrogels cross-linked with multivalent cations, Polymers 15 (2023) 3012.
[109] W. Liu, H. Madry, M. Cucchiarini, Application of alginate hydrogels for next-generation articular cartilage regeneration, Int. J. Mol. Sci. 23 (2022) 1147.
[110] P. Yu, Y. Li, H. Sun, X. Ke, J. Xing, Y. Zhao, X. Xu, M. Qin, J. Xie, J. Li, Cartilage-inspired hydrogel with mechanical adaptability, controllable lubrication, and inflammation regulation abilities, ACS Appl. Mater. Interfaces 14 (2022) 27360–27370.
[111] A.A. Golebiowska, S.P. Nukavarapu, Bio-inspired zonal-structured matrices for bone-cartilage interface engineering, Biofabrication 14 (2022) 025016.
[112] A. Dimaraki, P.J. Díaz-Payno, M. Minneboo, M. Nouri-Goushki, M. Hosseini, N. Kops, R. Narcisi, M.J. Mirzaali, G.J.V.M. van Osch, L.E. Fratila-Apachitei, A. A. Zadpoor, Bioprinting of a zonal-specific cell density scaffold: a biomimetic approach for cartilage tissue engineering, Appl. Sci. 11 (2021) 7821.
[113] Y. Cao, P. Cheng, S. Sang, C. Xiang, Y. An, X. Wei, Z. Shen, Y. Zhang, P. Li, Mesenchymal stem cells loaded on 3D-printed gradient poly(ε-caprolactone)/methacrylated alginate composite scaffolds for cartilage tissue engineering, Regen. Biomater. 8 (2021) rbab019.
[114] B. Sultankulov, D. Berillo, K. Sultankulova, T. Tokay, A. Saparov, Progress in the development of chitosan-based biomaterials for tissue engineering and regenerative medicine, Biomolecules 9 (2019) 470.
[115] H. Li, C. Hu, H. Yu, C. Chen, Chitosan composite scaffolds for articular cartilage defect repair: a review, RSC Adv. 8 (2018) 3736–3749.
[116] Y. Shen, Y. Xu, B. Yi, X. Wang, H. Tang, C. Chen, Y. Zhang, Engineering a highly biomimetic chitosan-based cartilage scaffold by using short fibers and a cartilage-decellularized matrix, Biomacromolecules 22 (2021) 2284–2297.
[117] P. Haghighi, A. Shamloo, Fabrication of a novel 3D scaffold for cartilage tissue repair: in-vitro and in-vivo study, Mater. Sci. Eng., C 128 (2021) 112285.
[118] C. Antich, J. de Vicente, G. Jimenez, C. Chocarro, E. Carrillo, E. Montanez, P. Galvez-Martin, J.A. Marchal, Bio-inspired hydrogel composed of hyaluronic acid and alginate as a potential bioink for 3D bioprinting of articular cartilage engineering constructs, Acta Biomater. 106 (2020) 114–123.
[119] T. He, B. Li, T. Colombani, K. Joshi-Navare, S. Mehta, J. Kisiday, S.A. Bencherif, A.G. Bajpayee, Hyaluronic acid-based shape-memory cryogel scaffolds for focal cartilage defect repair, Tissue Eng. 27 (2021) 748–760.
[120] Q. Zhang, H. Lu, N. Kawazoe, G. Chen, Pore size effect of collagen scaffolds on cartilage regeneration, Acta Biomater. 10 (2014) 2005–2013.
[121] V. Irawan, T.C. Sung, A. Higuchi, T. Ikoma, Collagen scaffolds in cartilage tissue engineering and relevant approaches for future development, Tissue Eng. Regen. Med. 15 (2018) 673–697.
[122] C. Intini, M. Lemoine, T. Hodgkinson, S. Casey, J.P. Gleeson, F.J. O'Brien, A highly porous type II collagen containing scaffold for the treatment of cartilage defects enhances MSC chondrogenesis and early cartilaginous matrix deposition, Biomater. Sci. 10 (2022) 970–983.
[123] C. Belda Marin, V. Fitzpatrick, D.L. Kaplan, J. Landoulsi, E. Guenin, C. Egles, Silk polymers and nanoparticles: a powerful combination for the design of versatile biomaterials, Front. Chem. 8 (2020) 604398.
[124] D. Dehghan-Baniani, B. Mehrjou, P.K. Chu, H. Wu, A biomimetic nano-engineered platform for functional tissue engineering of cartilage superficial zone, Adv. Healthcare Mater. 10 (2021) 2001018.
[125] H. Zheng, B. Zuo, Functional silk fibroin hydrogels: preparation, properties and applications, J. Mater. Chem. B 9 (2021) 1238–1258.
[126] A.A. Golebiowska, J.T. Intravaia, V.M. Sathe, S.G. Kumbar, S.P. Nukavarapu, Decellularized extracellular matrix biomaterials for regenerative therapies: advances, challenges and clinical prospects, Bioact. Mater. 32 (2024) 98–123.
[127] P. Xu, R.K. Kankala, S. Wang, A. Chen, Decellularized extracellular matrix-based composite scaffolds for tissue engineering and regenerative medicine, Regen. Biomater. 11 (2023) rbad107.
[128] X. Zhang, X. Chen, H. Hong, R. Hu, J. Liu, C. Liu, Decellularized extracellular matrix scaffolds: recent trends and emerging strategies in tissue engineering, Bioact, Mater 10 (2022) 15–31.
[129] S. Yeleswarapu, S. Chameettachal, A.K. Bera, F. Pati, Smooth muscle matrix bioink promotes myogenic differentiation of encapsulated adipose-derived stem cells, J. Biomed. Mater. Res. A. 110 (2022) 1761–1773.
[130] G. Tian, S. Jiang, J. Li, F. Wei, X. Li, Y. Ding, Z. Yang, Z. Sun, K. Zha, F. Wang, B. Huang, L. Peng, Q. Wang, Z. Tian, X. Yang, Z. Wang, Q. Guo, W. Guo, S. Liu, Cell-free decellularized cartilage extracellular matrix scaffolds combined with interleukin 4 promote osteochondral repair through immunomodulatory macrophages: in vitro and in vivo preclinical study, Acta Biomater. 127 (2021) 131–145.
[131] D.C. Browe, O.R. Mahon, P.J. Díaz-Payno, N. Cassidy, I. Dudurych, A. Dunne, C. T. Buckley, D.J. Kelly, Glyoxal cross-linking of solubilized extracellular matrix to produce highly porous, elastic, and chondro-permissive scaffolds for orthopedic tissue engineering, J. Biomed. Mater. Res. A. 107 (2019) 2222–2234.
[132] Y. Li, Y. Liu, X. Xun, W. Zhang, Y. Xu, D. Gu, Three-Dimensional porous scaffolds with biomimetic microarchitecture and bioactivity for cartilage tissue engineering, ACS Appl. Mater. Interfaces 11 (2019) 36359–36370.

[133] J. Li, B. Jiang, P. Zhang, J. Wu, N. Fan, Z. Chen, Y. Yang, E. Zhang, F. Wang, L. Yang, Cartilage decellularized extracellular matrix-based hydrogel with enhanced tissue adhesion and promoted chondrogenesis for cartilage tissue engineering, ACS Appl. Polym. Mater. 6 (2024) 4394–4408.
[134] Q. Li, H. Yu, F. Zhao, C. Cao, T. Wu, Y. Fan, Y. Ao, X. Hu, 3D printing of microenvironment-specific bioinspired and exosome-reinforced hydrogel scaffolds for efficient cartilage and subchondral bone regeneration, Adv. Sci. 10 (2023) 2303650.
[135] K.D. Ngadimin, A. Stokes, P. Gentile, A.M. Ferreira, Biomimetic hydrogels designed for cartilage tissue engineering, Biomater. Sci. 9 (2021) 4246–4259.
[136] Y. Han, M. Lian, B. Sun, B. Jia, Q. Wu, Z. Qiao, K. Dai, Preparation of high precision multilayer scaffolds based on Melt Electro-Writing to repair cartilage injury, Theranostics 10 (2020) 10214–10230.
[137] K.A. van Kampen, E. Olaret, I.C. Stancu, D.F. Duarte Campos, H. Fischer, C. Mota, L. Moroni, Hypotrochoidal scaffolds for cartilage regeneration, Mater. Today Bio. 23 (2023) 100830.
[138] D. Yari, M.H. Ebrahimzadeh, J. Movaffagh, A. Shahroodi, M. Shirzad, D. Qujeq, A. Moradi, Biochemical aspects of scaffolds for cartilage tissue engineering; from basic science to regenerative medicine, Arch. Bone Jt. Surg. 10 (2022) 229–244.
[139] K.N. Eckstein, J.E. Hergert, A.C. Uzcategui, S.A. Schoonraad, S.J. Bryant, R. R. McLeod, V.L. Ferguson, Controlled mechanical property gradients within a digital light processing printed hydrogel-composite osteochondral scaffold, Ann. Biomed. Eng. 52 (2024) 2162–2177.
[140] J.J. Li, M. Ebied, J. Xu, H. Zreiqat, Current approaches to bone tissue engineering: the interface between biology and engineering, Adv. Healthcare Mater. 7 (2018) e1701061.
[141] C. Shuai, L. Yu, P. Feng, C. Gao, S. Peng, Interfacial reinforcement in bioceramic/biopolymer composite bone scaffold: the role of coupling agent, Colloids Surf. B Biointerfaces 193 (2020) 111083.
[142] H. Ma, C. Feng, J. Chang, C. Wu, 3D-printed bioceramic scaffolds: from bone tissue engineering to tumor therapy, Acta Biomater. 79 (2018) 37–59.
[143] Y.M. Lv, Q.S. Yu, Repair of articular osteochondral defects of the knee joint using a composite lamellar scaffold, Bone Joint Res 4 (2015) 56–64.
[144] A. Tampieri, E. Kon, M. Sandri, E. Campodoni, M. Dapporto, S. Sprio, Marine-inspired approaches as a smart tool to face osteochondral regeneration, Mar. Drugs 21 (2023) 212.
[145] H. Shi, Z. Zhou, W. Li, Y. Fan, Z. Li, J. Wei, Hydroxyapatite based materials for bone tissue engineering: a brief and comprehensive introduction, Crystals 11 (2021) 149.
[146] Q. Zhang, L. Ma, X. Ji, Y. He, Y. Cui, X. Liu, C. Xuan, Z. Wang, W. Yang, M. Chai, X. Shi, High-strength hydroxyapatite scaffolds with minimal surface macrostructures for load-bearing bone regeneration, Adv. Funct. Mater. 32 (2022) 2204182.
[147] B. Liu, Y. Zhao, T. Zhu, S. Gao, K. Ye, F. Zhou, D. Qiu, X. Wang, Y. Tian, X. Qu, Biphasic double-network hydrogel with compartmentalized loading of bioactive glass for osteochondral defect repair, Front. Bioeng. Biotechnol. 8 (2020) 752.
[148] V. Bunpetch, X. Zhang, T. Li, J. Lin, E.P. Maswikiti, Y. Wu, D. Cai, J. Li, S. Zhang, C. Wu, H. Ouyang, Silicate-based bioceramic scaffolds for dual-lineage regeneration of osteochondral defect, Biomaterials 192 (2019) 323–333.
[149] Q. Yu, J. Chang, C. Wu, Silicate bioceramics: from soft tissue regeneration to tumor therapy, J. Mater. Chem. B 7 (2019) 5449–5460.
[150] Y. Wu, J. Liu, L. Kang, J. Tian, X. Zhang, J. Hu, Y. Huang, F. Liu, H. Wang, Z. Wu, An overview of 3D printed metal implants in orthopedic applications: present and future perspectives, Heliyon 9 (2023) e17718.
[151] S. Wang, L. Liu, K. Li, L. Zhu, J. Chen, Y. Hao, Pore functionally graded Ti6Al4V scaffolds for bone tissue engineering application, Mater. Des. 168 (2019) 107643.
[152] A. Diaz Lantada, H. Alarcon Iniesta, J.P. Garcia-Ruiz, Composite scaffolds for osteochondral repair obtained by combination of additive manufacturing, leaching processes and hMSC-CM functionalization, Mater. Sci. Eng., C 59 (2016) 218–227.
[153] C. Zhai, Q. Zuo, K. Shen, J. Zhou, J. Chen, X. Zhang, C. Luo, H. Fei, W. Fan, Utilizing an integrated tri-layered scaffold with Titanium-Mesh-Cage base to repair cartilage defects of knee in goat model, Mater. Des. 193 (2020) 108766.
[154] Z. Liu, M. Tamaddon, S.M. Chen, H. Wang, V. San Cheong, F. Gang, X. Sun, C. Liu, Determination of an initial stage of the bone tissue ingrowth into titanium matrix by cell adhesion model, Front. Bioeng. Biotechnol. 9 (2021) 736063.
[155] Y. Li, P. Pavanram, J. Zhou, K. Lietaert, P. Taheri, W. Li, H. San, M.A. Leeflang, J. M.C. Mol, H. Jahr, A.A. Zadpoor, Additively manufactured biodegradable porous zinc, Acta Biomater. 101 (2020) 609–623.
[156] F. Yang, Y. Li, L. Wang, H. Che, X. Zhang, H. Jahr, L. Wang, D. Jiang, H. Huang, J. Wang, Full-thickness osteochondral defect repair using a biodegradable bilayered scaffold of porous zinc and chondroitin sulfate hydrogel, Bioact. Mater. 32 (2024) 400–414.
[157] A. Farazin, A.H. Ghasemi, Design, synthesis, and fabrication of chitosan/hydroxyapatite composite scaffold for use as bone replacement tissue by sol–gel method, J. Inorg. Organomet. Polym. Mater. 32 (2022) 3067–3082.
[158] B.A.E. Ben-Arfa, R.C. Pullar, A comparison of bioactive glass scaffolds fabricated by robocasting from powders made by sol–gel and melt-quenching methods, Processes 8 (2020) 615.
[159] M. Costantini, C. Colosi, P. Mozetic, J. Jaroszewicz, A. Tosato, A. Rainer, M. Trombetta, W. Swieszkowski, M. Dentini, A. Barbetta, Correlation between porous texture and cell seeding efficiency of gas foaming and microfluidic foaming scaffolds, Mater. Sci. Eng., C 62 (2016) 668–677.
[160] Y. Li, S. Sun, P. Gao, M. Zhang, C. Fan, Q. Lu, C. Li, C. Chen, B. Lin, Y. Jiang, A tough chitosan-alginate porous hydrogel prepared by simple foaming method, J. Solid State Chem. 294 (2021) 121797.
[161] C.Y. Chen, C.J. Ke, K.C. Yen, H.C. Hsieh, J.S. Sun, F.H. Lin, 3D porous calcium-alginate scaffolds cell culture system improved human osteoblast cell clusters for cell therapy, Theranostics 5 (2015) 643–655.
[162] H. Kang, Y. Zeng, S. Varghese, Functionally graded multilayer scaffolds for in vivo osteochondral tissue engineering, Acta Biomater. 78 (2018) 365–377.
[163] H. Chen, A. Malheiro, C. van Blitterswijk, C. Mota, P.A. Wieringa, L. Moroni, Direct writing electrospinning of scaffolds with multidimensional fiber architecture for hierarchical tissue engineering, ACS Appl. Mater. Interfaces 9 (2017) 38187–38200.
[164] W.E. King 3rd, G.L. Bowlin, Near-field electrospinning and melt electrowriting of biomedical polymers-progress and limitations, Polymers 13 (2021) 1097.
[165] M. Bahraminasab, Challenges on optimization of 3D-printed bone scaffolds, Biomed. Eng. Online 19 (2020) 69.
[166] X. Zhou, T. Esworthy, S.J. Lee, S. Miao, H. Cui, M. Plesiniak, H. Fenniri, T. Webster, R.D. Rao, L.G. Zhang, 3D Printed scaffolds with hierarchical biomimetic structure for osteochondral regeneration, Nanomedicine 19 (2019) 58–70.
[167] J. Liu, L. Li, H. Suo, M. Yan, J. Yin, J. Fu, 3D printing of biomimetic multi-layered GelMA/nHA scaffold for osteochondral defect repair, Mater. Des. 171 (2019) 107708.
[168] C. Qin, J. Ma, L. Chen, H. Ma, H. Zhuang, M. Zhang, Z. Huan, J. Chang, N. Ma, C. Wu, 3D bioprinting of multicellular scaffolds for osteochondral regeneration, Mater, Today Off. 49 (2021) 68–84.
[169] A. Dewle, N. Pathak, P. Rakshasmare, A. Srivastava, Multifarious fabrication approaches of producing aligned collagen scaffolds for tissue engineering applications, ACS Biomater. Sci. Eng. 6 (2020) 779–797.
[170] G. Liu, X. Wei, Y. Zhai, J. Zhang, J. Li, Z. Zhao, T. Guan, D. Zhao, 3D printed osteochondral scaffolds: design strategies, present applications and future perspectives, Front. Bioeng. Biotechnol. 12 (2024) 1339916.
[171] S. Agarwal, S. Saha, V.K. Balla, A. Pal, A. Barui, S. Bodhak, Current developments in 3D bioprinting for tissue and organ regeneration–A review, Front. Mech. Eng. 6 (2020) 589171.
[172] Y. Wang, Y. Xue, J. Wang, Y. Zhu, Y. Zhu, X. Zhang, J. Liao, X. Li, X. Wu, Y.X. Qin, W. Chen, A composite hydrogel with high mechanical strength, fluorescence, and degradable behavior for bone tissue engineering, Polymers 11 (2019) 1112.
[173] S. Todros, S. Spadoni, S. Barbon, E. Stocco, M. Confalonieri, A. Porzionato, P. G. Pavan, Compressive mechanical behavior of partially oxidized polyvinyl alcohol hydrogels for cartilage tissue repair, Bioengineering 9 (2022) 789.
[174] W. Lan, M. Xu, X. Zhang, L. Zhao, D. Huang, X. Wei, W. Chen, Biomimetic polyvinyl alcohol/type II collagen hydrogels for cartilage tissue engineering, J. Biomater. Sci. Polym. Ed. 31 (2020) 1179–1198.
[175] Y. Liu, W. Wang, K. Gu, J. Yao, Z. Shao, X. Chen, Poly(vinyl alcohol) hydrogels with integrated toughness, conductivity, and freezing tolerance based on ionic liquid/water binary solvent systems, ACS Appl. Mater. Interfaces 13 (2021) 29008–29020.
[176] M. Hua, S. Wu, Y. Ma, Y. Zhao, Z. Chen, I. Frenkel, J. Strzalka, H. Zhou, X. Zhu, X. He, Strong tough hydrogels via the synergy of freeze-casting and salting out, Nature 590 (2021) 594–599.
[177] S. Liu, J.M. Yu, Y.C. Gan, X.Z. Qiu, Z.C. Gao, H. Wang, S.X. Chen, Y. Xiong, G. H. Liu, S.E. Lin, A. McCarthy, J.V. John, D.X. Wei, H.H. Hou, Biomimetic natural biomaterials for tissue engineering and regenerative medicine: new biosynthesis methods, recent advances, and emerging applications, Mil. Med. Res. 10 (2023) 16.
[178] J.J. Li, D.L. Kaplan, H. Zreiqat, Scaffold-based regeneration of skeletal tissues to meet clinical challenges, J. Mater. Chem. B 2 (2014) 7272–7306.
[179] Y. Zhu, L. Kong, F. Farhadi, W. Xia, J. Chang, Y. He, H. Li, An injectable continuous stratified structurally and functionally biomimetic construct for enhancing osteochondral regeneration, Biomaterials 192 (2019) 149–158.
[180] D. Gan, Z. Wang, C. Xie, X. Wang, W. Xing, X. Ge, H. Yuan, K. Wang, H. Tan, X. Lu, Mussel-inspired tough hydrogel with in situ nanohydroxyapatite mineralization for osteochondral defect repair, Adv. Healthcare Mater. 8 (2019) 1901103.
[181] H. Zhou, R. Chen, J. Wang, J. Lu, T. Yu, X. Wu, S. Xu, Z. Li, C. Jie, R. Cao, Y. Yang, Y. Li, D. Meng, Biphasic fish collagen scaffold for osteochondral regeneration, Mater. Des. 195 (2020) 108947.
[182] X. Wu, M. Zhou, F. Jiang, S. Yin, S. Lin, G. Yang, Y. Lu, W. Zhang, X. Jiang, Marginal sealing around integral bilayer scaffolds for repairing osteochondral defects based on photocurable silk hydrogels, Bioact. Mater. 6 (2021) 3976–3986.
[183] W. Jiang, X. Xiang, M. Song, J. Shen, Z. Shi, W. Huang, H. Liu, An all-silk-derived bilayer hydrogel for osteochondral tissue engineering, Mater. Today Bio. 17 (2022) 100485.
[184] X. Liu, Y. Wei, C. Xuan, L. Liu, C. Lai, M. Chai, Z. Zhang, L. Wang, X. Shi, A biomimetic biphasic osteochondral scaffold with layer-specific release of stem cell differentiation inducers for the reconstruction of osteochondral defects, Adv. Healthcare Mater. 9 (2020) 2000076.
[185] F. Gao, Z. Xu, Q. Liang, H. Li, L. Peng, M. Wu, X. Zhao, X. Cui, C. Ruan, W. Liu, Osteochondral regeneration with 3D-printed biodegradable high-strength supramolecular polymer reinforced-gelatin hydrogel scaffolds, Adv. Sci. 6 (2019) 1900867.
[186] L. Chen, L. Wei, X. Su, L. Qin, Z. Xu, X. Huang, H. Chen, N. Hu, Preparation and characterization of biomimetic functional scaffold with gradient structure for osteochondral defect repair, Bioengineering 10 (2023) 213.
[187] J. Liu, Q. Zou, C. Wang, M. Lin, Y. Li, R. Zhang, Y. Li, Electrospinning and 3D printed hybrid bi-layer scaffold for guided bone regeneration, Mater. Des. 210 (2021) 110047.

[188] S. Tamburaci, B. Cecen, O. Ustun, B.U. Ergur, H. Havitcioglu, F. Tihminlioglu, Production and characterization of a novel bilayer nanocomposite scaffold composed of chitosan/Si-nHap and zein/POSS structures for osteochondral tissue regeneration, ACS Appl. Mater. Interfaces 2 (2019) 1440–1455.
[189] F. Hejazi, S. Bagheri-Khoulenjani, N. Olov, D. Zeini, A. Solouk, H. Mirzadeh, Fabrication of nanocomposite/nanofibrous functionally graded biomimetic scaffolds for osteochondral tissue regeneration, J. Biomed. Mater. Res. A. 109 (2021) 1657–1669.
[190] C. Gegg, F. Yang, Spatially patterned microribbon-based hydrogels induce zonally-organized cartilage regeneration by stem cells in 3D, Acta Biomater. 101 (2020) 196–205.
[191] X. Wan, Y. Zhao, Z. Li, L. Li, Emerging polymeric electrospun fibers: from structural diversity to application in flexible bioelectronics and tissue engineering, Explorations 2 (2022) 20210029.
[192] M. Castilho, G. Hochleitner, W. Wilson, B. van Rietbergen, P.D. Dalton, J. Groll, J. Malda, K. Ito, Mechanical behavior of a soft hydrogel reinforced with three-dimensional printed microfibre scaffolds, Sci. Rep. 8 (2018) 1245.
[193] M. Castilho, V. Mouser, M. Chen, J. Malda, K. Ito, Bi-layered micro-fibre reinforced hydrogels for articular cartilage regeneration, Acta Biomater. 95 (2019) 297–306.
[194] A.F. Girão, Â. Semitela, G. Ramalho, A. Completo, P.A.A.P. Marques, Mimicking nature: fabrication of 3D anisotropic electrospun polycaprolactone scaffolds for cartilage tissue engineering applications, Compos. B Eng. 154 (2018) 99–107.
[195] N. Munir, A. McDonald, A. Callanan, Integrational technologies for the development of three-dimensional scaffolds as platforms in cartilage tissue engineering, ACS Omega 5 (2020) 12623–12636.
[196] T.J. Levingstone, A. Matsiko, G.R. Dickson, F.J. O'Brien, J.P. Gleeson, A biomimetic multi-layered collagen-based scaffold for osteochondral repair, Acta Biomater. 10 (2014) 1996–2004.
[197] R. Cao, Y. Xu, Y. Xu, D.D. Brand, G. Zhou, K. Xiao, H. Xia, J.T. Czernuszka, Development of tri-layered biomimetic atelocollagen scaffolds with interfaces for osteochondral tissue engineering, Adv. Healthcare Mater. 11 (2022) 2101643.
[198] S. Camarero-Espinosa, B. Rothen-Rutishauser, C. Weder, E.J. Foster, Directed cell growth in multi-zonal scaffolds for cartilage tissue engineering, Biomaterials 74 (2016) 42–52.
[199] O. Bas, S. Lucarotti, D.D. Angella, N.J. Castro, C. Meinert, F.M. Wunner, E. Rank, G. Vozzi, T.J. Klein, I. Catelas, E.M. De-Juan-Pardo, D.W. Hutmacher, Rational design and fabrication of multiphasic soft network composites for tissue engineering articular cartilage: a numerical model-based approach, Chem. Eng. J. 340 (2018) 15–23.
[200] M. Nowicki, W. Zhu, K. Sarkar, R. Rao, L.G. Zhang, 3D printing multiphasic osteochondral tissue constructs with nano to micro features via PCL based bioink, Bioprinting 17 (2020) e00066.
[201] X. Hu, W. Li, L. Li, Y. Lu, Y. Wang, R. Parungao, S. Zheng, T. Liu, Y. Nie, H. Wang, K. Song, A biomimetic cartilage gradient hybrid scaffold for functional tissue engineering of cartilage, Tissue Cell 58 (2019) 84–92.
[202] C.A. Tee, J. Han, J.H.P. Hui, E.H. Lee, Z. Yang, Perspective in achieving stratified articular cartilage repair using zonal chondrocytes, Tissue Eng., Part B 29 (2023) 310–330.
[203] C.A. Tee, Z. Yang, Y. Wu, X. Ren, M. Baranski, D.J. Lin, A. Hassan, J. Han, E. H. Lee, A pre-clinical animal study for zonal articular cartilage regeneration using stratified implantation of microcarrier expanded zonal chondrocytes, Cartilage 13 (2022) 1–16.
[204] Y. Peng, Y. Zhuang, Y. Zhang, J. Zuo, J. Ding, Dynamically adaptive scaffolds for cartilage tissue engineering, MedComm – Biomaterials and Applications 2 (2023) e49.
[205] D. Clearfield, A. Nguyen, M. Wei, Biomimetic multidirectional scaffolds for zonal osteochondral tissue engineering via a lyophilization bonding approach, J. Biomed. Mater. Res. A. 106 (2018) 948–958.
[206] D.C. Browe, P.J. Diaz-Payno, F.E. Freeman, R. Schipani, R. Burdis, D.P. Ahern, J. M. Nulty, S. Guler, L.D. Randall, C.T. Buckley, P.A.J. Brama, D.J. Kelly, Bilayered extracellular matrix derived scaffolds with anisotropic pore architecture guide tissue organization during osteochondral defect repair, Acta Biomater. 143 (2022) 266–281.
[207] S. Zadegan, B. Vahidi, J. Nourmohammadi, A. Shojaee, N. Haghighipour, Evaluation of rabbit adipose derived stem cells fate in perfused multilayered silk fibroin composite scaffold for Osteochondral repair, J. Biomed. Mater. Res. B Appl. Biomater. 112 (2024) e35396.
[208] J. Chakraborty, J. Fernández-Pérez, K.A. van Kampen, S. Roy, T. Ten Brink, C. Mota, S. Ghosh, L. Moroni, Development of a biomimetic arch-like 3D bioprinted construct for cartilage regeneration using gelatin methacryloyl and silk fibroin-gelatin bioinks, Biofabrication 15 (2023) 035009.
[209] M. Younesi, V.M. Goldberg, O. Akkus, A micro-architecturally biomimetic collagen template for mesenchymal condensation based cartilage regeneration, Acta Biomater. 30 (2016) 212–221.
[210] T. Yamamoto, R. Randriantsilefisoa, C.M. Sprecher, M. D'Este, Fabrication of collagen-hyaluronic acid cryogels by directional freezing mimicking cartilage arcade-like structure, Biomolecules 12 (2022) 1809.
[211] J.N. Fu, X. Wang, M. Yang, Y.R. Chen, J.Y. Zhang, R.H. Deng, Z.N. Zhang, J.K. Yu, F.Z. Yuan, Scaffold-based tissue engineering strategies for osteochondral repair, Front. Bioeng. Biotechnol. 9 (2021) 812383.
[212] J. Liang, P. Liu, X. Yang, L. Liu, Y. Zhang, Q. Wang, H. Zhao, Biomaterial-based scaffolds in promotion of cartilage regeneration: recent advances and emerging applications, J. Orthop. Translat. 41 (2023) 54–62.
[213] Y. Yu, J. Wang, Y. Li, Y. Chen, W. Cui, Cartilaginous organoids: advances, applications, and perspectives, Adv. Nanobiomed Res. 3 (2022) 2200114.
[214] Y. Wang, Y. Guo, Q. Wei, X. Li, K. Ji, K. Zhang, Current researches on design and manufacture of biopolymer-based osteochondral biomimetic scaffolds, Bio-Des, Man (Lond.) 4 (2021) 541–567.
[215] Š. Rýglová, M. Braun, T. Suchý, M. Hříbal, M. Žaloudková, L.J.F.R.I. Vištějnová, The investigation of batch-to-batch variabilities in the composition of isolates from fish and mammalian species using different protocols, Food Res. Int. 169 (2023) 112798.
[216] J. Du, Z. Zhu, J. Liu, X. Bao, Q. Wang, C. Shi, C. Zhao, G. Xu, D. Li, 3D-printed gradient scaffolds for osteochondral defects: current status and perspectives, Int. J. Bioprinting. 9 (2023) 724.
[217] D. Kilian, P. Sembdner, H. Bretschneider, T. Ahlfeld, L. Mika, J. Lützner, S. Holtzhausen, A. Lode, R. Stelzer, M. Gelinsky, 3D printing of patient-specific implants for osteochondral defects: workflow for an MRI-guided zonal design, Bio-Des, Man (Lond.) 4 (2021) 818–832.
[218] T. Ahlfeld, N. Cubo-Mateo, S. Cometta, V. Guduric, C. Vater, A. Bernhardt, A. R. Akkineni, A. Lode, M. Gelinsky, A novel plasma-based bioink stimulates cell proliferation and differentiation in bioprinted, mineralized constructs, ACS Appl. Mater. Interfaces 12 (2020) 12557–12572.
[219] P. Gonzalez-Fernandez, C. Rodriguez-Nogales, O. Jordan, E. Allemann, Combination of mesenchymal stem cells and bioactive molecules in hydrogels for osteoarthritis treatment, Eur. J. Pharm. Biopharm. 172 (2022) 41–52.
[220] S. Critchley, E.J. Sheehy, G. Cunniffe, P. Diaz-Payno, S.F. Carroll, O. Jeon, E. Alsberg, P.A.J. Brama, D.J. Kelly, 3D printing of fibre-reinforced cartilaginous templates for the regeneration of osteochondral defects, Acta Biomater. 113 (2020) 130–143.
[221] D. Pearce, S. Fischer, F. Huda, A. Vahdati, Applications of computer modeling and simulation in cartilage tissue engineering, Tissue Eng. Regen. Med. 17 (2020) 1–13.
[222] B.L. Devlin, M.C. Allenby, J. Ren, E. Pickering, T.J. Klein, N.C. Paxton, M. A. Woodruff, Materials design innovations in optimizing cellular behavior on melt electrowritten (MEW) scaffolds, Adv. Funct. Mater. 16 (2024) 2313092.
[223] H. Nosrati, M. Nosrati, Artificial intelligence in regenerative medicine: applications and implications, Biomimetics 8 (2023) 442.
[224] O. Yue, X. Wang, M. Hou, M. Zheng, D. Hao, Z. Bai, X. Zou, B. Cui, C. Liu, X. Liu, Smart nanoengineered electronic-scaffolds based on triboelectric nanogenerators as tissue batteries for integrated cartilage therapy, Nano Energy 107 (2023) 108158.
[225] A. Puiggalí-Jou, R. Rizzo, A. Bonato, P. Fisch, S. Ponta, D.M. Weber, M. Zenobi-Wong, FLight biofabrication supports maturation of articular cartilage with anisotropic properties, Adv. Healthcare Mater. 13 (2024) 2302179.
[226] H. Meng, X. Liu, R. Liu, Y. Zheng, A. Hou, S. Liu, W. He, Y. Wang, A. Wang, Q. Guo, J. Peng, Decellularized laser micro-patterned osteochondral implants exhibit zonal recellularization and self-fixing for osteochondral regeneration in a goat model, J. Orthop. Translat. 46 (2024) 18–32.
[227] J. Lai, Y. Liu, G. Lu, P. Yung, X. Wang, R.S. Tuan, Z.A. Li, 4D bioprinting of programmed dynamic tissues, Bioact. Mater. 37 (2024) 348–377.
[228] A.N. Aufa, Z. Ismail, M. Zaki Hassan, Emerging trends in 4d printing of hydrogels in the biomedical field: a review, in: Materials Today: Proceedings, 2023, https://doi.org/10.1016/j.matpr.2023.01.101.
[229] S. Naficy, R. Gately, R. Gorkin, H. Xin, G.M. Spinks, 4D printing of reversible shape morphing hydrogel structures, Macromol. Mater. Eng. 302 (2017) 1600212–n/a.
[230] S.H. Kim, Y.B. Seo, Y.K. Yeon, Y.J. Lee, H.S. Park, M.T. Sultan, J.M. Lee, J.S. Lee, O.J. Lee, H. Hong, H. Lee, O. Ajiteru, Y.J. Suh, S.-H. Song, K.-H. Lee, C.H. Park, 4D-bioprinted silk hydrogels for tissue engineering, Biomaterials 260 (2020) 120281.
[231] A. Ding, O. Jeon, D. Cleveland, K.L. Gasvoda, D. Wells, S.J. Lee, E. Alsberg, Jammed micro-flake hydrogel for four-dimensional living cell bioprinting, Adv Mater. 34 (2022).
[232] A. Ding, S.J. Lee, R. Tang, K.L. Gasvoda, F. He, E. Alsberg, 4D cell-condensate bioprinting, Small 18 (2022).
[233] P.J. Díaz-Payno, M. Kalogeropoulou, I. Muntz, E. Kingma, N. Kops, M. D'Este, G. H. Koenderink, L.E. Fratila-Apachitei, G.J.V.M. van Osch, A.A. Zadpoor, Swelling-dependent shape-based transformation of a human mesenchymal stromal cells-laden 4D bioprinted construct for cartilage tissue engineering, Adv. Healthcare Mater. 12 (2023).
[234] K. Loukelis, Z.A. Helal, A.G. Mikos, M. Chatzinikolaidou, Nanocomposite bioprinting for tissue engineering applications, Gels 9 (2023).
[235] L. Ricotti, A. Cafarelli, C. Manferdini, D. Trucco, L. Vannozzi, E. Gabusi, F. Fontana, P. Dolzani, Y. Saleh, E. Lenzi, M. Columbaro, M. Piazzi, J. Bertacchini, A. Aliperta, M. Cain, M. Gemmi, P. Parlanti, C. Jost, Y. Fedutik, G.D. Nessim, M. Telkhozhayeva, E. Teblum, E. Dumont, C. Delbaldo, G. Codispoti, L. Martini, M. Tschon, M. Fini, G. Lisignoli, Ultrasound stimulation of piezoelectric nanocomposite hydrogels boosts chondrogenic differentiation in vitro, in both a normal and inflammatory milieu, ACS Nano 18 (2024) 2047–2065.
[236] C. Lesage, M. Lafont, P. Guihard, P. Weiss, J. Guicheux, V. Delplace, Material-assisted strategies for osteochondral defect repair, Adv. Sci. 9 (2022).
[237] P.P.W. van Hugten, R.M. Jeuken, E.E. Asik, H. Oevering, T.J.M. Welting, C.C. van Donkelaar, J.C. Thies, P.J. Emans, A.K. Roth, In vitro and in vivo evaluation of the osseointegration capacity of a polycarbonate-urethane zirconium-oxide composite material for application in a focal knee resurfacing implant, J. Biomed. Mater. Res., Part A 112 (2024) 1424–1435.
[238] H. Meng, X. Liu, R. Liu, Y. Zheng, A. Hou, S. Liu, W. He, Y. Wang, A. Wang, Q. Guo, J. Peng, Decellularized laser micro-patterned osteochondral implants exhibit zonal recellularization and self-fixing for osteochondral regeneration in a goat model, J. Orthop. Transl. 46 (2024) 18–32.

[239] Y. Huo, B. Bai, R. Zheng, Y. Sun, Y. Yu, X. Wang, H. Chen, Y. Hua, Y. Zhang, G. Zhou, X. Wang, In vivo stable allogenic cartilage regeneration in a goat model based on immunoisolation strategy using electrospun semipermeable membranes, Adv. Healthcare Mater. 12 (2023).
[240] T.J. Levingstone, E.J. Sheehy, C.J. Moran, G.M. Cunniffe, P.J. Diaz Payno, R. T. Brady, H.V. Almeida, S.F. Carroll, J.M. O'Byrne, D.J. Kelly, P.A. Brama, F.J. O' Brien, Evaluation of a co-culture of rapidly isolated chondrocytes and stem cells seeded on tri-layered collagen-based scaffolds in a caprine osteochondral defect model, Biomater. Biosyst. 8 (2022).
[241] D.C. Browe, P.J. Díaz-Payno, F.E. Freeman, R. Schipani, R. Burdis, D.P. Ahern, J. M. Nulty, S. Guler, L.D. Randall, C.T. Buckley, P.A.J. Brama, D.J. Kelly, Bilayered extracellular matrix derived scaffolds with anisotropic pore architecture guide tissue organization during osteochondral defect repair, Acta Biomater. 143 (2022) 266–281.
[242] D.C. Browe, R. Burdis, P.J. Díaz-Payno, F.E. Freeman, J.M. Nulty, C.T. Buckley, P. A.J. Brama, D.J. Kelly, Promoting endogenous articular cartilage regeneration using extracellular matrix scaffolds, Mater, Today Bio. 16 (2022).
[243] M. de Ruijter, P. Diloksumpan, I. Dokter, H. Brommer, I.H. Smit, R. Levato, P. R. van Weeren, M. Castilho, J. Malda, Orthotopic equine study confirms the pivotal importance of structural reinforcement over the pre-culture of cartilage implants, Bioeng. Trans. Med. 9 (2024).
[244] R. Chen, J.S. Pye, J. Li, C.B. Little, J.J.J.B.M. Li, Multiphasic Scaffolds for the Repair of Osteochondral Defects: Outcomes of Preclinical Studies, vol. 27, 2023, pp. 505–545.
[245] J.S. Wayne, C.L. McDowell, K.J. Shields, R.S. Tuan, In vivo response of polylactic acid–alginate scaffolds and bone marrow-derived cells for cartilage tissue engineering, Tissue Eng. 11 (2005) 953–963.
[246] M. Maglio, S. Brogini, S. Pagani, G. Giavaresi, M. Tschon, Current trends in the evaluation of osteochondral lesion treatments: histology, histomorphometry, and biomechanics in preclinical models, BioMed Res. Int. 2019 (2019) 4040236, 27.
[247] P. Mainil-Varlet, T. Aigner, M. Brittberg, P. Bullough, A. Hollander, E. Hunziker, R. Kandel, S. Nehrer, K. Pritzker, S. Roberts, E. Stauffer, Histological assessment of cartilage repair : a report by the histology endpoint committee of the international cartilage repair society (ICRS), JBJS 85 (2003) 45–57.
[248] S.S. Glasson, M.G. Chambers, W.B. Van Den Berg, C.B. Little, The OARSI histopathology initiative – recommendations for histological assessments of osteoarthritis in the mouse, Osteoarthritis Cartilage 18 (2010) S17–S23.
[249] S. Wakitani, T. Goto, S.J. Pineda, R.G. Young, J.M. Mansour, A.I. Caplan, V. M. Goldberg, Mesenchymal cell-based repair of large, full-thickness defects of articular cartilage, JBJS 76 (1994) 579–592.
[250] S.W. O'Driscoll, R.G. Marx, D.E. Beaton, Y. Miura, S.H. Gallay, J.S. Fitzsimmons, Validation of a simple histological-histochemical cartilage scoring system, Tissue Eng. 7 (2001) 313–320.
[251] B. Hiemer, B. Genz, J. Ostwald, A. Jonitz-Heincke, A. Wree, T. Lindner, T. Tischer, S. Dommerich, R. Bader, Repair of cartilage defects with devitalized osteochondral tissue: a pilot animal study, J. Biomed. Mater. Res., Part B 107 (2019) 2354–2364.
[252] B.A. Lakin, B.D. Snyder, M.W. Grinstaff, Assessing cartilage biomechanical properties: techniques for evaluating the functional performance of cartilage in health and disease, Annu. Rev. Biomed. Eng. 19 (2017) 27–55.
[253] F. Gullotta, D. Izzo, F. Scalera, B. Palazzo, I. Martin, A. Sannino, F. Gervaso, Biomechanical evaluation of hMSCs-based engineered cartilage for chondral tissue regeneration, J. Mech. Behav. Biomed. Mater. 86 (2018) 294–304.
[254] A.J. de Kanter, K.R. Jongsma, M.C. Verhaar, A.L. Bredenoord, The ethical implications of tissue engineering for regenerative purposes: a systematic review, Tissue Eng., Part B 29 (2023) 167–187.
[255] A.M. Gonçalves, A. Moreira, A. Weber, G.R. Williams, P.F. Costa, Osteochondral tissue engineering: the potential of electrospinning and additive manufacturing, Pharmaceutics 13 (2021) 983.
[256] D. Bicho, S. Pina, R.L. Reis, J.M. Oliveira, Commercial products for osteochondral tissue repair and regeneration, Adv. Exp. Med. Biol. 1058 (2018) 415–428.
[257] X. Guo, Y. Ma, Y. Min, J. Sun, X. Shi, G. Gao, L. Sun, J. Wang, Progress and prospect of technical and regulatory challenges on tissue-engineered cartilage as therapeutic combination product, Bioact. Mater. 20 (2023) 501–518.
[258] K.B. McGowan, G. Stiegman, Regulatory challenges for cartilage repair technologies, Cartilage 4 (2013) 4–11.
[259] C.V. Oberweis, J.A. Marchal, E. López-Ruiz, P. Gálvez-Martín, A worldwide overview of regulatory frameworks for tissue-based products, Tissue Eng., Part B 26 (2020) 181–196.